

**Synthesis and Characterization of Ethylene  
Carbonate Modified Polyisobutylene Succinimide  
Dispersants**

by

Yulin Wang

A thesis  
presented to the University of Waterloo  
in fulfillment of the  
thesis requirement for the degree of  
Master of Science  
in  
Chemistry

Waterloo, Ontario, Canada, 2010

© Yulin Wang 2010

# **Author`s Declaration**

I hereby declare that I am the sole author of this thesis. This is a true copy of the thesis, including any required final version, as accepted by my examiners.

I understand that my thesis may be made electronically available to the public.

# Abstract

Succinimide-based dispersants are the most commonly used dispersants in the oil industry. They are used in engine oil to prevent the aggregation of carbon-rich particles generated during engine operation, and consequently reduce the production of sludge and the emission of fine particles into the air that cause air pollution. This project aims at studying the efficiency of a series of non-ionic dispersants at stabilizing carbon-rich particles in an apolar solvent. The dispersants are composed of two polyisobutylene apolar chains and a polyamine core that was modified by reacting the dispersant with ethylene carbonate. This thesis describes the synthesis of a series of unmodified and modified dispersants with different amine contents. It also includes different techniques used in the characterization of the chemical composition of the dispersants, as well as the synthesis of the model compounds which enabled the characterization of the dispersants. A preliminary study on the micelle formation of the dispersants is also presented in this thesis.

# Acknowledgements

I would like to thank my supervisor Dr. Jean Duhamel for his patient guidance and generous help throughout this learning process. This thesis would not have been accomplished without Dr. Duhamel's selfless help.

I would also like to thank all my committee members: Dr. Mario Gauthier and Dr. Costa Tzoganakis, with special thanks to Dr. Mike Chong for his help with the model compound synthesis and NMR spectra analysis.

Thanks go to Dr. Mark Ingratta who taught me numerous lab skills during my first research project, as well as to all the Duhamel and Gauthier lab members who have made my time here at UW fun and memorable.

Special thanks go to my parents for their support and encouragement over the years.

Finally, I would like to thank NSERC, Imperial Oil, and the University of Waterloo for financial support.

# Dedication

To my parents,

Wei Wang and Fangsheng Lin

# Table of Contents

<b>AUTHOR'S DECLARATION .....</b>	<b>II</b>
<b>ABSTRACT.....</b>	<b>III</b>
<b>ACKNOWLEDGEMENTS .....</b>	<b>IV</b>
<b>DEDICATION.....</b>	<b>V</b>
<b>TABLE OF CONTENTS .....</b>	<b>VI</b>
<b>LIST OF FIGURES .....</b>	<b>X</b>
<b>LIST OF SCHEMES .....</b>	<b>XIII</b>
<b>LIST OF TABLES .....</b>	<b>XIV</b>
<b>LIST OF ABBREVIATIONS .....</b>	<b>XV</b>
<b>CHAPTER 1 .....</b>	<b>1</b>
<b>INTRODUCTION.....</b>	<b>1</b>
1.1. INTRODUCTION .....	2
1.2. DISPERSANTS.....	2
1.3. MICELLIZATION OF DISPERSANTS.....	5
1.4. PROJECT GOAL .....	6
<b>CHAPTER 2 .....</b>	<b>10</b>
<b>SYNTHESIS OF THE MODEL COMPOUNDS AND THEIR USE FOR THE</b>	
<b>ASSIGNMENT OF THE <sup>1</sup>H NMR SPECTRA OF THE DISPERSANTS .....</b>	<b>10</b>

2.1 INTRODUCTION.....	11
2.2 EXPERIMENTAL PROCEDURES .....	12
2.2.1 <i>Chemicals</i> .....	12
2.2.2 <i>Instrumentation: Nuclear Magnetic Resonance (NMR)</i> .....	12
2.3 ASSIGNMENT OF THE PEAKS IN THE <sup>1</sup> H NMR SPECTRUM OF PIBSA.....	13
2.4. SAMPLE REACTION OF METHYL SUCCINIC ANHYDRIDE WITH DIETHYLENTRIAMINE	16
2.4.1 <i>Synthesis of bis-methyl succinimide-DETA</i> .....	17
2.4.2. <i>Purification of b-MSI-DETA</i> .....	18
2.4.3. <i>Assignment of the proton peaks in the <sup>1</sup>H NMR spectra of b-MSI-DETA and b-PIBSI-DETA</i> .....	19
2.5. SYNTHESIS OF 2-HYDROXYETHYL <i>N,N</i> -DIBUTYL CARBAMATE .....	21
2.5.1. <i>Synthesis of 2-hydroxyethyl N,N-dibutyl carbamate</i> .....	22
2.5.2. <i>Purification of 2-hydroxyethyl N,N-dibutyl carbamate</i> .....	24
2.5.3. <i>Dilute sample reaction</i> .....	28
2.5.4. <i>Assignment of the <sup>1</sup>H NMR spectrum of HEDBC and M-b-PIBSI-DETA</i> .....	29
2.6. SUMMARY OF <sup>1</sup> H NMR SPECTRA.....	31
<b>CHAPTER 3 .....</b>	<b>33</b>
<b>SYNTHESIS AND CHARACTERIZATION OF MODIFIED</b>	
<b>POLYISOBUTYLENE SUCCINIMIDE DISPERSANTS .....</b>	<b>33</b>
3.1 INTRODUCTION.....	34
3.2. EXPERIMENTAL PROCEDURES .....	35
3.2.1 <i>Chemicals</i> .....	35
3.2.2 <i>Instrumentation</i> .....	35

3.3 CHARACTERIZATION OF PIBSA.....	36
3.3.1. Purification of PIBSA .....	36
3.3.2. Dehydration of PIBSA .....	36
3.3.3. Chemical composition of PIBSA.....	38
3.4. SYNTHESIS AND CHARACTERIZATION OF PIBSI DISPERSANTS .....	42
3.4.1 Synthesis of PIBSI dispersants .....	42
3.4.2. Purification of the PIBSI dispersants .....	44
3.4.3. Characterization of PIBSI dispersants .....	47
3.4.3.1. FT-IR .....	47
3.4.3.2. <sup>1</sup> H NMR.....	51
3.4.3.3. Summary of the $N_{SI}/N_{IB}$ ratios.....	54
3.5. SYNTHESIS AND CHARACTERIZATION OF M-B-PIBSI.....	56
3.5.1. Synthesis of M-b-PIBSI-DETA .....	57
3.5.2. Synthesis and characterization of M-b-PIBSI-TEPA .....	61
3.6. CONCLUSIONS .....	63
<b>CHAPTER 4.....</b>	<b>65</b>
<b>PRELIMINARY RESULTS FOR THE DETERMINATION OF THE CRITICAL</b>	
<b>MICELLE CONCENTRATION OF THE DISPERSANTS .....</b>	<b>65</b>
4.1 INTRODUCTION.....	66
4.2 EXPERIMENTAL PROCEDURES .....	68
4.2.1 Chemicals .....	68
4.2.2 Instrumentation: Steady-state Spectrofluorometer.....	69
4.2.3. Sample Preparation for CMC measurements.....	69



4.3 CHROMOPHORE: <i>BIS</i> -(2,2'-BIPYRIDINE)-RUTHENIUM(II)-5-AMINO-1,10-PHENANTHROLINE HEXAFLUOROPHOSPHATE.....	69
4.3.1 <i>Synthesis of [RuNH<sub>2</sub>]<sub>2</sub>PF<sub>6</sub></i> .....	70
4.3.2 <i>Purification of [RuNH<sub>2</sub>]<sub>2</sub>PF<sub>6</sub></i> .....	71
4.4. CMC MEASUREMENTS .....	72
4.5. CONCLUSIONS .....	77
<b>CHAPTER 5.....</b>	<b>78</b>
<b>CONCLUSIONS AND FUTURE WORK.....</b>	<b>78</b>
5.1 CONCLUSIONS .....	79
5.2 FUTURE WORK.....	84
5.2.1. <i>Why are the <math>N_{SA}/N_{IB}</math> ratio of PIBSA and the <math>N_{SI}/N_{IB}</math> ratio of b-PIBSI dispersants different?</i> .....	84
5.2.2. <i>Determination of the CMC of b-PIBSI and M-b-PIBSI dispersants</i> .....	85
5.2.3. <i>Adsorption of the M-b-PIBSI dispersants onto carbon black particles</i> .....	85
<b>REFERENCES.....</b>	<b>88</b>

## List of Figures

Figure 1.1. Aggregation of UFPs in engine oil without (top) and with dispersant present (bottom).....	3
Figure 1.2. Synthesis of the M- <i>b</i> -PIBSI dispersant .....	8
Figure 2.1. Structures of MSA (A) and PIBSA (B).....	13
Figure 2.2. <sup>1</sup> H NMR spectrum of MSA (300 MHz, CDCl <sub>3</sub> ).....	14
Figure 2.3. <sup>1</sup> H NMR spectrum of PIBSA (300MHz, CDCl <sub>3</sub> ).....	15
Figure 2.4. <sup>1</sup> H NMR spectrum of MSA (upper) and <i>b</i> -MSI-DETA (lower) (300 MHz, CDCl <sub>3</sub> ).....	19
Figure 2.5. <sup>1</sup> H NMR spectra of <i>b</i> -MSI-DETA (top) and <i>b</i> -PIBSI-DETA (bottom) (300 MHz, CDCl <sub>3</sub> ).....	20
Figure 2.6. <sup>1</sup> H NMR spectra of EC (top), DBA (middle), and the reaction product (bottom) (300 MHz, CDCl <sub>3</sub> ).....	23
Figure 2.7. Chemical structure of 2-(dibutylamino)ethanol .....	23
Figure 2.8. <sup>1</sup> H NMR spectra of neutral (top) and basic products (bottom) of the reaction shown in Scheme 2.4 (300 MHz, CDCl <sub>3</sub> ) .....	25
Figure 2.9. <sup>1</sup> H NMR spectra of the neutral products found in the reaction mixture (300 MHz, CDCl <sub>3</sub> ).....	26
Figure 2.10. Comparison of the <sup>1</sup> H NMR spectra of DBA and HEDBC (300 MHz, CDCl <sub>3</sub> ).....	27
Figure 2.11. <sup>1</sup> H NMR spectra of the neutral (top) and the basic products (bottom) obtained during the synthesis of HEDBC under dilute conditions (300 MHz, CDCl <sub>3</sub> ) .....	29

Figure 2.12. $^1\text{H}$ NMR spectra of HEDBC (top) and M- <i>b</i> -PIBSI-DETA (bottom) (300 MHz, $\text{CDCl}_3$ ).....	30
Figure 2.13. $^1\text{H}$ NMR spectra of PIBSA (top), <i>b</i> -PIBSI-DETA (middle), and M- <i>b</i> -PIBSI-DETA (bottom).....	31
Figure 3.1. FT-IR spectra of hydrated (top) and dehydrated (bottom) PIBSA.....	38
Figure 3.2. $^1\text{H}$ NMR spectrum of PIBSA .....	40
Figure 3.3. GPC trace of crude PIBSA. Elution volume $v_{\text{el}} = 31$ mL: PIBSA ( $M_n = 1200$ g/mol); $v_{\text{el}} = 33$ mL: non-maleated PIB impurity ( $M_n = 280$ g/mol); $v_{\text{el}} = 35$ mL: solvent peak. The molecular weights are obtained according to a calibration curve based on polystyrene standards .....	41
Figure 3.4. GPC trace of PIBSA (bottom) and <i>b</i> -PIBSI-DETA (top). .....	45
Figure 3.5. GPC traces of crude <i>b</i> -PIBSI-DETA (bottom) and purified <i>b</i> -PIBSI-DETA sample (top). .....	46
Figure 3.6. Calibration curve relating the ratio of the number of SI to IB units to the peak ratio of absorption bands at $1705\text{ cm}^{-1}$ and $1390\text{ cm}^{-1}$ .....	48
Figure 3.7. Calibration curve relating the $N_{\text{SI}}/N_{\text{IB}}$ ratio to the ratio of the integrated absorption bands at $1705\text{ cm}^{-1}$ and $1390\text{ cm}^{-1}$ in the FT-IR spectra.....	50
Figure 3.8. $^1\text{H}$ NMR spectrum of <i>b</i> -PIBSI-DETA.....	51
Figure 3.9. Integration of the peak at 3.5 ppm in the $^1\text{H}$ NMR spectrum.....	53
Figure 3.10. $^1\text{H}$ NMR spectrum of <i>b</i> -PIBSI-DETA.....	53
Figure 3.11. FT-IR spectra of <i>b</i> -PIBSI-PEHA (top), <i>b</i> -PIBSI-TEPA (middle), and <i>b</i> -PIBSI-DETA (bottom) .....	55
Figure 3.12. Chemical structure of succinamide .....	56

Figure 3.13. <sup>1</sup> H NMR spectra of <i>b</i> -PIBSI-DETA (top) and M- <i>b</i> -PIBSI-DETA (bottom); peaks at 3.8 and 4.2 ppm are shown with an asterisk.....	59
Figure 3.14. <sup>1</sup> H NMR spectra of <i>m</i> -PIBSI-DETA (top) and M- <i>m</i> -PIBSI-DETA (bottom); Peaks at 3.8 and 4.2 ppm are shown with an asterisk.....	60
Figure 3.15. <sup>1</sup> H NMR spectrum of M- <i>b</i> -PIBSI-TEPA .....	62
Figure 4.1. Chemical structure of <i>b</i> -PIBSI (top) and M- <i>b</i> -PIBSI (bottom).....	66
Figure 4.2. Formation of reverse micelles by an amphiphilic polymeric dispersant.....	68
Figure 4.3. Fluorescence spectra of [RuNH <sub>2</sub> ] <sub>2</sub> PF <sub>6</sub> in acetone and hexane; the peak at 520 nm for the spectrum in hexane is due to light scattering. (λ <sub>ex</sub> =452 nm) .....	70
Figure 4.4. Mass spectrometry spectrum of [RuNH <sub>2</sub> ] <sub>2</sub> PF <sub>6</sub> .....	72
Figure 4.5. Fluorescence spectra of dispersant with [RuNH <sub>2</sub> ] <sub>2</sub> PF <sub>6</sub> added, dispersant, and [RuNH <sub>2</sub> ] <sub>2</sub> PF <sub>6</sub> ; [PIBSI]=0.13 g/L, [[RuNH <sub>2</sub> ] <sub>2</sub> PF <sub>6</sub> ]= 4 μM.....	73
Figure 4.6. Time study of the fluorescence intensity of [RuNH <sub>2</sub> ] <sub>2</sub> PF <sub>6</sub> in the dispersant solution; [ <i>b</i> -PIBSI-TEPA]=1.1 g/L (top), [M- <i>b</i> -PIBSI-TEPA]=0.8 g/L (bottom); [[RuNH <sub>2</sub> ] <sub>2</sub> PF <sub>6</sub> ]=4 μM for both solutions. ....	75
Figure 4.7. CMC measurement of <i>b</i> -PIBSI-TEPA after the dispersant/[RuNH <sub>2</sub> ] <sub>2</sub> PF <sub>6</sub> solution was stirred for 5 days.....	76
Figure 5.1. Structures of MSA (left) and PIBSA (right).....	81
Figure 5.2. Chemical structures of <i>b</i> -MSI-DETA (top) and <i>b</i> -PIBSI-DETA (bottom)....	81
Figure 5.3. Chemical structures of HEDBC (top) and M- <i>b</i> -PIBSI-DETA (bottom).....	82

# List of Schemes

Scheme 2.1. Synthesis of PIBSI dispersants, $n=49$ ; $m=1, 3,$ and $4$ for DETA, TEPA and PEHA, respectively .....	16
Scheme 2.2. Reaction of MSA and DETA to yield b-MSI-DETA.....	18
Scheme 2.3 Modification of b-PIBSI with EC .....	21
Scheme 2.4. Sample Reaction of DBA and EC .....	22
Scheme 3.1. Reversible hydration and dehydration of PIBSA.....	37
Scheme 3.2. Alder-ene reaction used to synthesize PIBSA shown with one of the possible isomers.....	42
Scheme 3.3. Synthesis of b-PIBSI dispersant.....	44
Scheme 3.4. Synthesis of M-b-PIBSI .....	57

# List of Tables

Table 3.1. Polyamines used to prepare the PIBSI dispersants.....	43
Table 3.2. Apparent number-average molecular weight of PIBSA, b-PIB-DETA, and purified b-PIB-DETA obtained by using a GPC instrument calibrated with polystyrene standards .....	47
Table 3.3. $N_{SA}/N_{IB}$ ratio of PIBSA and $N_{SI}/N_{IB}$ ratios of the b-PIBSI dispersants.....	54
Table 3.4. Yield of M-b-PIBSI-DETA by conducting the modification reaction in different solvents. ....	58

## List of Abbreviations

CMC	critical micelle concentration
DETA	diethylene triamine
EC	ethylene carbonate
HEDBC	2-hydroxyethyl <i>N,N</i> -dibutyl carbamate
<i>M-b</i> -PIBSI	modified <i>bis</i> -polyisobutylene succinimide
MSA	methyl succinic anhydride
<i>b</i> -MSA	<i>b</i> -methyl succinic anhydride
PEHA	pentaethylene hexamine
PIB	polyisobutylene
PIBSA	polyisobutylene succinic anhydride
PIBSI	polyisobutylene succinimide
<i>b</i> -PIBSI	<i>bis</i> -polyisobutylene succinimide
SA	succinic anhydride
SI	succinimide
TEPA	tetraethylene pentamine
THF	tetrahydrofuran

# **Chapter 1**

## **Introduction**



## **1.1. Introduction**

This thesis deals with polymeric dispersants used as additives in engine oils. Additives are chemicals that are added to lubricating oils to enhance some desirable properties of the finished oils. Additives for lubricating oils were first used during the 1920s.<sup>1</sup> Over the years, customers have increasingly relied on automobiles resulting in an ever increasing number of requirements that lubricants are expected to meet. In turn, this led to much research effort being devoted to the improvement of improved lubricants used in automotive engines. Additives are able to improve the lubricating and aging properties of engine oil even under many severe end use conditions, such as high temperature, high pressure, and possible exposure to air.<sup>2</sup> Since their introduction in the 1920s, the use of oil additives has increased tremendously. Today, practically all types of lubricating oils contain at least one additive, and usually more than one. The amount of additive used in the oil varies from less than 1 weight percent to over 30 weight percent or more.<sup>1</sup> Among the additives commonly used in lubricants are those that inhibit oxidation, corrosion, rust, and foam formation whereas others reduce the friction between the moving part of the engine or act as pour point depressants, detergents, and dispersants.

## **1.2. Dispersants**

The research developed in this project focuses on dispersants. Dispersants are chemical compounds that disperse or suspend particulate matter generated in the engine oil that eventually leads to the formation of sludge in the engine. During the regular operation of an internal combustion engine, ultrafine particles (UFPs) are generated that have a diameter smaller than 100 nm. UFPs are either metallic or carbon-rich in nature

depending on whether they originate from engine wear or combustion, respectively.<sup>3</sup> The surface of carbon-rich particles (CRPs) is covered by polar groups. As a greater number of carbon-rich UFPs are generated through sustained use of the engine, UFPs self-aggregate into larger CRPs with a diameter greater than 1  $\mu\text{m}$  in order to minimize the exposure of the polar surface of the UFPs to the apolar oil. As the size of the CRPs increases, they precipitate out of the oil and form sludge which if not attended to results in oil blockage followed by engine failure (top panel of Figure 1).<sup>4</sup> This leads to the obvious conclusion that the presence of large CRPs in the oil must be minimized if sludge formation is to be prevented.<sup>5,6</sup>

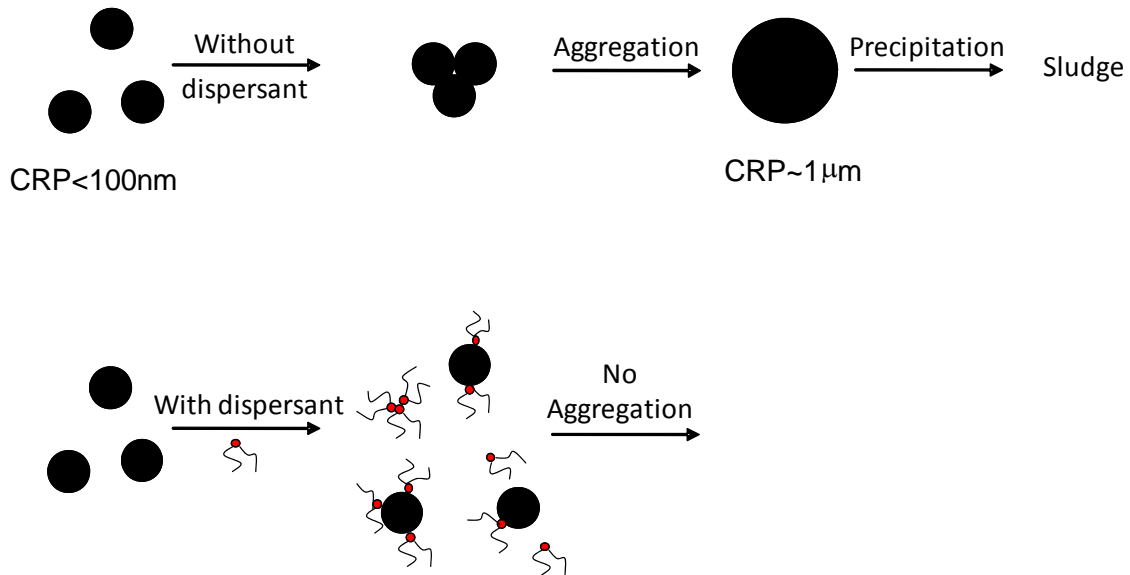


Figure 1.1. Aggregation of UFPs in engine oil without (top) and with dispersant present (bottom)

On the other hand, widespread health concerns about the adverse effect of releasing UFPs into the environment have led to ever more draconian governmental regulations that aim at reducing the release of UFPs from engines.<sup>7</sup> In order to meet those regulations, truck engine manufacturers bubble the UFPs loaded exhaust gas in the oil before releasing it to the air, further enriching the oil in sludge forming CRPs. In order to prevent sludge formation and the emission of CRPs, dispersants are introduced into the engine oil.<sup>4</sup>

The dispersant studied in this project is a polymeric amphiphile composed of two long non-polar chains and a polar core. In the engine oil, the polar core of the dispersant adsorbs onto the surface of the CRPs. As two particles coated with dispersant approach one another, interpenetration of the dispersant layer occurs. This interpenetration is accompanied by a loss of disorder in the dispersant layer that results in a decrease in entropy that disfavors interpenetration. Consequently, adsorption of the dispersant onto the CRP surface favors interparticle repulsion between the two coated particles and minimizes the aggregation of the CRPs. As a result, sludge formation is significantly reduced. On the other hand, the use of dispersant also stabilizes the CRPs in the oil which enables the emission of fewer UFPs and contributes to improving air quality while maintaining good engine oil performance.

Some of the dispersants in use today are referred to as polymeric succinimides. The preparation of succinimide dispersants was first described by Le Suer and Stuart in 1966.<sup>8-10</sup> They are based on long chain hydrocarbons which are acidified and then neutralized with a compound containing basic nitrogen. The hydrocarbon portion of the

dispersant provides oil solubility, while the nitrogen portion provides an active site that attracts and holds tightly onto the surface of CRPs to keep them suspended in the oil.

### **1.3. Micellization of Dispersants**

The presence of hydrophilic and hydrophobic moieties in the structure of dispersants leads to several interesting phenomena. One of the most important ones is their self-association to form micelles. In aqueous solution, dispersants start to aggregate above a set concentration and form micelles in which the apolar groups form the micellar core and the polar head groups are localized at the aggregate surface. In contrast, the aggregation of dispersants in apolar organic solvent results in the formation of reverse micelles in which the polar groups of the dispersants form the micellar core and the apolar tails are exposed to the solvent. The dispersant concentration at the onset of micelle formation is called the critical micelle concentration (CMC).

This project focuses on the study of the formation of the reverse micelles in the apolar solvent hexane. Reverse micelles can be viewed as aggregates of dispersants composed of a polar group and hydrocarbon-based tails. Reverse micelles are formed as the result of interactions between the dispersant polar groups due to dipole-dipole interactions and possible hydrogen bonding.<sup>11,12</sup>

The formation of reverse micelles in non polar solvents was observed later than in aqueous solutions because reverse micelles are much smaller than their water-based equivalents, resulting in less pronounced changes in the physico-chemical properties of the dispersant solution.<sup>13</sup> As a result, many techniques which are useful to study micellization in aqueous solution are not sensitive enough to characterize the aggregation

of reverse micelles. For example, surface tension which is a reliable tool for detecting aggregation in water is not used to study the micellization of dispersants in organic solvents.

Since the core of the reverse micelles is able to host polar compounds in the apolar solvent, the solubilisation of polar compounds by a dispersant solution is a strong indication of aggregate formation. Fluorescence is one of the most powerful techniques that is able to characterize reverse micelle formation. In the Duhamel laboratory, the technique has been successfully applied to study the micellization of a series of succinimide dispersants.<sup>14</sup> A chromophore insoluble in an apolar solvent was added to the dispersant solutions. As the dispersants started to form micelles, a strong fluorescence signal was detected from the dispersant solution as the chromophore was solubilised by the polar core of the reverse micelle formed. In contrast, weak or no fluorescence signal was detected at low dispersant concentration when no micelles formed. Fluorescence will be used to characterize the micellization of the dispersants that will be prepared in this thesis.

#### **1.4. Project Goal**

Traditional succinimide dispersants use polyamines for their polar core. The high basicity of the polyamine enhances the deposit control and antifouling performance of the oil.<sup>15</sup> However, a number of problems are associated with the use of polyamines.<sup>15</sup> These problems include higher viscosities that make the dispersant solution more difficult to handle, and a tendency for the viscosity of such mixtures to increase over time. In order to minimize the viscosity built up of the oil, oil is often added to the mixture, resulting in less concentrated and so less efficient additives. To reduce the problems encountered

with the use of polyamines, the polyamine core of dispersants are often modified by reacting them with ethylene carbonate or boric acid.<sup>16</sup> The modified dispersants have been shown to provide improved deposit control and antifouling performance.<sup>16</sup>

The Duhamel laboratory has investigated the micellization of a series of *bis*-polyisobutylene succinimide (*b*-PIBSI) dispersants. The dispersants were synthesized by reacting two molar equivalents of polyisobutylene succinic anhydride (PIBSA) with one molar equivalent of polyamine. The polyamines used were diethylene triamine (DETA), tetraethylene pentamine (TEPA), and pentaethylene hexamine (PEHA) (top reaction in Figure 1.2). The CMCs of the *b*-PIBSI-DETA, *b*-PIBSI-TEPA, and *b*-PIBSI-PEHA dispersants were obtained. Up to a dispersant concentration of 1 g/L, no CMC was found for *b*-PIBSI-DETA. A CMC was found for *b*-PIBSI-TEPA and *b*-PIBSI-PEHA. The adsorption of the dispersants onto carbon black particles (CBPs) was characterized. In these adsorption experiments the CBPs were used as a model of the CRPs found in the engine oil. At the dispersant concentration close to CMC a decrease in the adsorption of the dispersant onto the CBPs was observed for both *b*-PIBSI-TEPA and *b*-PIBSI-PEHA suggesting that micellization of the dispersants might hinder the adsorption of the dispersants onto the CBPs.<sup>14</sup>

In this thesis modified *bis*-polyisobutylene succinimide dispersants (*M*-*b*-PIBSI) were synthesized by reacting *b*-PIBSI with ethylene carbonate (EC) (bottom reaction in Figure 1.2). The modified dispersants have been shown to possess better dispersancy than PIBSI when used in the engine oil.<sup>16</sup> As a result, it would be interesting to determine the CMC and the adsorption isotherm of the modified dispersants and compare these results

with those obtained for the *b*-PIBSI dispersants in order to investigate whether micellization of the modified dispersants also affects the adsorption of the dispersant.

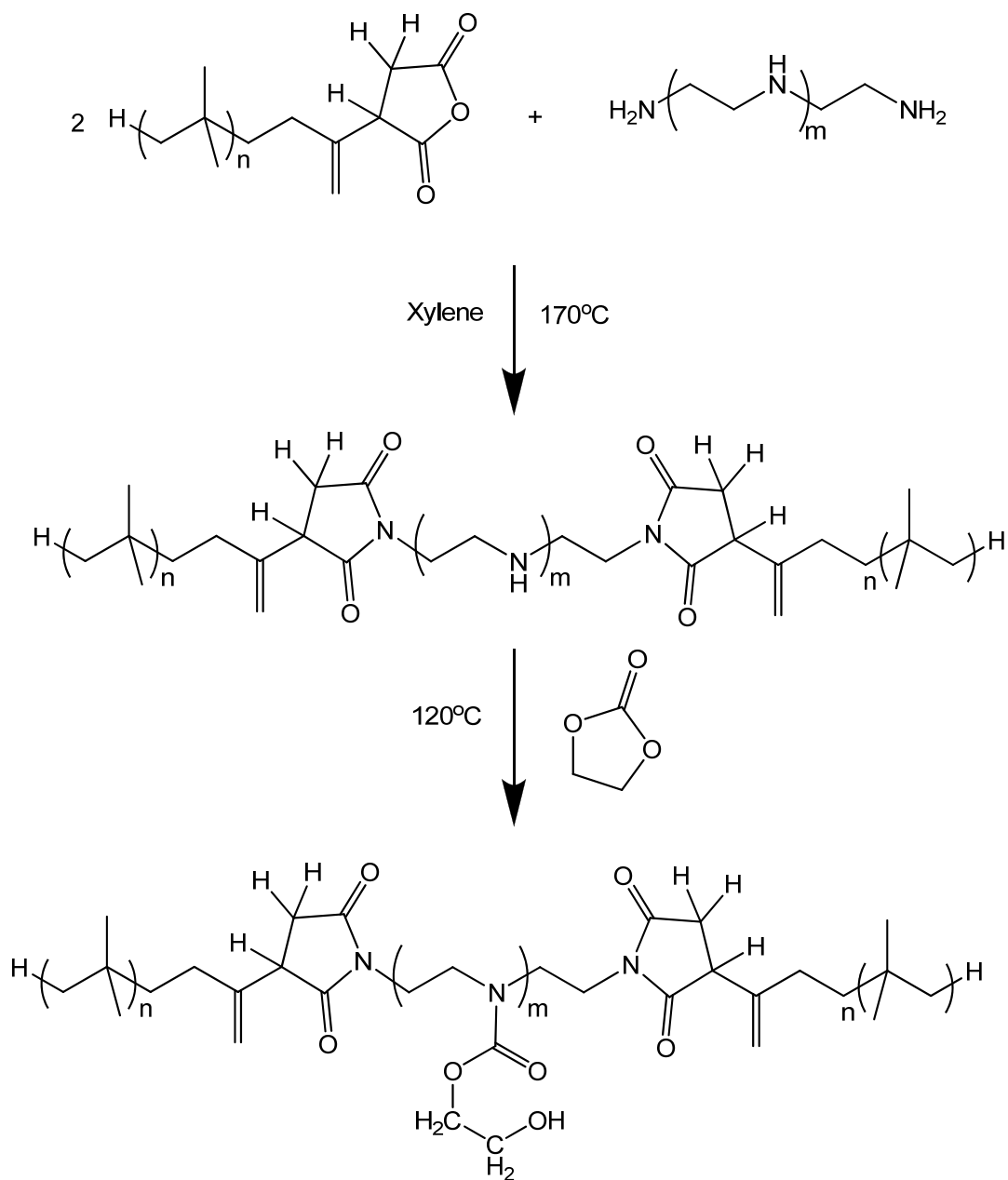


Figure 1.2. Synthesis of the M-*b*-PIBSI dispersant

In this project, *M-b*-PIBSI-DETA and *M-b*-PIBSI-TEPA were prepared. Their synthesis and characterization is described in Chapter 3. The dispersants were characterized by FT-IR and  $^1\text{H}$  NMR spectroscopy. Unfortunately, FT-IR was found to be not sensitive enough to characterize the modified dispersants. As a result,  $^1\text{H}$  NMR was used to characterize *M-b*-PIBSI dispersants. To this end, several model compounds were synthesized to assist in the assignment of the  $^1\text{H}$  NMR spectra of the dispersants. The assignment of the  $^1\text{H}$  NMR spectra of the dispersants based on the preparation of model compounds is described in Chapter 2. Chapter 4 reports on the preliminary results obtained for the determination of the CMC of the dispersants by fluorescence. Conclusions drawn from this project are given in Chapter 5, along with future work that needs to be done in order to complete the project.



## **Chapter 2**

# **Synthesis of the Model Compounds and their Use for the Assignment of the $^1\text{H}$ NMR spectra of the Dispersants**

## 2.1 Introduction

Polymers are high molecular weight molecules composed of a variety of functional groups. When modified by reacting small amounts of a foreign molecule, characterization of the extent to which the polymer has been modified is made difficult by the relatively much weaker signal emanating from the foreign molecule now covalently attached to the polymer. Assignment of the NMR chemical shifts of the protons of the foreign molecule used to modify the polymer is facilitated by synthesizing relevant model compounds.

The polymer studied in this project was prepared by first reacting two molar equivalents of polyisobutylene succinic anhydride (PIBSA) with one molar equivalent of polyamine to synthesize *bis*-polyisobutylene succinimide (*b*-PIBSI).<sup>1</sup> *b*-PIBSI was modified by reacting its polyamine core with ethylene carbonate (EC) to yield modified *b*-PIBSI (M-*b*-PIBSI).<sup>2</sup>

At the early stage of the project, the <sup>1</sup>H NMR peaks in the NMR spectrum of the modified (M-*b*-PIBSI) and unmodified (*b*-PIBSI) dispersants were difficult to assign. The number of protons of the isobutylene (IB) monomers is significantly larger than the number of protons found in the polar core of the dispersants making them difficult to detect. To facilitate the assignment of the chemical shift of the core protons, several model compounds were prepared that would mimic the polar core of the dispersants. The <sup>1</sup>H NMR spectra of the model compounds were obtained to be used as references for the polymer spectra. The chemical shift of the protons of the model compounds were expected to be similar to that of the dispersant protons. The <sup>1</sup>H NMR peaks characteristic of the dispersants were generally broader since the dispersants are larger and tumble

more slowly than the model compounds. Nevertheless comparison of the model compounds to those of the dispersants enabled the assignment of the  $^1\text{H}$  NMR peaks of the dispersant polar core.

This chapter describes the synthesis of the model compounds used to mimic the polar core of one type of *b*-PIBSI dispersant and its modified equivalent. The  $^1\text{H}$  NMR spectra of the model compounds were then acquired and used to assign the  $^1\text{H}$  NMR spectra of PIBSA and of the unmodified and modified *b*-PIBSI dispersants.

## **2.2 Experimental Procedures**

### **2.2.1 Chemicals**

The solvents xylene (reagent grade, 98.5%, EMD), hexane (HPLC grade, Caledon), acetone (HPCL grade, Caledon), ethyl ether (reagent grade, Caledon), and ethyl acetate (HPLC grade, Caledon) were used as received.

Diethylene triamine (DETA) (99%, Sigma-Aldrich), methyl succinic anhydride (MSA) (98%, Aldrich), dibutylamine (DBA) (99.5%, Sigma-Aldrich) and ethylene carbonate (98%, Sigma-Aldrich) were used as received.

### **2.2.2 Instrumentation: Nuclear Magnetic Resonance (NMR)**

The  $^1\text{H}$  NMR spectra of the samples were obtained with Bruker 300 MHz high resolution NMR spectrometer. Deuterated chloroform (99.8%, Cambridge Isotope Laboratory Inc.) was used as the solvent. The sample concentration used to acquire the polymer spectra was equal to or greater than 30 mg/mL.

### 2.3 Assignment of the peaks in the $^1\text{H}$ NMR spectrum of PIBSA.

PIBSA is composed of a polyisobutylene (PIB) apolar chain capped at one end with a succinic anhydride (SA) group (Figure 2.1, Compound B). The ratio of the number of IB units over the number of SA groups was found to equal 49:1 by FT-IR. How this ratio was obtained will be described in more details in Chapter 4. Since the number of IB units was significantly larger than the number of SA groups, the IB protons in the  $^1\text{H}$  NMR spectrum of PIBSA yielded strong signals while the protons of the SA groups resulted in a weaker signal that was more difficult to monitor. To assign the accurate chemical shift of the SA proton peaks of PIBSA in the  $^1\text{H}$  NMR spectrum, the  $^1\text{H}$  NMR spectrum of methyl succinic anhydride (MSA, Figure 2.1, Compound A, purchased from Sigma-Aldrich) was acquired. It is shown in Figure 2.2.

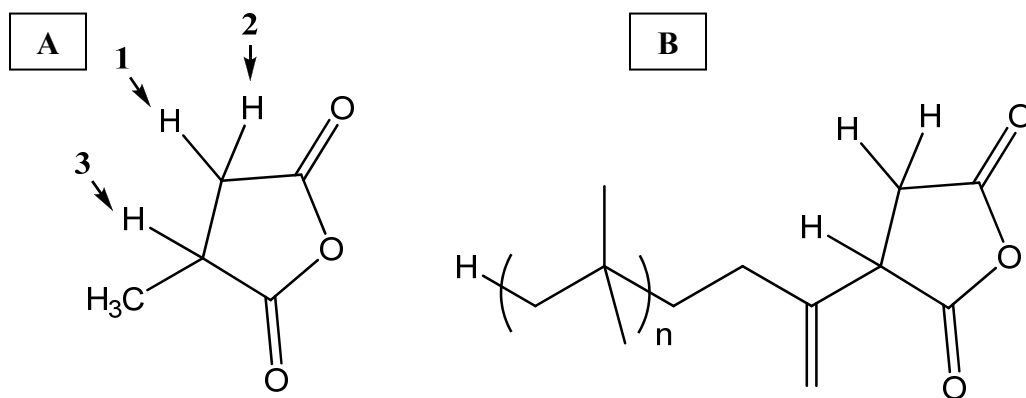


Figure 2.1. Structures of MSA (A) and PIBSA (B)

MSA and PIBSA both contain identical SA groups although. The SA rings of MSA and PIBSA are substituted with a methyl group and a long PIB chain via an

isobutylene linker, respectively. The  $^1\text{H}$  NMR spectrum of MSA in Figure 2.2 was obtained in deuterated chloroform. Since proton **1** and **2** are diastereotopic, the two protons do not have the same chemical shift. Proton **1** is doubled by proton **2** and **3**, so that its peak appears at 2.6 ppm as a doublet of doublet, and the small peaks in the center are due to the virtual coupling of the methyl group. Proton **3** is strongly deshielded by the methyl group, and its proton peak appears at 3.2 ppm. Due to the rigid ring structure, and the complexity of the shielding and deshielding of the carbonyl group, proton **2** gives a peak at 3.2 ppm which overlaps with that of proton **3**. The doublet at 1.45 ppm represents the protons of the methyl group. The single peaks at 1.5 and 7.25 ppm represent the water and chloroform protons, respectively. Since PIBSA possesses the same protons **1**, **2**, and **3** as MSA, the peaks located at 2.5 and 3.5 ppm were expected to be found in the  $^1\text{H}$  NMR spectrum of PIBSA.

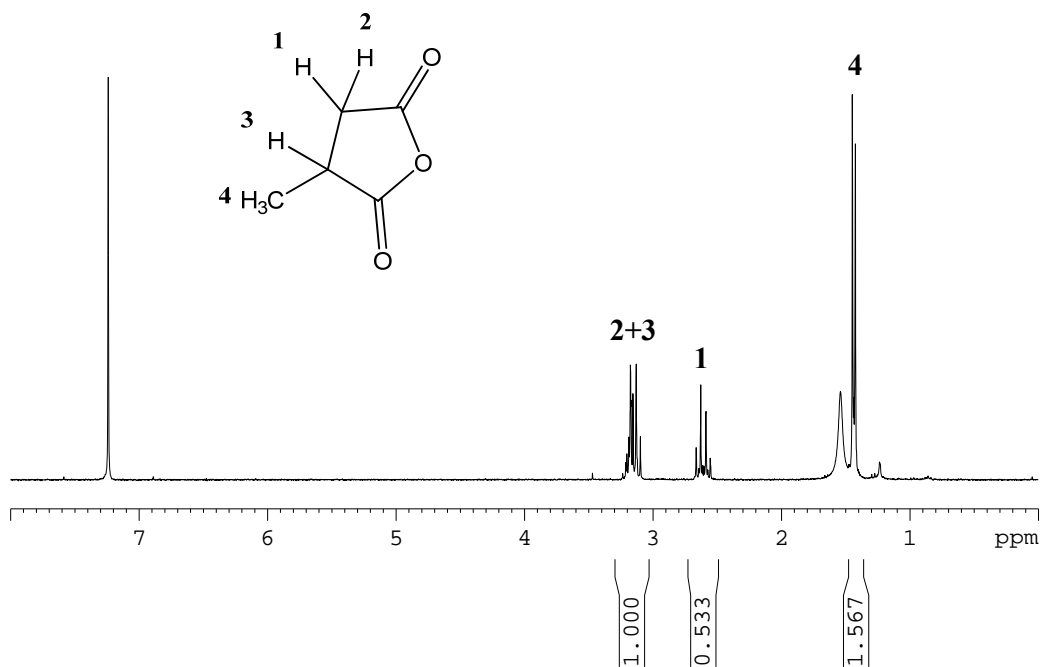


Figure 2.2.  $^1\text{H}$  NMR spectrum of MSA (300 MHz,  $\text{CDCl}_3$ )

The  $^1\text{H}$  NMR spectrum of PIBSA is shown in Figure 2.3. Two large peaks appeared at 1.1 and 1.5 ppm with a 3:1 ratio. These peaks represent the protons of the IB units in the polyisobutylene chain of PIBSA.

Since the ratio of IB to SA was found to be 49:1 for PIBSA, the signal of SA protons was expected to be significantly smaller than that of the IB protons. In order to improve the SA proton signal, the PIBSA spectrum was magnified in the insert of Figure 2.3. The SA proton peaks were clearly visible in the magnified spectrum. They appeared at 2.6 and 3.3 ppm, close to the chemical shifts of 2.6 and 3.2 ppm found for the protons on the SA ring of MSA (Figure 2.2).

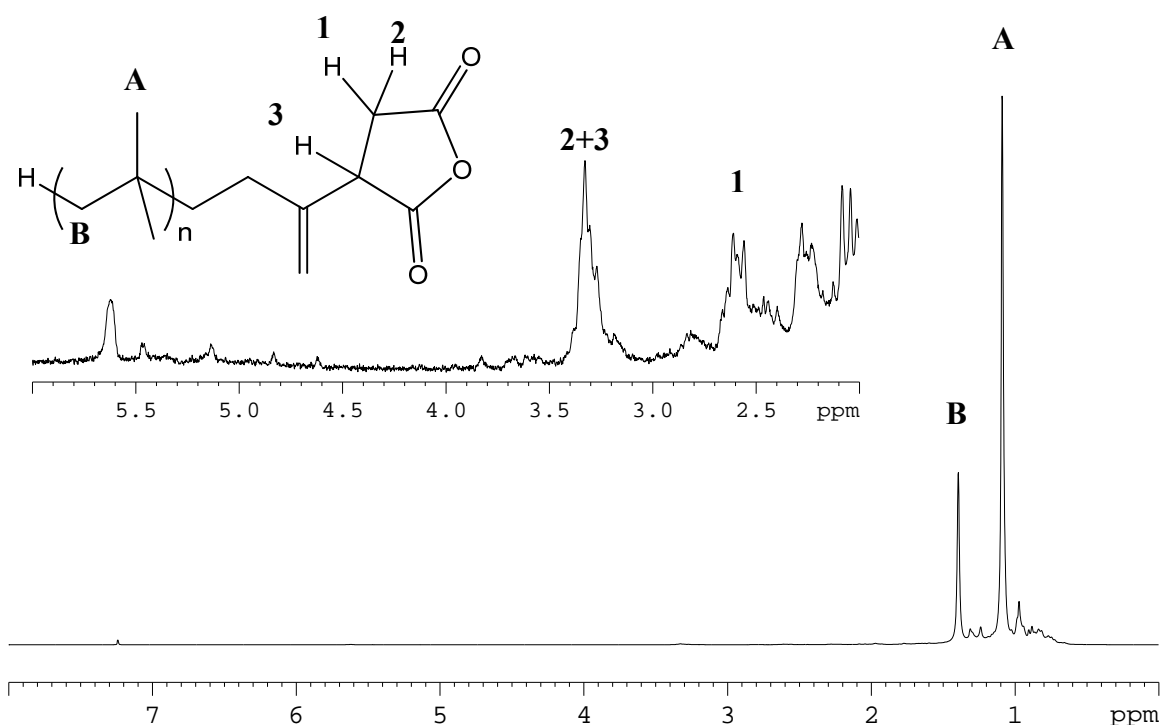
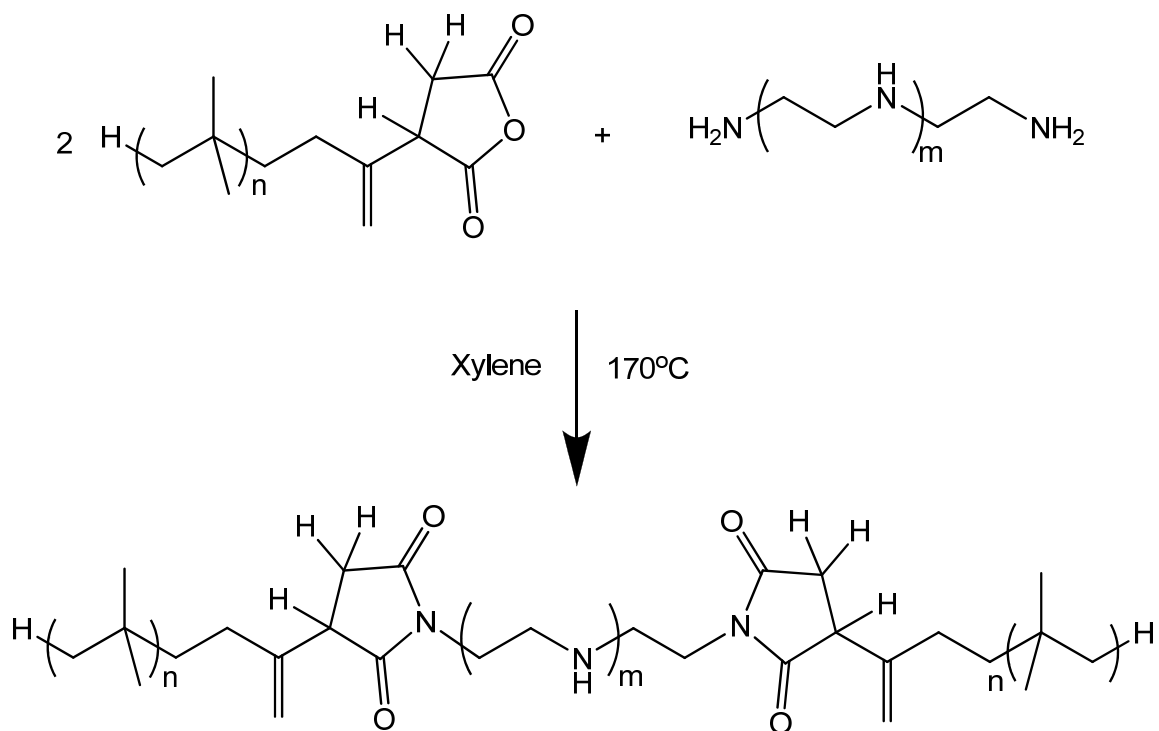


Figure 2.3.  $^1\text{H}$  NMR spectrum of PIBSA (300MHz,  $\text{CDCl}_3$ )

## 2.4. Sample reaction of methyl succinic anhydride with diethylenetriamine

In a previous study done in the Duhamel laboratory on PIBSI dispersants, FT-IR was used to characterize the structure of the dispersants. However, the technique is not sensitive enough to detect the modification of the PIBSI dispersants and even worse to quantify its extent. In order to monitor the degree of modification of the *b*-PIBSI dispersants,  $^1\text{H}$  NMR was used. The *b*-PIBSI dispersants studied in this project were composed of two apolar chains linked via a polar core. Their synthesis involves the reaction of two molar equivalents of PIBSA with one molar equivalent of polyamine as shown in Scheme 2.1. <sup>1</sup>



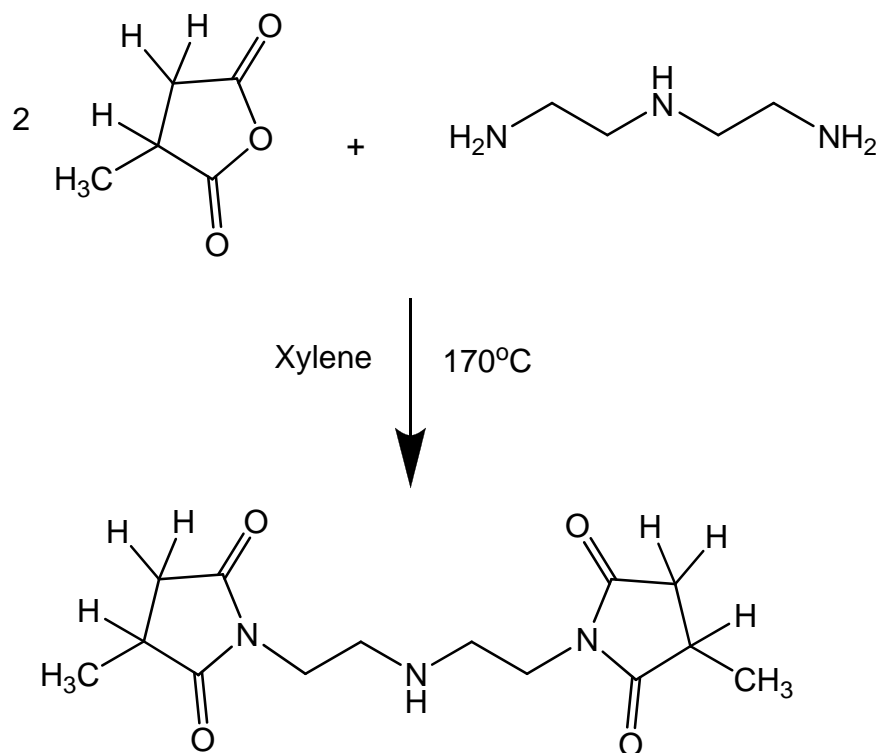
Scheme 2.1. Synthesis of PIBSI dispersants,  $n=49$ ;  $m=1, 3,$  and  $4$  for DETA, TEPA and PEHA, respectively

Depending on whether diethylene triamine (DETA), tetraethylene pentamine (TEPA), or pentaethylene hexamine (PEHA) is used, the number of secondary amines in the polymer core is different. The amine proton is usually broad and hard to quantify due to quadrupolar relaxation by  $^{14}\text{N}$ .<sup>2</sup> In order to minimize the number of the amine protons in the  $^1\text{H}$  NMR spectra, the *b*-PIBSI-DETA dispersant which contains only one secondary amine in its polar core was selected for this study. Assignment of the proton peaks found in the polar core of *b*-PIBSI-DETA was enabled by acquiring the  $^1\text{H}$  NMR spectrum of *b*-methyl succinimide-DETA which was synthesized in the laboratory as a model compound.

#### 2.4.1 Synthesis of *bis*-methyl succinimide-DETA

*bis*-Methyl succinimide-DETA (*b*-MSI-DETA) was prepared by reacting 2 molar equivalents of MSA with one molar equivalent of DETA in xylene at 170 °C according to Scheme 2.2. A typical reaction proceeded as follows. MSA (0.5 g, 4.4 mmol) and DETA (0.23 g, 2.2 mmol) were dissolved in 10 mL of xylene. The reaction mixture was added in a two neck round bottom flask, onto which a water condenser with a nitrogen inlet and outlet was mounted. The reaction mixture was heated in an oil bath at 170 °C for 20 hours.





Scheme 2.2. Reaction of MSI and DETA to yield *b*-MSI-DETA

#### 2.4.2. Purification of *b*-MSI-DETA

After the reaction, 50 mL of xylene were added to the 10 mL reaction mixture. The 60 mL solution was washed separately with 10 mL of 0.5 M HCl solution, 10 mL of 0.5 M NaHCO<sub>3</sub>, and 10 mL of Milli-Q water. Each extraction was repeated three times in order to remove most of the unreacted DETA. The organic fraction was collected. After the extractions were completed, xylene was removed with a rotary evaporator and the product was dried in a vacuum oven. Since *b*-MSI-DETA is water soluble, the isolated yield of the extraction was low around 10%.

### 2.4.3. Assignment of the proton peaks in the $^1\text{H}$ NMR spectra of *b*-MSI-DETA and *b*-PIBSI-DETA

The  $^1\text{H}$  NMR spectrum of *b*-MSI-DETA is shown in Figure 2.4. Comparison of the  $^1\text{H}$  NMR spectra of MSA and *b*-MSI-DETA indicates that the peaks at 2.6 and 3.3 ppm in the spectrum of MSA shifted to respectively 2.3 and 2.9 ppm in the  $^1\text{H}$  NMR spectrum of *b*-MSI-DETA. Since oxygen in the SA ring was substituted by nitrogen which is less electron negative, the protons on the SA group shifted to lower frequency.

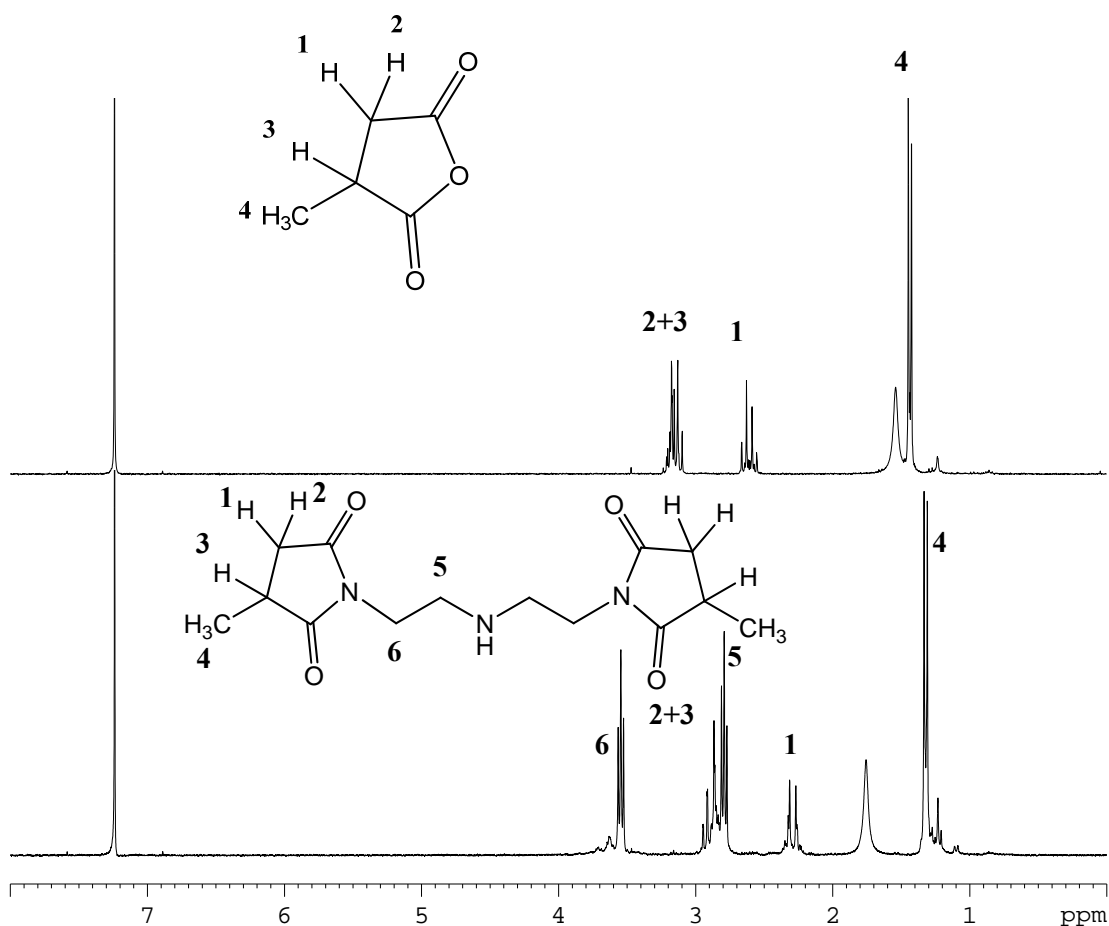


Figure 2.4.  $^1\text{H}$  NMR spectrum of MSA (upper) and *b*-MSI-DETA (lower) (300 MHz,  $\text{CDCl}_3$ )

Meanwhile, two symmetric triplets appeared in the spectrum of *b*-MSI-DETA at 2.8 ppm and 3.55 ppm. These two peaks represented the protons **5** and **6** of the ethylene segments in the core of *b*-MSI-DETA.

The spectra of *b*-MSI-DETA and *b*-PIBSI-DETA are compared in Figure 2.5. Using the spectrum of *b*-MSI-DETA as reference, the peaks at 2.5 and 3.0 ppm were assigned to the protons on the SA ring, and the peaks at 2.7 and 3.5 ppm to the protons on the ethylene segments in the polar core of *b*-PIBSI-DETA.

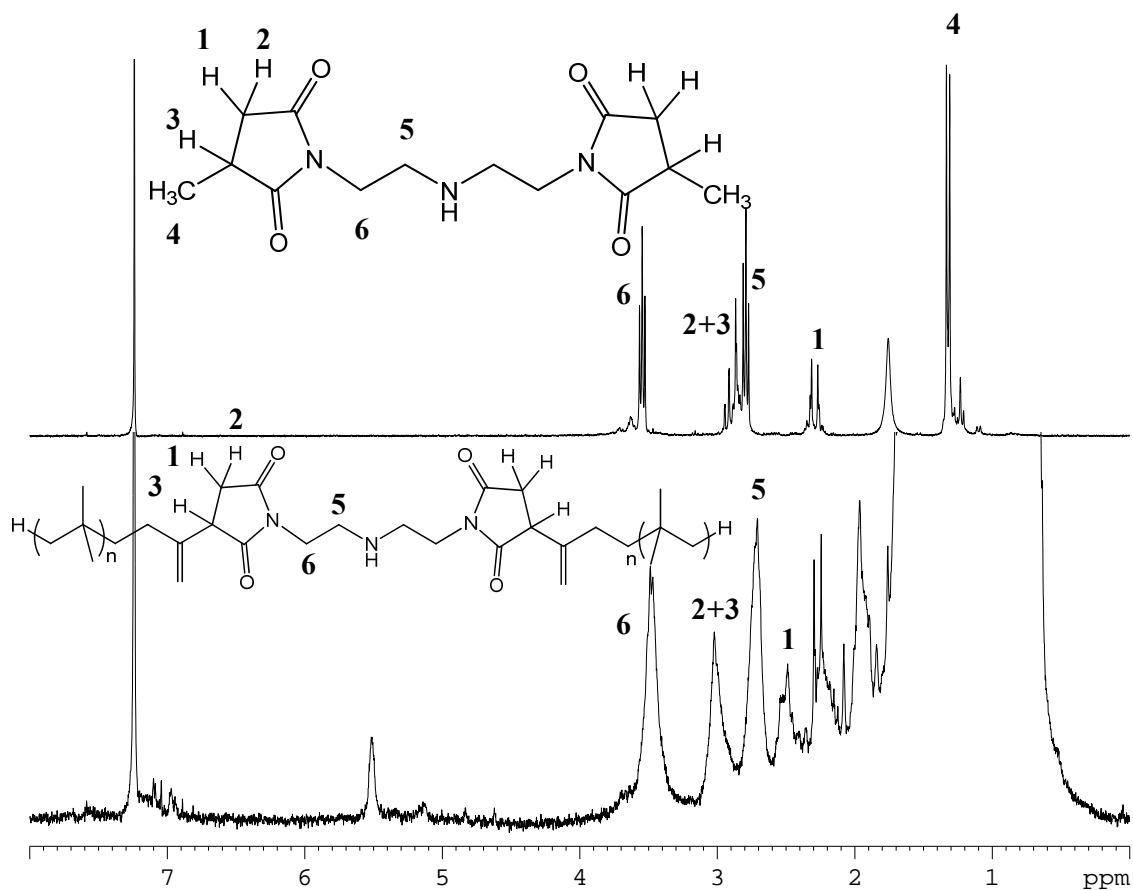
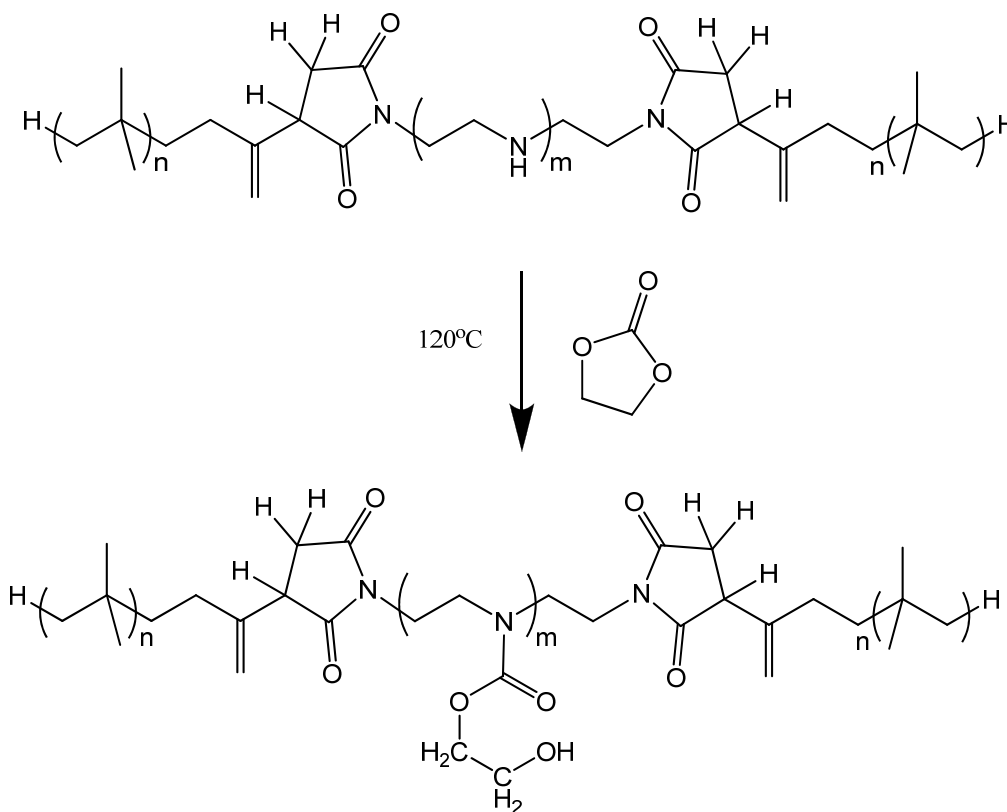


Figure 2.5. <sup>1</sup>H NMR spectra of *b*-MSI-DETA (top) and *b*-PIBSI-DETA (bottom) (300 MHz, CDCl<sub>3</sub>)

## 2.5. Synthesis of 2-hydroxyethyl *N,N*-dibutyl carbamate

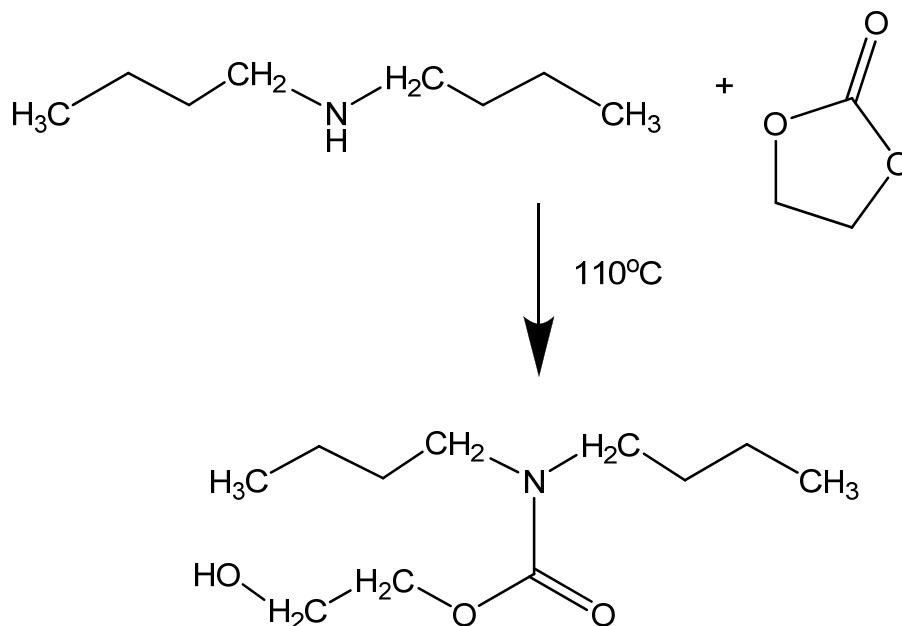
As the  $^1\text{H}$  NMR spectra of PIBSA and *b*-PIBSI-DETA were assigned, another model compound was prepared to assign the proton peaks in the  $^1\text{H}$  NMR spectrum of *M-b*-PIBSI-DETA. The modified dispersant was synthesized by reacting PIBSI with ethylene carbonate (EC) following Scheme 2.3. The proton on the secondary amine in the core of PIBSI-DETA was substituted by a carbamate side chain (Scheme 2.3).<sup>3</sup> Assignment of the new proton peaks that appeared in the  $^1\text{H}$  NMR spectrum was achieved by comparison with the  $^1\text{H}$  NMR spectrum obtained for the model compound 2-hydroxyethyl *N,N*-dibutyl carbamate which was synthesized in the laboratory.



Scheme 2.3 Modification of *b*-PIBSI with EC

### 2.5.1. Synthesis of 2-hydroxyethyl *N,N*-dibutyl carbamate

2-Hydroxyethyl *N,N*-dibutyl carbamate was prepared by reacting 1 molar equivalents of dibutylamine (DBA) and ethylene carbonate (EC) according to Scheme 2.4.



Scheme 2.4. Sample Reaction of DBA and EC

DBA (3.0 g, 23.8 mmol) and EC (2.1 g, 23.8 mmol) were added in a two neck round bottom flask which was mounted with a water condenser and a nitrogen inlet and outlet. The reaction was carried out without solvent at 110 °C for 20 hours. The spectrum of the product mixture is shown in Figure 2.6. It confirmed that unreacted DBA and EC remained in the mixture, but also that new peaks appeared. The methylene protons in the carbamate side chain were expected to be those at 3.8 and 4.2 ppm.

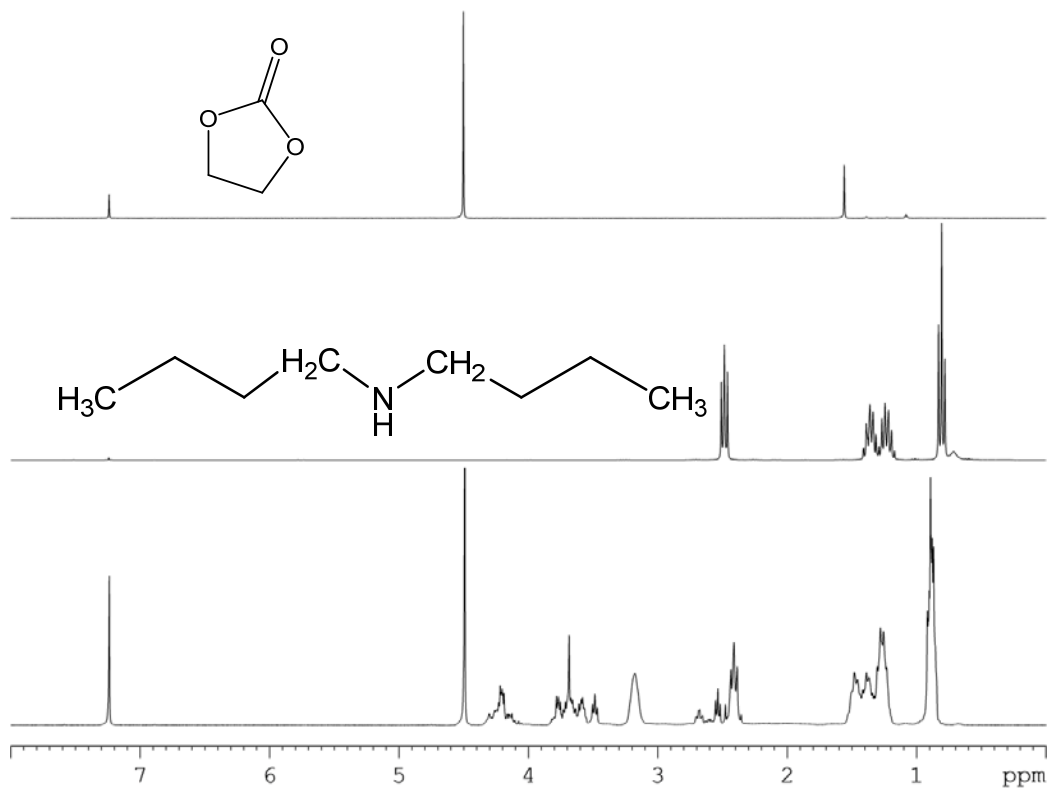


Figure 2.6.  $^1\text{H}$  NMR spectra of EC (top), DBA (middle), and the reaction product (bottom) (300 MHz,  $\text{CDCl}_3$ )

However, other unknown peaks were present in the spectrum, which suggested the existence of side products, one of them being 2-(dibutylamino)ethanol (DBAE) whose structure is shown in Figure 2.7.

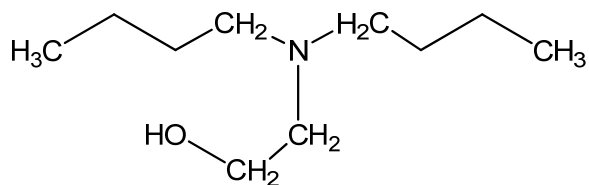


Figure 2.7. Chemical structure of 2-(dibutylamino)ethanol

### 2.5.2. Purification of 2-hydroxyethyl *N,N*-dibutyl carbamate

With their tertiary and secondary amine, DBAE and unreacted DBA behave as bases, while the carbamate product is neutral. Extractions were performed to separate the two species. The product mixture was dissolved in 50 mL of ethyl ether, and extracted with 50 mL of 1 M HCl aqueous solution. Upon mixing, DBA and DBAE were protonated and dissolved in the water phase. EC being water-soluble was also removed from the organic fraction after the extraction, and the carbamate product which was not acid soluble remained in the ether fraction. Magnesium sulfate anhydrous was used to dry the ether fraction and was removed by filtration afterward. The solvent was evaporated, and the  $^1\text{H}$  NMR spectrum was obtained (Figure 2.8).

The water fraction with protonated amines was neutralized with a 5 M NaOH solution. The aqueous solution of DBA and DBAE was mixed with ethyl ether to extract the deprotonated DBA and DBAE into the ether layer. The organic phase was dried and the solvent was removed. The  $^1\text{H}$  NMR spectra of the basic and neutral products are shown in Figure 2.8.

Several peaks found in the spectrum of the neutral products in Figure 2.8 indicated the presence of 2-hydroxyethyl *N,N*-dibutyl carbamate (HEDBC), however, side products were also observed.

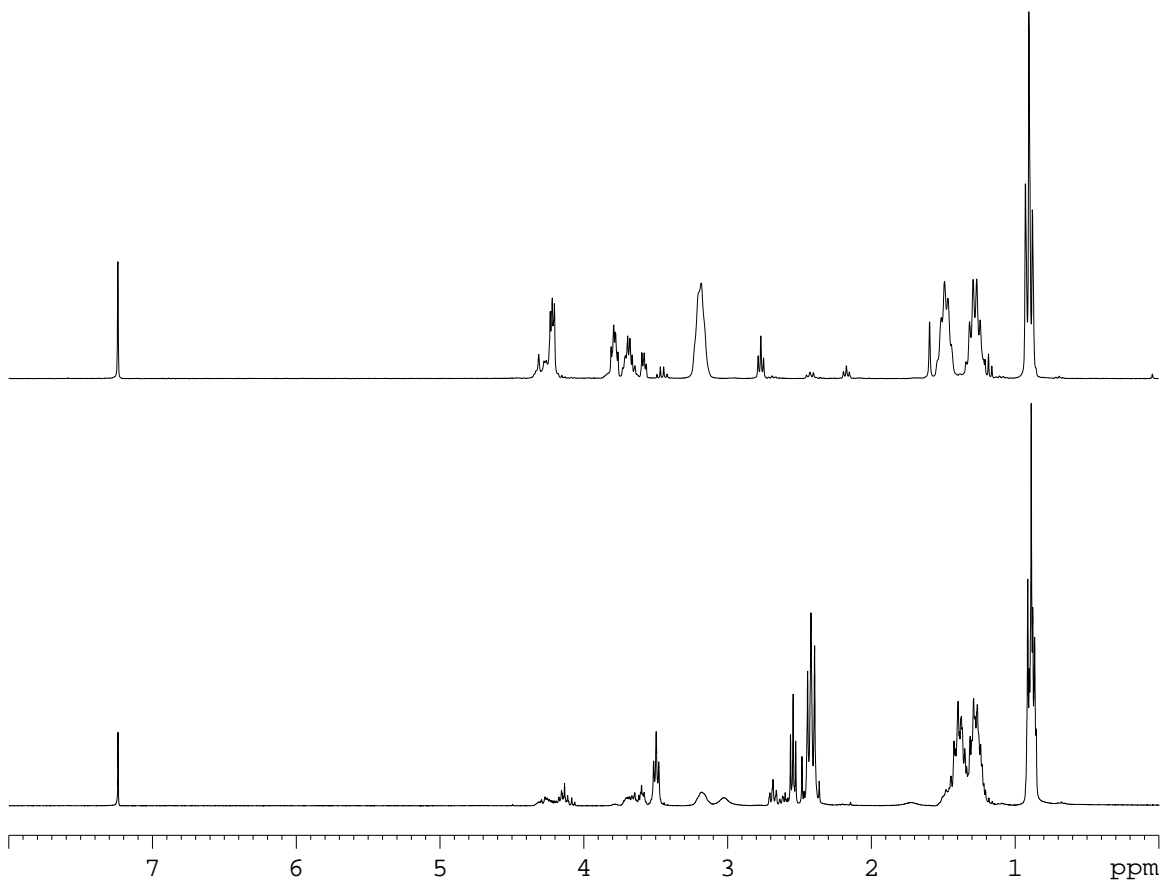


Figure 2.8.  $^1\text{H}$  NMR spectra of neutral (top) and basic products (bottom) of the reaction shown in Scheme 2.4 (300 MHz,  $\text{CDCl}_3$ )

In order to separate the side products from the HEDBC product, column chromatography was performed. A 1:1 ratio of ethyl acetate (EA) and hexane solution was used as the eluent, and the products were separated. Three different compounds were found in the neutral product mixture. The spectra are shown in Figure 2.9. The chemical structure of the compounds obtained after separation via column chromatography of the reaction mixture was determined from the NMR spectra. They are also shown in Figure 2.9.



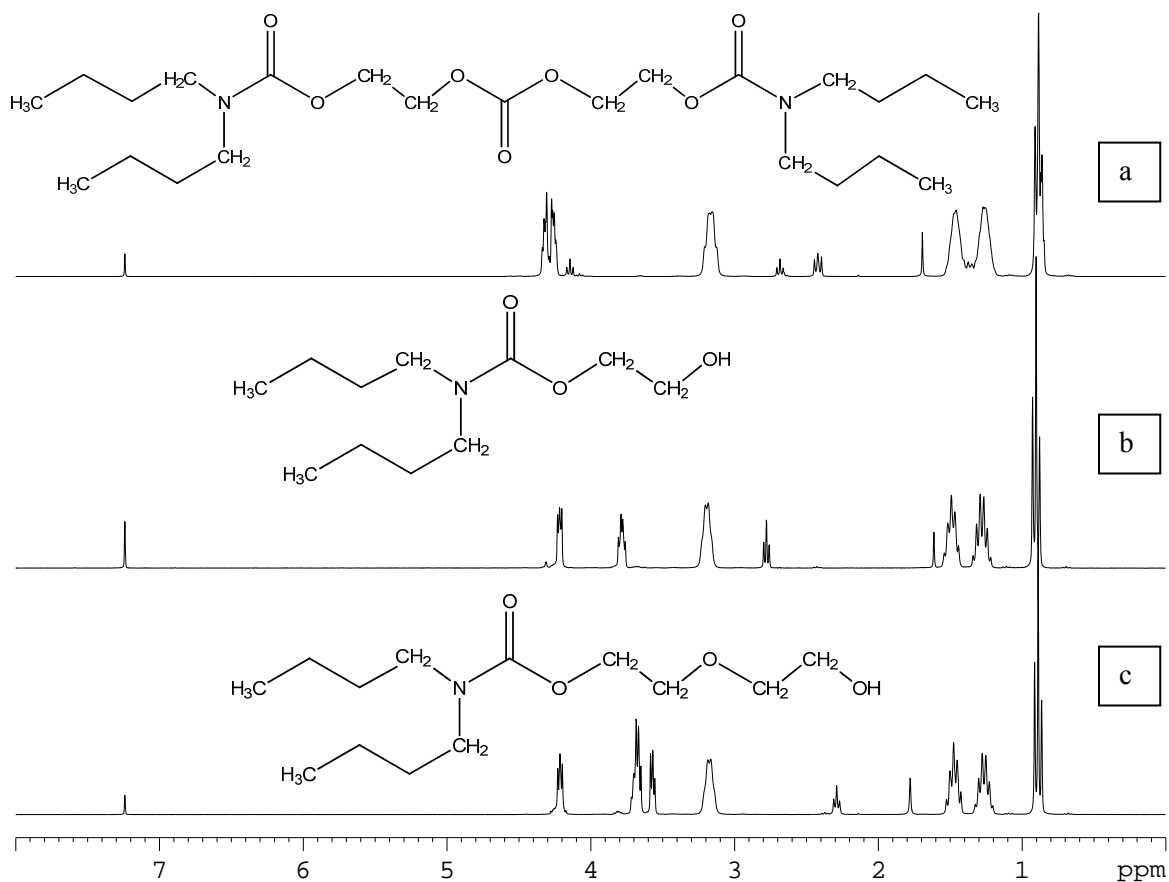


Figure 2.9.  $^1\text{H}$  NMR spectra of the neutral products found in the reaction mixture (300 MHz,  $\text{CDCl}_3$ )

Product “a” was a HEDBC dimer linked by an ethylene carbonate unit. Product “b” was the expected HEDBC product. Product “c” was a HEDBC derivative bearing an extra glycol group. The yield of HEDBC was 19%. Unfortunately, the yields of the side products were not recorded.

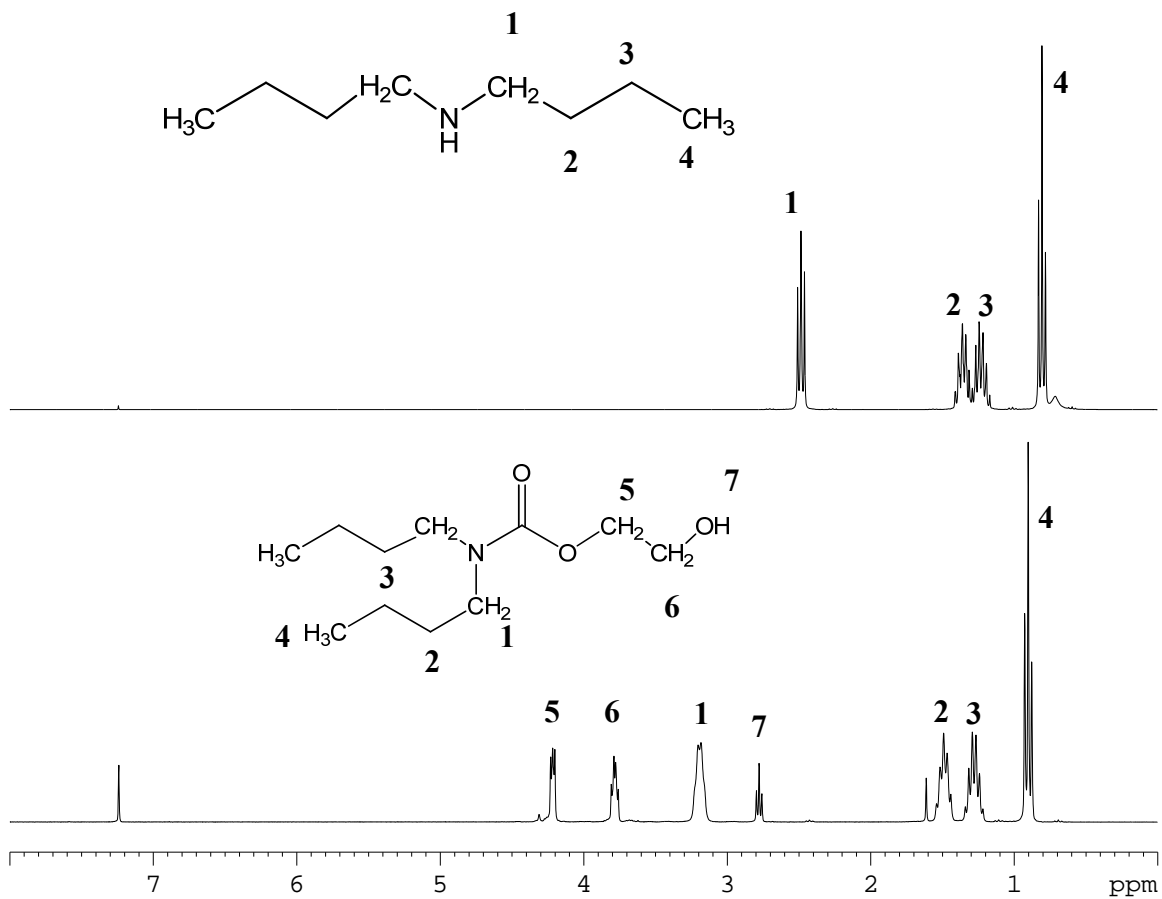


Figure 2.10. Comparison of the  $^1\text{H}$  NMR spectra of DBA and HEDBC (300 MHz,  $\text{CDCl}_3$ )

Comparison of the spectra of DBA and HEDBC is shown in Figure 2.10. The spectra indicate that the peak of the butyl protons  $\alpha$  to the nitrogen is shifted from 2.5 to 3.15 ppm. It is also broader since the amine proton of DBA is substituted by a carbamate group in HEDBC. New peaks appeared at 2.8, 3.8, and 4.2 ppm representing the alcohol proton, the methylene protons  $\alpha$  to the alcohol, and  $\beta$  to the alcohol, respectively.

### 2.5.3. Dilute sample reaction

*b*-PIBSI-DETA dispersant was found to be composed of succinimide and isobutylene units in a 1:30 ratio. As a result, the modification reaction of *b*-PIBSI-DETA occurs under conditions that are more dilute compared to those of the sample reaction shown in Scheme 2.4. In order to mimic the conditions used for the PIBSI modification more closely, HEDBC was synthesized in the presence of xylene as the solvent.

DBA (2.0 g, 15.9 mmol) and EC (1.4 g, 23.8 mmol) were dissolved in 35 mL of xylene, and the mixture was added in a two neck round bottom flask capped with a condenser. The reaction was carried out under nitrogen at 110 °C for 20 hours. The product was separated by extraction as described in section 2.3.2. The <sup>1</sup>H NMR spectra of the neutral and basic reaction products are shown in Figure 2.11. Xylene was used as the diluent in the reaction, and it appeared to possess a boiling point similar to that of the neutral products. As a result, the spectrum of the neutral products was taken with xylene present.

The <sup>1</sup>H NMR spectrum of the neutral products found in the ether layer showed two peaks at 3.8 and 4.2 ppm. In Figure 2.11, no peaks appeared at 3.55, 3.6 or 4.3 ppm as the proton peaks of compound **c** and **a** shown in Figure 2.9. This spectrum demonstrates that none of the side products found when HEDBC was synthesized without xylene as solvent was present in the ether layer. The spectrum of the basic product was identical to that of DBA, which proved that no 2-(dibutylamino)ethanol side product was generated when the reaction was conducted under dilute conditions.

In conclusion, the reaction of DBA with EC under dilute conditions seems to yield HEDBC as the only product. This result suggests that a single reaction product might be obtained when reacting a *b*-PIBSI dispersant with ethylene carbonate.

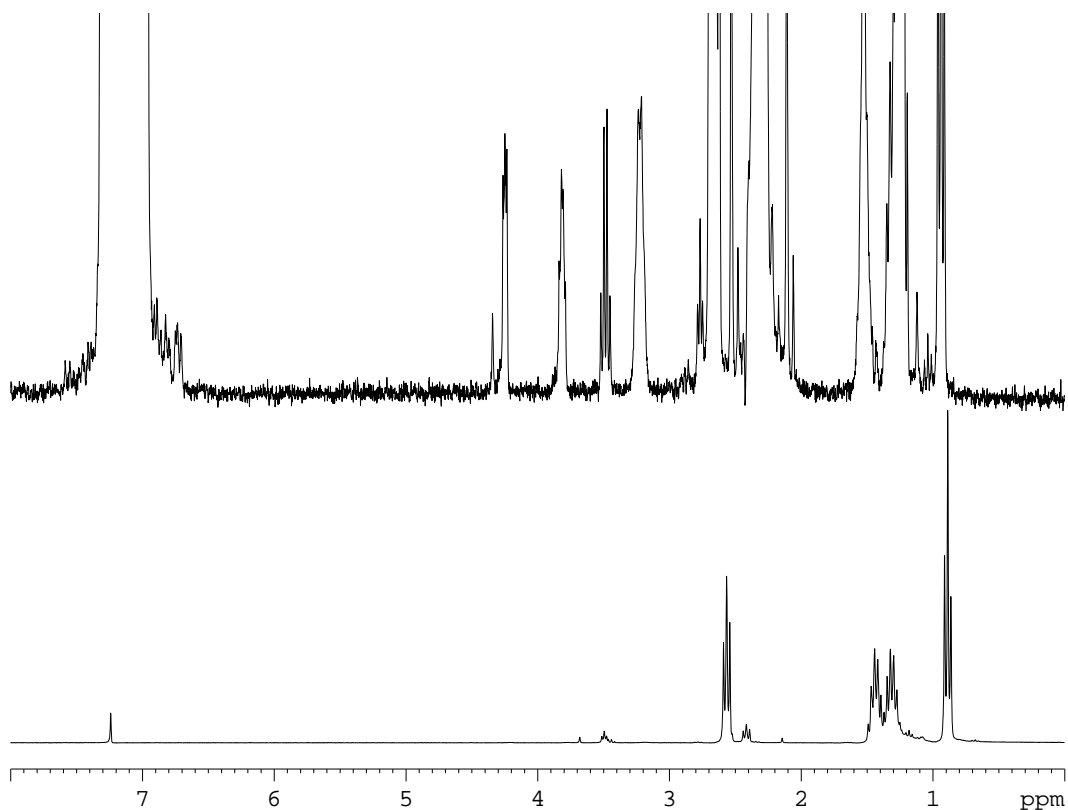


Figure 2.11.  $^1\text{H}$  NMR spectra of the neutral (top) and the basic products (bottom) obtained during the synthesis of HEDBC under dilute conditions (300 MHz,  $\text{CDCl}_3$ )

#### 2.5.4. Assignment of the $^1\text{H}$ NMR spectrum of HEDBC and *M-b*-PIBSI-DETA

The  $^1\text{H}$  NMR spectrum of *M-b*-PIBSI-DETA is presented in Figure 2.12 with that of HEDBC. The two peaks at 3.8 and 4.1 ppm found in the NMR spectrum of *M-b*-PIBSI-DETA correspond to the methylene protons in the carbamate side chain, with a chemical shift similar to that of 3.8 and 4.2 ppm found in the NMR spectrum of HEDBC.

The peak at 4.1 ppm in the NMR spectrum of M-*b*-PIBSI-DETA is relatively well-resolved and will be used to determine the level of modification of the modified succinimide dispersants. The small peak at 4.2 ppm might be due to the polymerized ethylene carbonate. However it is small, so it does not have a strong effect on the integration of the 4.1 ppm peak.

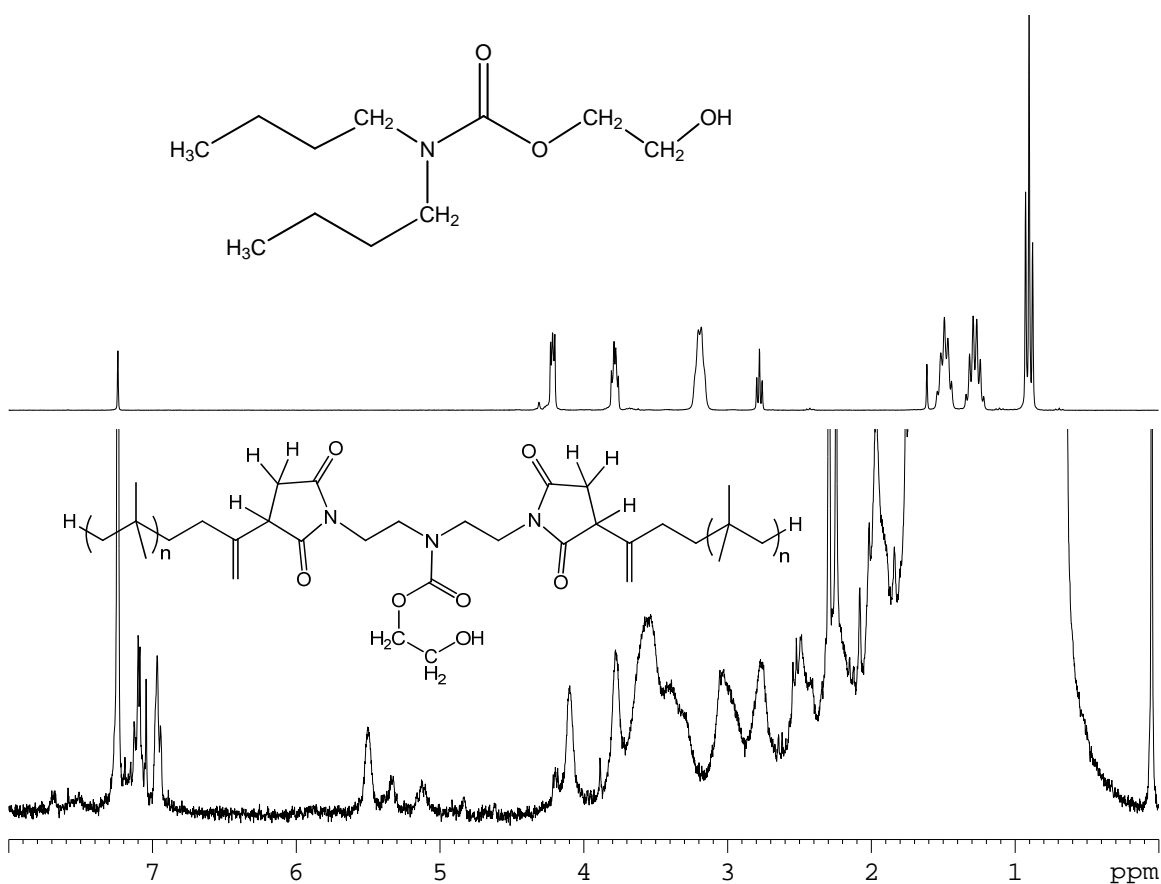


Figure 2.12. <sup>1</sup>H NMR spectra of HEDBC (top) and M-*b*-PIBSI-DETA (bottom) (300 MHz, CDCl<sub>3</sub>)

## 2.6. Summary of $^1\text{H}$ NMR spectra

PIBSA was used as the starting material in the synthesis of M-*b*-PIBSI-DETA. PIBSA reacted with DETA to produce *b*-PIBSI-DETA which was reacted with EC to form the M-*b*-PIBSI-DETA. The spectra of PIBSA, *b*-PIBSI-DETA, and M-*b*-PIBSI-DETA are shown in Figure 2.13.

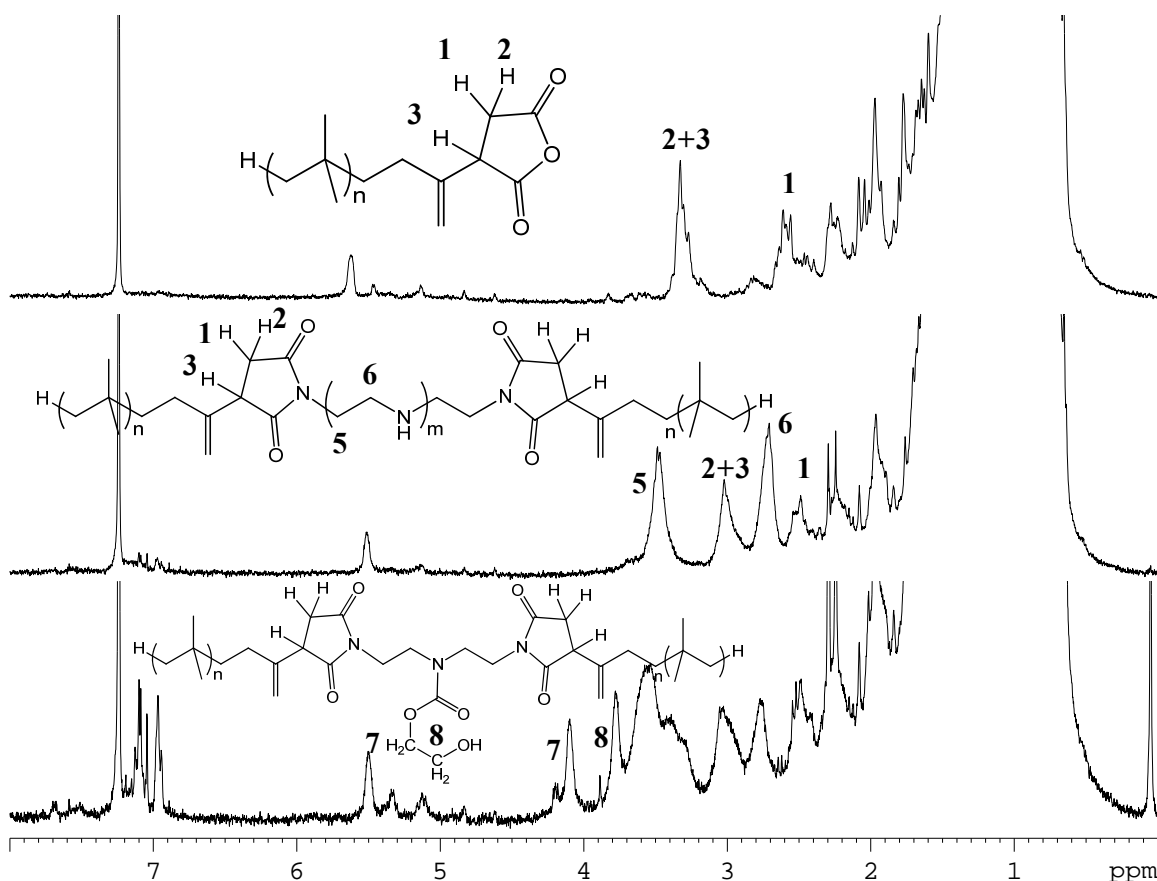


Figure 2.13.  $^1\text{H}$  NMR spectra of PIBSA (top), *b*-PIBSI-DETA (middle), and M-*b*-PIBSI-DETA (bottom)

In the spectrum of PIBSA, the peaks at 2.6 and 3.3 ppm represent the protons in the succinic anhydride ring. After the reaction with polyamine, these peaks shifted to 2.5 and 3.0 ppm, and new peaks appeared at 2.7 and 3.5 ppm representing the ethylene protons in the polar core of PIBSI. As PIBSI was modified by reaction with EC, the peak at 2.7 ppm was reduced, and the peak at 3.5 ppm was enlarged as the environment of the methylene protons in the  $\alpha$  position to the central carbamate became similar to that of the methylene protons in the  $\alpha$  position to the succinimide groups. Also, the two new peaks representing the modified carbamate side chain methylene protons appeared at 3.8 and 4.1 ppm. The peaks around 7 ppm in the bottom spectrum in Figure 2.13 are due to the presence of residual xylene. The peaks at 5.5 ppm is found in all polymer samples and might be due to the presence of vinyl groups generated during the Alder-Ene reaction of PIBSA.<sup>4,5</sup>

## **Chapter 3**

# **Synthesis and Characterization of Modified Polyisobutylene Succinimide Dispersants**



### 3.1 Introduction

Modified polyisobutylene succinimide (M-PIBSI) dispersants used in engine oils exhibit a better dispersancy capability than the unmodified polyisobutylene succinimide (PIBSI) dispersants. M-PIBSI is derived from PIBSI by substituting some of the secondary amine protons of the dispersant polyamine core with a carbamate ethanol side chain.<sup>1</sup> An earlier study from the Duhamel Laboratory has characterized *bis*-polyisobutylene succinimide (*b*-PIBSI) dispersants which are composed of two long apolar polyisobutylene (PIB) tails linked by a succinimide moiety to a polyamine core.<sup>2</sup> In this project, the properties of the modified *b*-PIBSI (M-*b*-PIBSI) dispersants are investigated.

To obtain *b*-PIBSI, two molar equivalents of polyisobutylene succinic anhydride (PIBSA) were reacted with one molar equivalent of a polyamine. PIBSA is a polyisobutylene chain terminated at one end with one succinic anhydride moiety. Diethylene triamine (DETA), tetraethylene pentamine (TEPA), and pentaethylene hexamine (PEHA) were used in the synthesis of *b*-PIBSI. M-*b*-PIBSI was synthesized by reacting *b*-PIBSI with ethylene carbonate (EC) to form the carbamate ethanol side chain. This chapter focuses on the synthesis of the *b*-PIBSI and M-*b*-PIBSI dispersants, the characterization of their chemical composition in terms of the ratio of the number of succinimide units ( $N_{SI}$ ) over the number of isobutylene units ( $N_{IB}$ ), as well as the degree of modification of M-*b*-PIBSI.

## **3.2. Experimental Procedures**

### **3.2.1 Chemicals**

The solvents xylene (reagent grade, 98.5%, EMD), tetrahydrofuran (THF) (distilled in glass, Caledon), hexane (HPLC grade, Caledon), acetone (HPLC grade, Caledon) were used as received. Diethylene triamine (DETA) (99%, Sigma-Aldrich), tetraethylene pentamine (TEPA) (technical grade, Sigma-Aldrich), pentaethylene hexamine (PEHA) (technical grade, Sigma-Aldrich) and ethylene carbonate (98%, Sigma-Aldrich) were used as received. PIBSA was provided by Imperial Oil.

### **3.2.2 Instrumentation**

#### **Gel Permeation Chromatography (GPC)**

A divinylbenzene (DVB) mixed bed 500×10 mm Jordi column and a Waters 410 differential refractometer were used in the GPC instrument. All samples were filtered using a 0.2 µm Millipore filter before GPC measurement. THF was used as the solvent in the GPC experiments. The samples were run at a flow rate of 1.0 mL/min. The GPC instrument was calibrated with polystyrene standards so that the molecular weights obtained by GPC analysis of the polymeric dispersants are apparent molecular weights.

#### **Fourier Transform Infrared (FT-IR)**

The FT-IR spectra of the samples deposited as thin films on NaCl FT-IR cells were obtained with a Bruker Tensor 27 FT-IR spectrophotometer.

## **Nuclear Magnetic Resonance (NMR)**

The  $^1\text{H}$  NMR spectra of the samples were obtained with a Bruker 300 MHz high resolution NMR spectrometer. Deuterated chloroform (99.8%, Cambridge Isotope Laboratory Inc.) was used as the solvent. The concentration of all polymer solutions for  $^1\text{H}$  NMR was over 30 mg/mL.

### **3.3 Characterization of PIBSA**

Since PIBSA is one of the starting materials used in the synthesis of M-PIBSI, it was important to determine its chemical composition. As mentioned earlier, PIBSA is composed of a long apolar PIB chain bearing a succinic anhydride group at one end. PIBSA was provided by Imperial Oil.

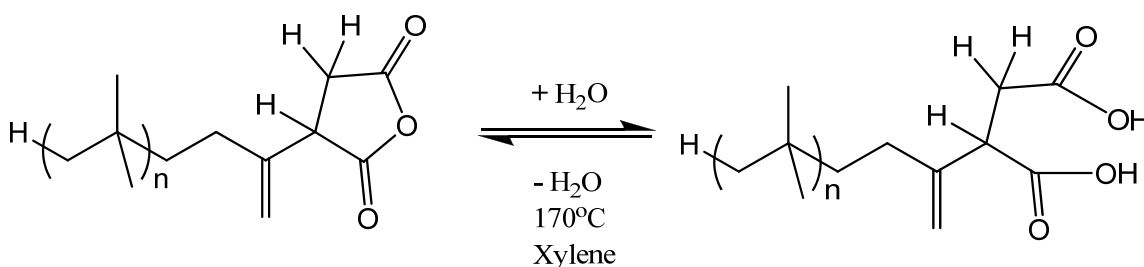
#### **3.3.1. Purification of PIBSA**

A minimum amount of hexane (around 10 mL) was used to dissolve 10 g of crude PIBSA at 60 °C. The hot PIBSA solution was added dropwise into 500 mL of acetone which was cooled in an ice bath. The PIBSA precipitate and the supernatant were separated by centrifugation at 7000 g. The precipitate was dissolved in hexane and it was precipitated in the same manner for two more times. After the precipitations, PIBSA was dried in a vacuum oven at 60 °C for 48 hours.

#### **3.3.2. Dehydration of PIBSA**

Since the succinic anhydride group of PIBSA is moisture sensitive, the SA unit of PIBSA can react with water present as moisture in the air to yield succinic acid. This process can be reversed by “cooking” the acid form of PIBSA at high temperature (Scheme 3.1). The dehydration of PIBSA was conducted by dissolving 2 g of PIBSA in

20 mL of xylene placed in a 50 mL round bottom flask which was connected to a Dean-Stark trap, a water condenser, and a nitrogen inlet and outlet. The flask was heated at 170 °C for 16 hours. After the reaction was complete, xylene was removed under reduced pressure, and the dehydrated PIBSA was further dried in a vacuum oven at 80 °C for 16 hours.



Scheme 3.1. Reversible hydration and dehydration of PIBSA

The FT-IR spectra of PIBSA acquired before and after dehydration are shown in Figure 3.1. The bands at  $1705\text{ cm}^{-1}$  and  $1785\text{ cm}^{-1}$  represent the carbonyl group of the succinic acid and succinic anhydride, respectively.<sup>3</sup> The disappearance of the peak at  $1705\text{ cm}^{-1}$  in the bottom FT-IR spectrum illustrates that all the succinic acid is converted to succinic anhydride after PIBSA was subject to the process described in Scheme 3.1. In this project, PIBSA was always used in the dehydrated form.

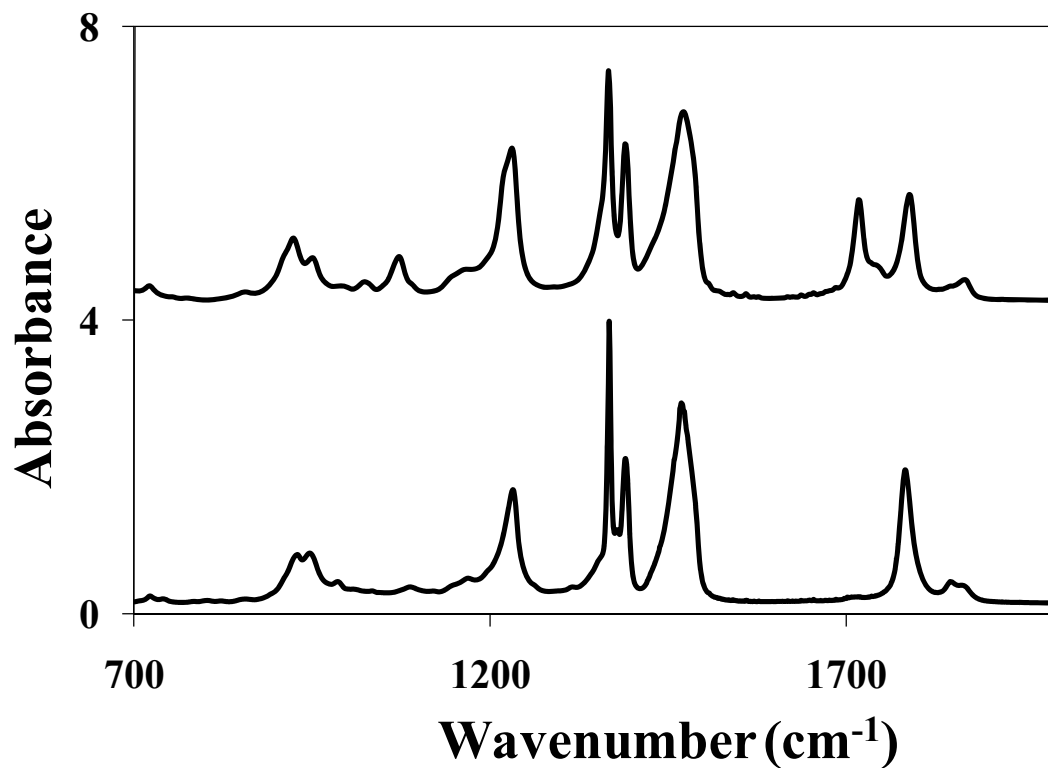


Figure 3.1. FT-IR spectra of hydrated (top) and dehydrated (bottom) PIBSA

### 3.3.3. Chemical composition of PIBSA

FT-IR was used to determine the average number of IB units in a PIBSA molecule per SA moiety. A small amount of THF was used as the solvent to prepare the PIBSA solutions which were cast onto a sodium chloride FT-IR cell. In the FT-IR spectrum, the absorption at  $1785\text{ cm}^{-1}$  represents the carbonyl of SA and that at  $1390\text{ cm}^{-1}$  represents the isobutylene monomers of the PIB backbone (Figure 3.2). The carbonyl stretching absorption is one of the strongest IR absorptions, and is very useful in structure determination as one can determine both the number of carbonyl groups but also the form under which it is present such as in an acid, an anhydride, an amide, etc. Walch and Gaymans established a calibration curve to determine the ratio of SA to IB units for

an unknown PIBSA sample.<sup>3</sup> Known amounts of methyl succinic anhydride (MSA) were mixed with a matrix of polyisobutylene and the absorption of the mixtures was measured by FT-IR as a function of MSA content. The ratio of the absorbance at 1785 cm<sup>-1</sup> characteristic of the SA carbonyls over that at 1390 cm<sup>-1</sup> characteristic of the methyls of the PIB backbone was plotted as a function of the MSA content. A straight line was drawn through the data points which relates the ratio of FT-IR absorptions  $\text{abs}(1785 \text{ cm}^{-1})/\text{abs}(1390 \text{ cm}^{-1})$  to the ratio of the number of moles of SA units ( $N_{SA}$ ) over that of IB units ( $N_{IB}$ ). The slope of this line yielded Equation 1 which can then be used to determine the SA content of PIBSA.<sup>3</sup> It is worth pointing out that peak heights were used in the procedure.

$$\frac{N_{SA}}{N_{IB}} = 0.024 \times \frac{\text{abs}(1785\text{cm}^{-1})}{\text{abs}(1390\text{cm}^{-1})} \quad (1)$$

Furthermore, if all the polyisobutylene chains are assumed to be capped at one end with one SA group, this ratio provides an estimate of the molecular weight of PIBSA. Based on the absorptions measured in Figure 3.1, the average number of IB monomers per SA unit was found to equal 49:1, giving a number-average molecular weight estimate of 2,874 g/mol for PIBSA. The  $N_{IB}/N_{SA}$  ratio was also estimated by <sup>1</sup>H NMR (Figure 3.2).

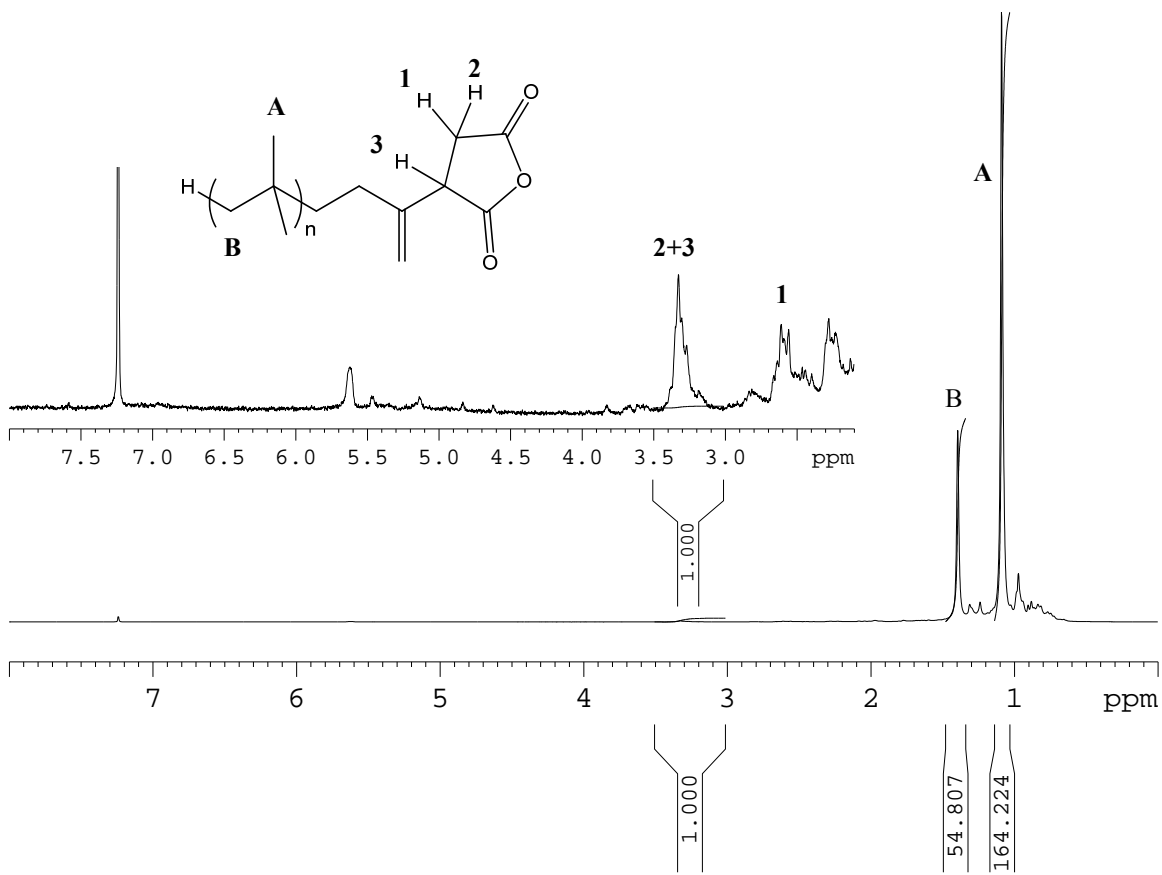


Figure 3.2.  $^1\text{H}$  NMR spectrum of PIBSA

In the  $^1\text{H}$  NMR spectrum, the peak at 3.3 ppm represents the protons **2** and **3** of SA. The peak at 1.4 ppm represents the methylene protons (proton **B**) of the IB group. The ratio of the peak integrals of the proton **B** and **2+3** is equal to the  $N_{\text{IB}}/N_{\text{SA}}$  ratio. The  $N_{\text{IB}}/N_{\text{SA}}$  ratio obtained by  $^1\text{H}$  NMR is 1:55. This ratio is similar to the one of 1:49 obtained by FT-IR.

After using FT-IR and  $^1\text{H}$  NMR to estimate the chemical composition of PIBSA, GPC was used to determine the molecular weight distribution of PIBSA. The GPC trace

of PIBSA in Figure 3.3 shows a low molecular weight impurity at high elution volume ( $v_{el} = 33$  mL).

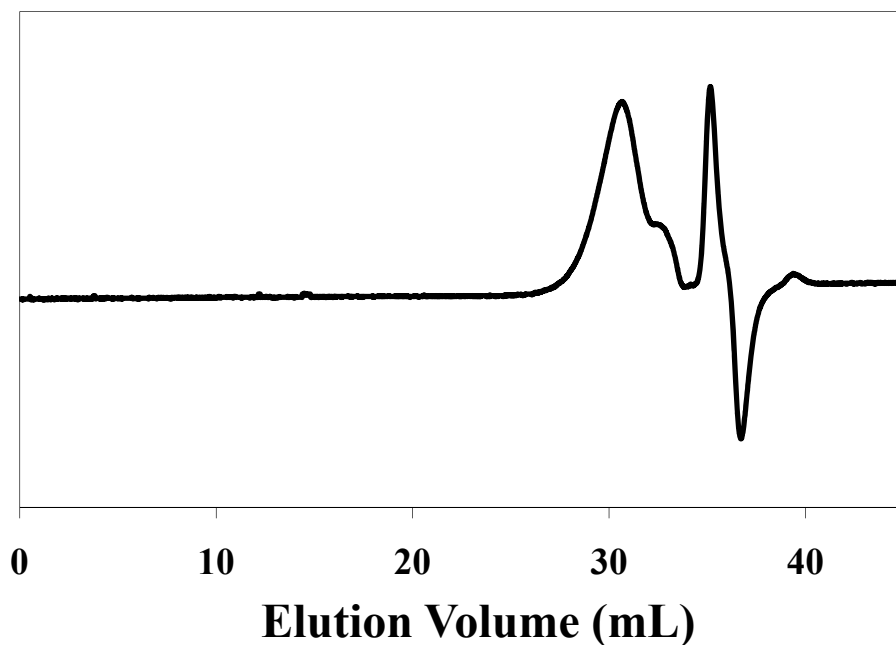
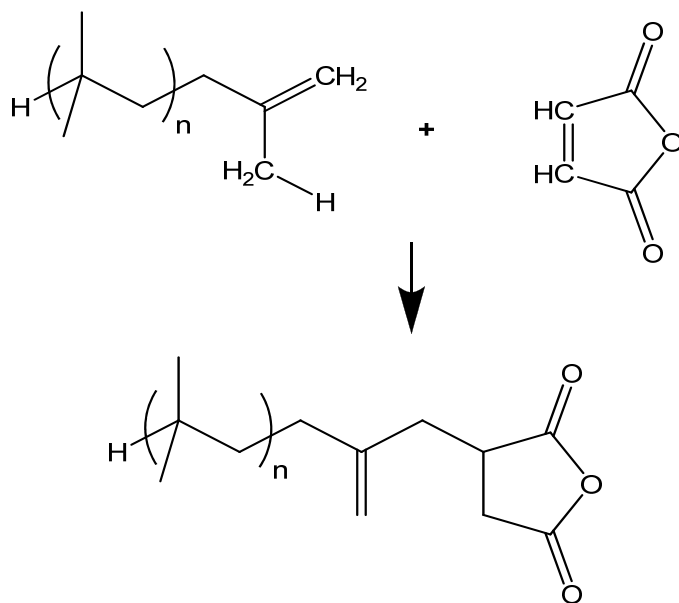


Figure 3.3. GPC trace of crude PIBSA. Elution volume  $v_{el} = 31$  mL: PIBSA ( $M_n = 1200$  g/mol);  $v_{el} = 33$  mL: non-maleated PIB impurity ( $M_n = 280$  g/mol);  $v_{el} = 35$  mL: solvent peak. The molecular weights are obtained according to a calibration curve based on polystyrene standards

Since PIBSA is usually synthesized by an Alder-ene reaction (Scheme 3.2),<sup>4,5</sup> the impurity could be unreacted polyisobutylene. According to Shen and Duhamel,<sup>2</sup> the impurity can be removed by column chromatography.





Scheme 3.2. Alder-ene reaction used to synthesize PIBSA shown with one of the possible isomers.

### 3.4. Synthesis and characterization of PIBSI dispersants

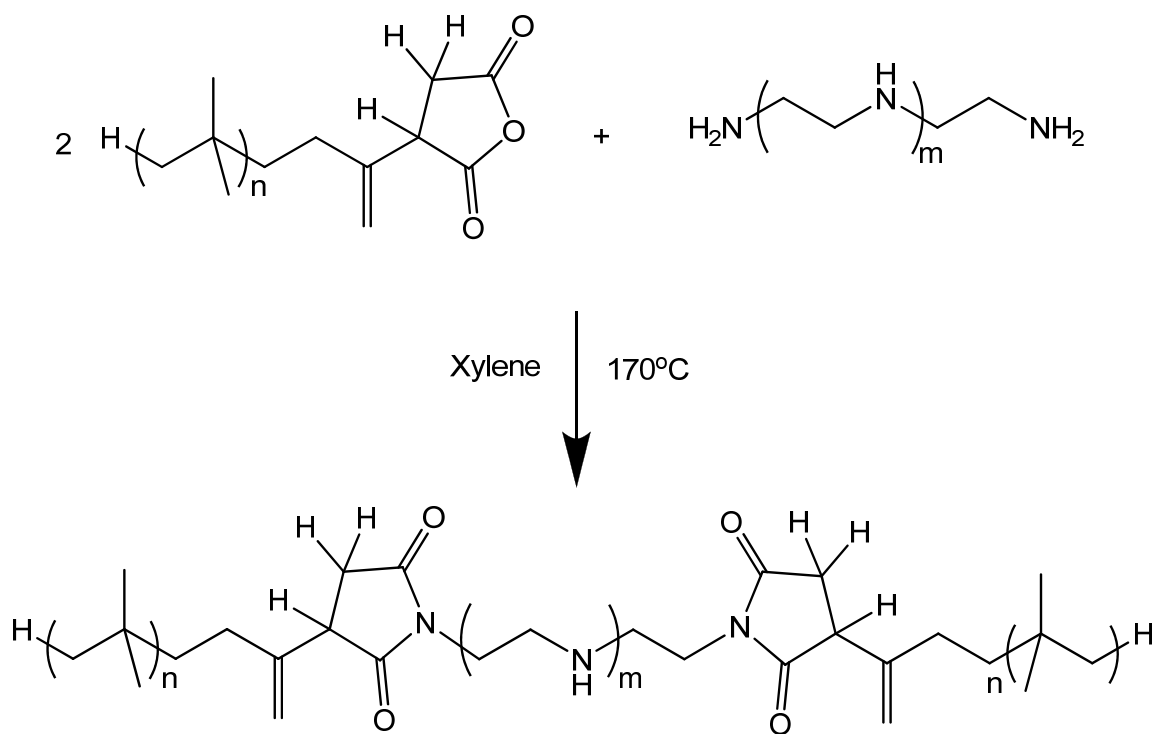
#### 3.4.1 Synthesis of PIBSI dispersants

A PIBSI dispersant is synthesized by reacting two molar equivalents of PIBSA with one molar equivalent of polyamine. Three different polyamines were used to prepare the modified PIBSI dispersant (Table 3.1), namely diethylenetriamine (DETA), tetraethylenepentamine (TEPA), and pentaethylenehexamine (PEHA). The secondary amine groups of the polyamines are evenly separated by an ethylene unit.

Table 3.1. Polyamines used to prepare the PIBSI dispersants

	Chemical Structure	Number of Secondary Amines
Diethylenetriamine (DETA)	$\text{H}_2\text{N}-\text{CH}_2\text{CH}_2-\text{NH}-\text{CH}_2\text{CH}_2-\text{NH}_2$	1
Tetraethylenepentamine (TEPA)	$\text{H}_2\text{N}-(\text{CH}_2\text{CH}_2-\text{NH})_3-\text{CH}_2\text{CH}_2-\text{NH}_2$	3
Pentaethylenehexamine (PEHA)	$\text{H}_2\text{N}-(\text{CH}_2\text{CH}_2-\text{NH})_4-\text{CH}_2\text{CH}_2-\text{NH}_2$	4

The synthesis of the PIBSI dispersant begins typically by dissolving PIBSA (9 g, 3 mmol) in 30 mL of xylene where it is heated at 170 °C for 10 hours under nitrogen to dehydrate any succinic acid into succinic anhydride using a Dean-Stark apparatus. DETA (0.16 g, 1.55 mmol) is then added and the mixture is refluxed for 10 hours by keeping it in an oil bath whose temperature is set at 170 °C (Scheme 3.3). In order to remove unreacted polyamine, 50 mL of xylene were added to the reaction mixture and the solution was washed three times with a 0.5 M HCl solution, 0.5 M NaHCO<sub>3</sub> solution, and Milli-Q water.



Scheme 3.3. Synthesis of b-PIBSI dispersant.

### 3.4.2. Purification of the PIBSI dispersants

As shown in Figure 3.4, a low molecular weight impurity is present in PIBSA. According to a previous study,<sup>2</sup> the impurity is unreacted PIB generated during the Alder-ene reaction for the synthesis of PIBSA. As a result, the impurity should not affect the synthesis of PIBSI.

Figure 3.4 shows the GPC traces of PIBSA (bottom trace) and *b*-PIBSI-DETA (top trace). A major shift in the main peak was observed with respect to PIBSA, reflecting a significant increase in the molecular weight of the product, from 1200 g/mol

to 2000 g/mol. This molecular weight increase is expected since coupling of two PIBSA molecules into one *b*-PIBSI-DETA dispersant results in a twice larger molecule. The impurity hump at  $v_{el} = 33$  mL did not shift, however, yielding an apparent molecular weight of 280 g/mol in the PIBSA sample and 290 g/mol in the *b*-PIB-DETA sample. This observation suggests that the low molecular weight impurity in the PIBSA sample did not participate in the reaction and supports the assumption made earlier that the impurity could be unmaleated PIB.<sup>2</sup>

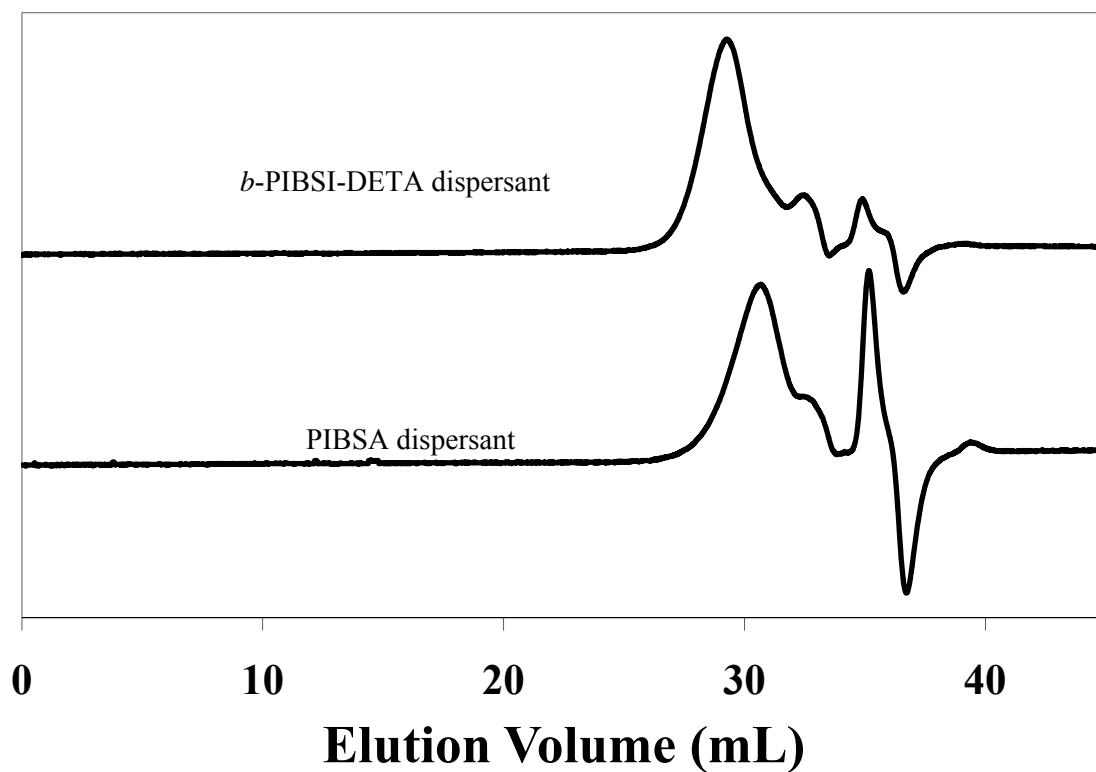


Figure 3.4. GPC trace of PIBSA (bottom) and *b*-PIBSI-DETA (top).

The *b*-PIBSI-DETA sample was then purified by column chromatography following the procedure established by Shen and Duhamel.<sup>2</sup> A 1:10 ratio of ethyl acetate to hexane mixture was used as the eluent for the column followed by a THF flush. The PIB impurity eluted out of the column with the ethyl acetate/hexane solution, and the purified *b*-PIBSI-DETA sample was obtained with the THF flush. The GPC traces of the *b*-PIBSI-DETA and purified *b*-PIBSI-DETA sample are shown in Figure 3.5.

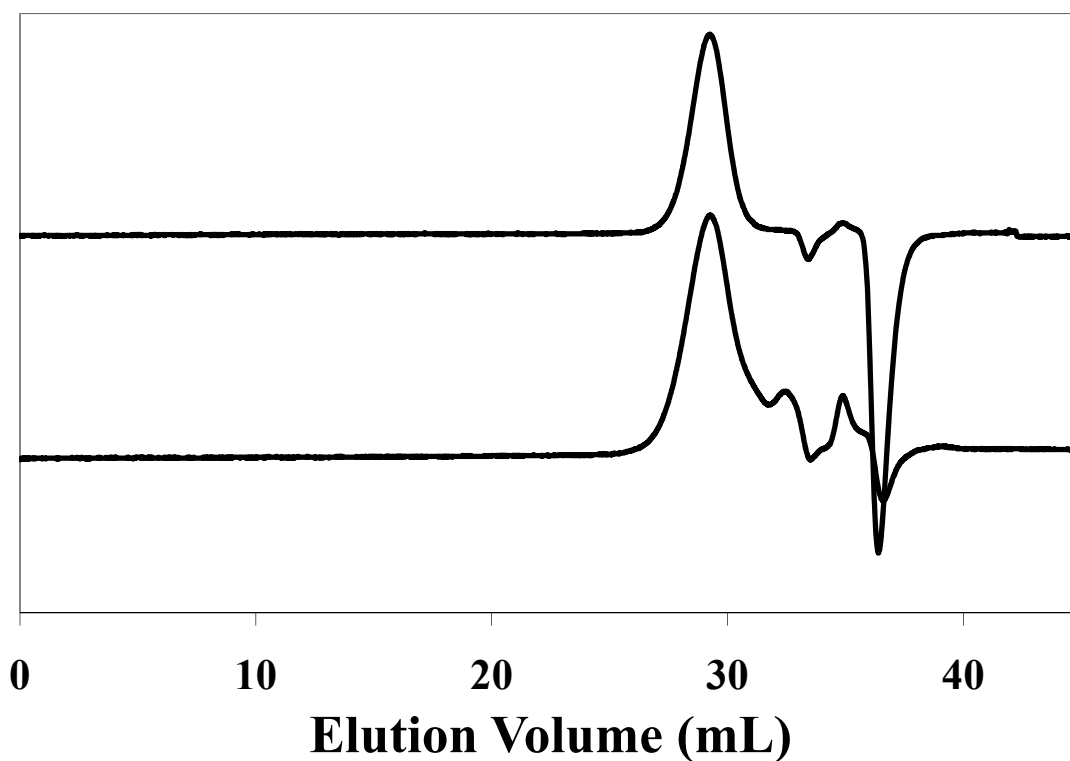


Figure 3.5. GPC traces of crude *b*-PIBSI-DETA (bottom) and purified *b*-PIBSI-DETA sample (top).

The small impurity hump at  $v_{el} = 33$  mL disappeared in the GPC trace of the purified *b*-PIBSI-DETA dispersant. The apparent number-averaged molecular weight  $M_n$  for *b*-PIB-DETA equaled 2440 g/mol, about twice larger than the  $M_n$  value obtained for PIBSA. The  $M_n$  values of PIBSA, *b*-PIBSI-DETA, and the purified *b*-PIBSI-DETA are compared in Table 3.2. However, the yield of the column was found to be substantially lower than originally reported.<sup>2</sup> The yield obtained was less than 10%. Since large amounts of *b*-PIBSI-DETA were needed to carry out the modification reaction later on, and since the low molecular weight impurity did not participate in the reaction, the low molecular weight impurity was not removed before the synthesis of M-PIBSI.

Table 3.2. Apparent number-average molecular weight of PIBSA, *b*-PIB-DETA, and purified *b*-PIB-DETA obtained by using a GPC instrument calibrated with polystyrene standards

	$M_n$ ; PDI of the Major Component(g/mol)	$M_n$ ; PDI of the Impurity Component(g/mol)
PIBSA	1200; 1.6	280; 1.1
<i>b</i> -PIB-DETA	2000; 1.6	290; 1.1
Purified <i>b</i> -PIB-DETA	2400; 1.3	-

### 3.4.3. Characterization of PIBSI dispersants

#### 3.4.3.1. FT-IR

Walch and Gaymans used the absorption of the carbonyl of SA and of the methyl of PIB to establish a calibration curve that would yield the  $N_{SA}/N_{IB}$  ratio of an unknown

PIBSA sample.<sup>1</sup> A similar method was used to obtain a calibration curve to determine the ratio of the number of moles of succinimide units ( $N_{SI}$ ) over that of isobutylene units ( $N_{IB}$ ).<sup>2</sup> *N*-methyl succinimide (NMSI) was used as a model of the SI group found in the PIBSI dispersants. Mixtures of NMSI and PIB were prepared in different proportions. The ratio of the absorbance at  $1705\text{ cm}^{-1}$  characteristic of the SI carbonyls over that at  $1390\text{ cm}^{-1}$  characteristic of the methyls of the PIB backbone was plotted as a function of the  $N_{SI}/N_{IB}$  ratio in Figure 3.6.

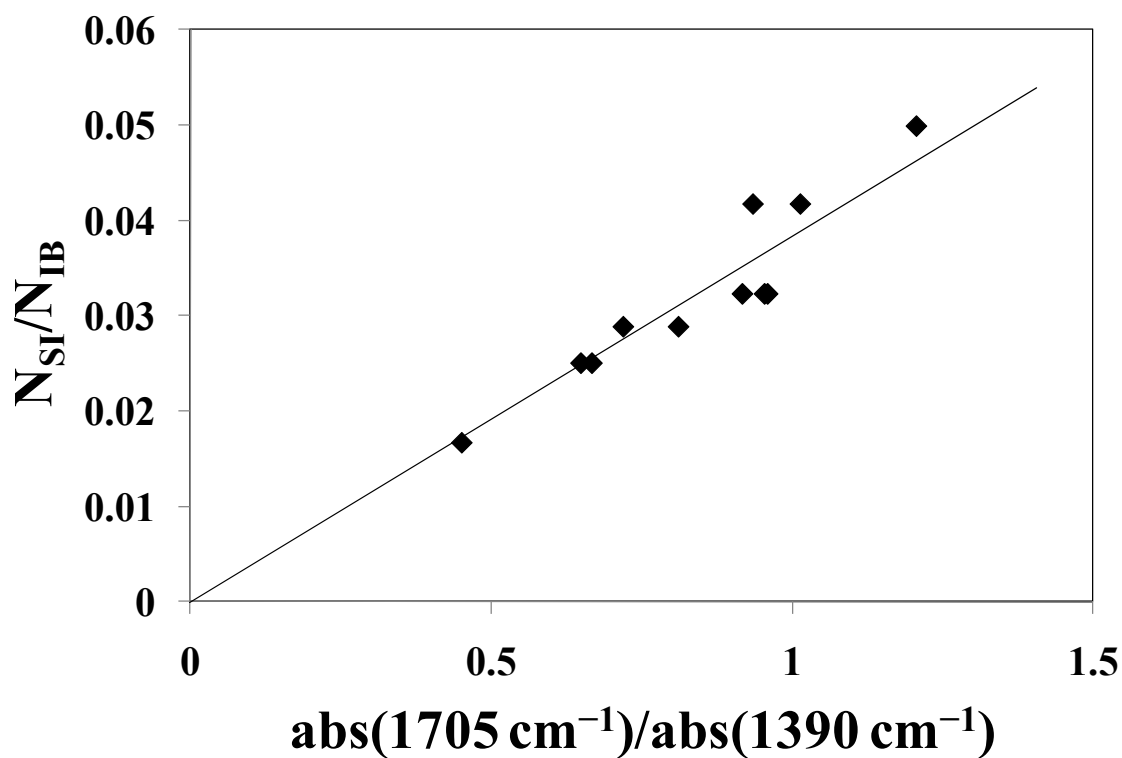


Figure 3.6. Calibration curve relating the ratio of the number of SI to IB units to the peak ratio of absorption bands at  $1705\text{ cm}^{-1}$  and  $1390\text{ cm}^{-1}$

A straight line was drawn through the data points and its slope was determined. It was found to equal  $0.038 \pm 0.001$ . By using Equation 2, the  $N_{SI}/N_{IB}$  ratios of *b*-PIBSI-DETA, *b*-PIBSI-TEPA, and *b*-PIBSI-PEHA were determined to equal  $1:29 \pm 1$ ,  $1:31 \pm 1$ , and  $1:36 \pm 1$ , respectively.

$$\frac{N_{SI}}{N_{IB}} = 0.038 \times \frac{abs(1705cm^{-1})}{abs(1390cm^{-1})} \quad (2)$$

A calibration curve was also established by using the integral of the absorption bands instead of the peak height. To this end, the  $1705 \text{ cm}^{-1}$  peak characteristic of the SI carbonyls was integrated from  $1680 \text{ cm}^{-1}$  to  $1764 \text{ cm}^{-1}$ , and the  $1390 \text{ cm}^{-1}$  peak characteristic of the methyls of the PIB backbone was integrated from  $1377 \text{ cm}^{-1}$  to  $1415 \text{ cm}^{-1}$ . The ratio of the two peak integrals were obtained and plotted as a function of the  $N_{SI}/N_{IB}$  ratio in Figure 3.7.

Within experimental error, the ratio of the number of SI to IB units was found to increase linearly with increasing SI content in the mixtures. The slope of the calibration curve equaled  $0.024 \pm 0.001$ .



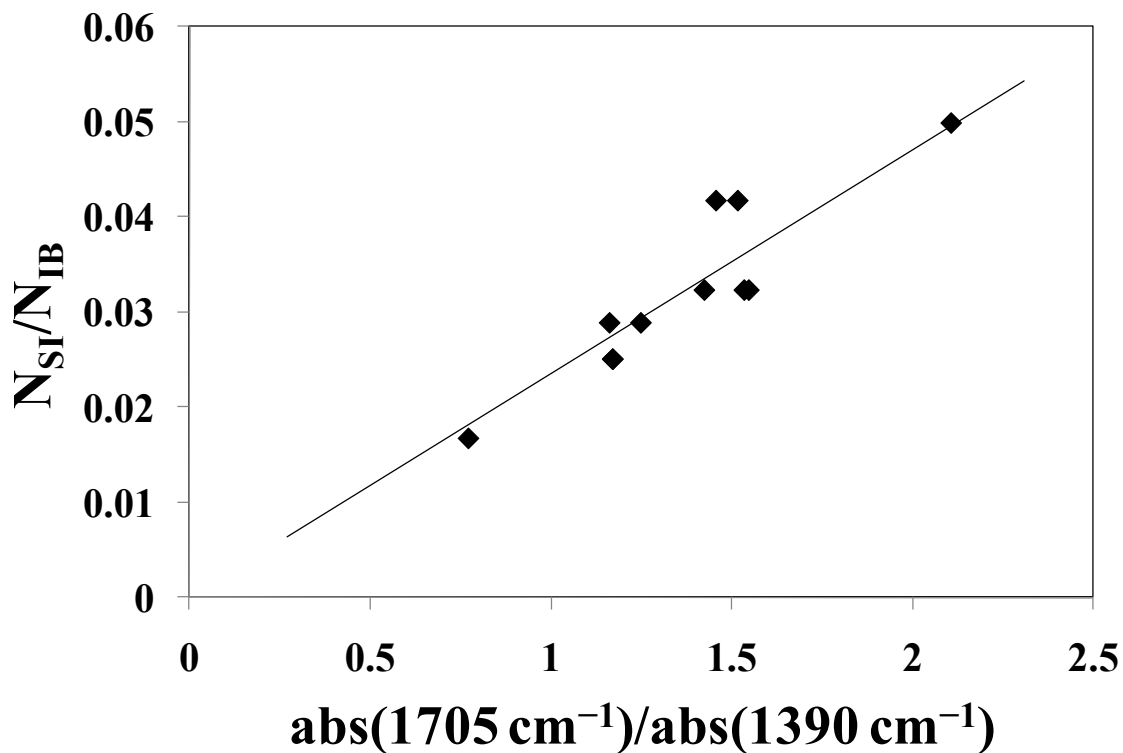


Figure 3.7. Calibration curve relating the  $N_{SI}/N_{IB}$  ratio to the ratio of the integrated absorption bands at  $1705\text{ cm}^{-1}$  and  $1390\text{ cm}^{-1}$  in the FT-IR spectra

Using Equation 3, the  $N_{SI}/N_{IB}$  ratios of *b*-PIBSI-DETA, *b*-PIBSI-TEPA, and *b*-PIBSI-PEHA were found to equal  $1:37\pm 1$ ,  $1:39\pm 1$ , and  $1:47\pm 2$ , respectively.

$$\frac{N_{SI}}{N_{IB}} = 0.024 \times \frac{\text{Integration}(1705\text{cm}^{-1}\text{Peak})}{\text{Integration}(1390\text{cm}^{-1}\text{Peak})} \quad (3)$$

### 3.4.3.2. $^1\text{H}$ NMR

$^1\text{H}$  NMR was used to determine the  $N_{\text{SI}}/N_{\text{IB}}$  ratio of *b*-PIBSI-DETA. The  $^1\text{H}$  NMR spectrum is shown in Figure 3.8. As found in Chapter 2, the peaks at 3.5, 3.0, 2.7, and 2.5 ppm in Figure 3.8 represent the protons **5**, **2** and **3**, **6**, and **1** of *b*-PIBSI-DETA, respectively. The peak at 1.4 and 1.1 ppm represent the methylene protons and the methyl protons of the PIB backbone, respectively.

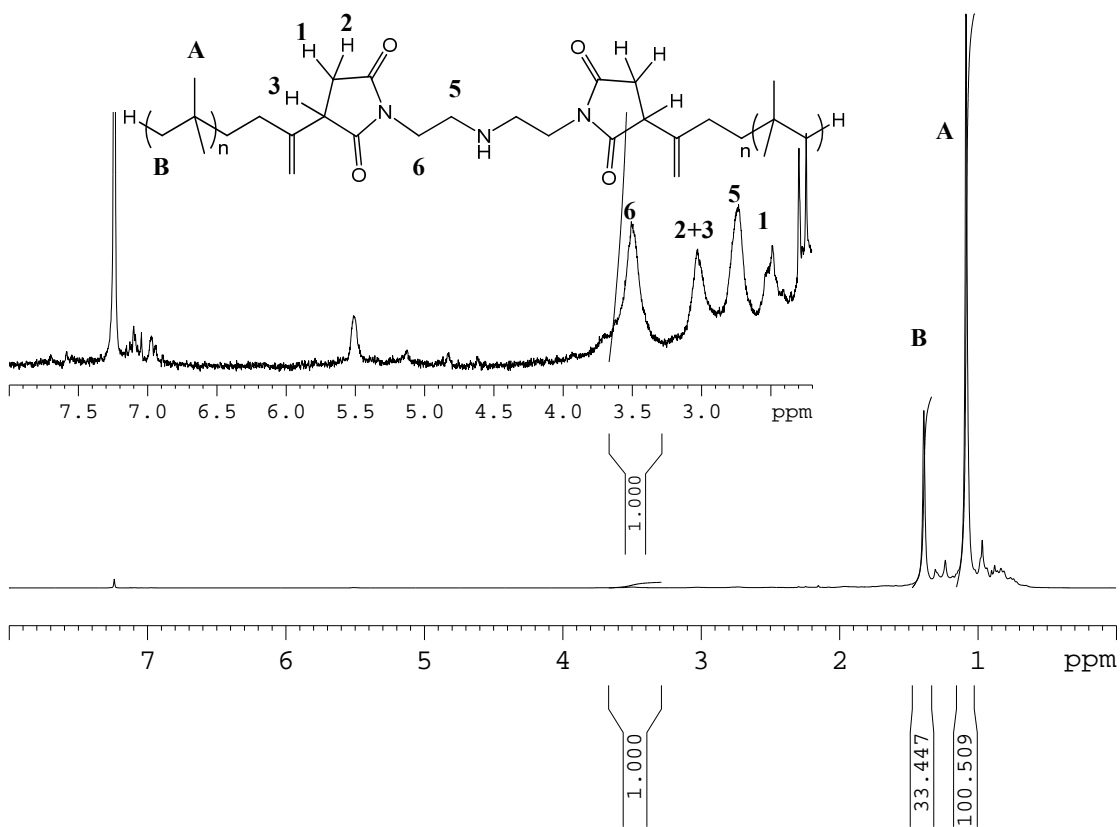


Figure 3.8.  $^1\text{H}$  NMR spectrum of *b*-PIBSI-DETA

The ratio of the integrals of the peaks at 3.5 and 1.4 ppm yields the ratio of  $N_{SI}/N_{IB}$  for the *b*-PIBSI-DETA dispersant. The ratio of the integrals of the peaks located at 1.4 and 1.1 ppm is found to equal 1/3 as expected since these peaks represent the **B** and **A** protons of the PIB chain, respectively. The small peaks around 7 ppm and the sharp peaks at 2.25 and 2.3 ppm are due to the solvent xylene and its additives. Since the dispersants are highly viscous, the solvents are difficult to remove completely. Fortunately, the solvent peaks do not interfere with the peaks of interest, and they do not affect the integration results.

The peak at 3.5 ppm representative of the methylene protons of the polyamine core is well isolated from the other peaks in the  $^1\text{H}$  NMR spectrum shown in Figure 3.8. However, a small shoulder is observed on the left side of the main peak which complicates its integration.

Starting the integration at 3.65 ppm in Figure 3.10 discards the shoulder. The procedure yields an  $N_{IB}/N_{SI}$  ratio of 33 for *b*-PIBSI-DETA. Since the peak at 3.5 ppm is broad, a substantial fraction of peak might be excluded as illustrated in Figure 3.11 if the integration is started at 3.65 ppm, resulting in a smaller  $N_{SI}/N_{IB}$  ratio.

On the other hand, if the shoulder is included in the integration by starting the integration at 3.8 ppm, the area **A** in Figure 3.9 which does not belong to the main peak becomes part of the area under the peak. Consequently, the  $N_{SI}/N_{IB}$  ratio will be overestimated. The integration of the peak at 3.5 ppm in Figure 3.10 yields an  $N_{SI}/N_{IB}$  ratio equal to 1/28.

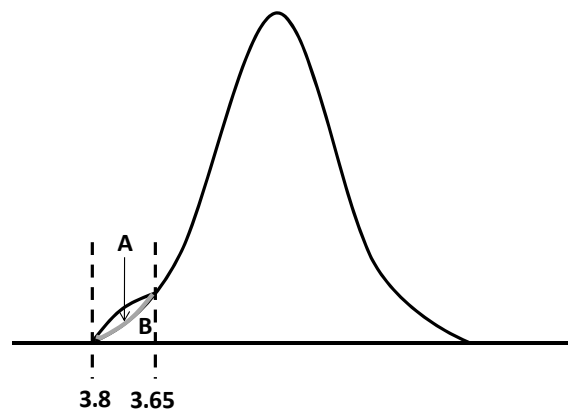


Figure 3.9. Integration of the peak at 3.5 ppm in the  $^1\text{H}$  NMR spectrum

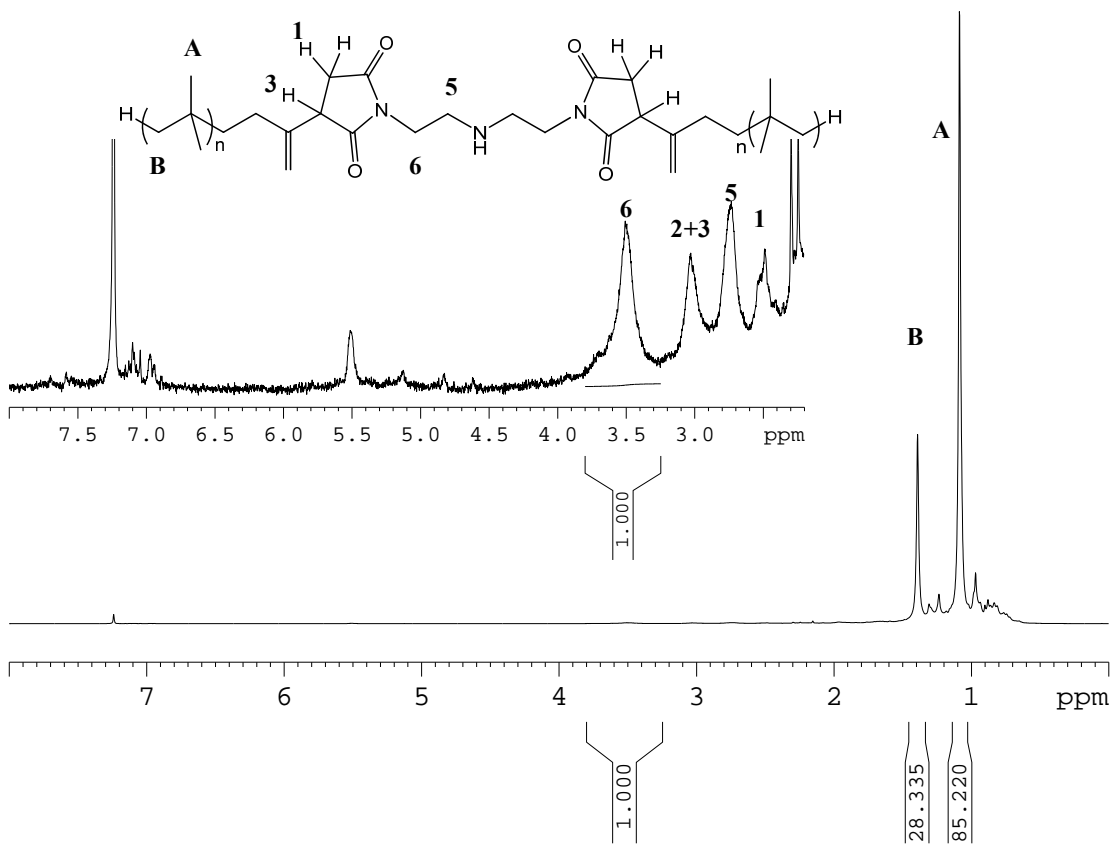


Figure 3.10.  $^1\text{H}$  NMR spectrum of *b*-PIBSI-DETA

The presence of the additional secondary amines for *b*-PIBSI-TEPA and *b*-PIBSI-PEHA complicated the <sup>1</sup>H NMR spectra to such an extent that <sup>1</sup>H NMR was not used to determine their chemical composition.

### 3.4.3.3. Summary of the N<sub>SI</sub>/N<sub>IB</sub> ratios

The N<sub>SI</sub>/N<sub>IB</sub> ratios of the *b*-PIBSI dispersants were obtained by FT-IR using the peak height or integral and by <sup>1</sup>H NMR. The results are listed in Table 3.3.

Table 3.3. N<sub>SA</sub>/N<sub>IB</sub> ratio of PIBSA and N<sub>SI</sub>/N<sub>IB</sub> ratios of the *b*-PIBSI dispersants

Dispersants	<sup>1</sup> H NMR	<sup>1</sup> H NMR	FT-IR (Peak Height)	FT-IR (Peak Integration)	Average from FT-IR
PIBSA	1:55		1:49		
<i>b</i> -PIBSI-DETA	1:33±1 <sup>a</sup>	1:29±1 <sup>b</sup>	1:29±1	1:37±1	1:33±4
<i>b</i> -PIBSI-TEPA	–	-	1:31±1	1:39±1	1:34±5
<i>b</i> -PIBSI-PEHA	–	-	1:36±1	1:47±2	1:41±5

a: shoulder excluded for the integration of the peak at 3.5 ppm;

b: shoulder included for the integration of the peak at 3.5 ppm.

As mentioned earlier, the N<sub>SA</sub>/N<sub>IB</sub> ratio of PIBSA obtained by using <sup>1</sup>H NMR and FT-IR agree relatively well with each other. The N<sub>SI</sub>/N<sub>IB</sub> ratio of *b*-PIBSI-DETA obtained by <sup>1</sup>H NMR and FT-IR equal 1:31±3 and 1:33±4, respectively. The chemical composition of the *b*-PIBSI dispersants obtained by applying the procedures described above agree relatively well with each other suggesting that each procedure yields a reliable measure

of the chemical composition of the dispersants. Using FT-IR, the  $N_{SI}/N_{IB}$  ratios of *b*-PIBSI-DETA, *b*-PIBSI-TEPA, and *b*-PIBSI-PEHA were determined to equal  $1:33\pm 4$ ,  $1:34\pm 5$ , and  $1:41\pm 5$ .

Interestingly, the  $N_{SI}/N_{IB}$  ratio of *b*-PIBSI-PEHA obtained by FT-IR is lower than that of *b*-PIBSI-DETA and *b*-PIBSI-TEPA. The FT-IR spectra of the three dispersants are shown in Figure 3.11.

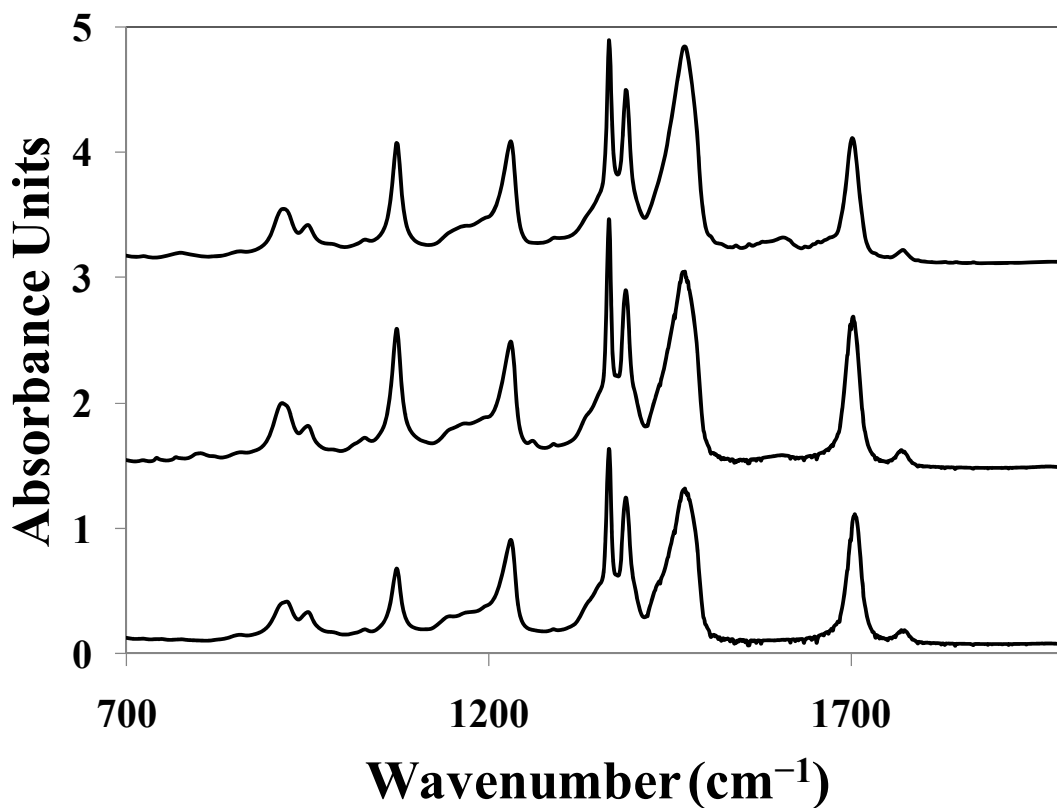


Figure 3.11. FT-IR spectra of *b*-PIBSI-PEHA (top), *b*-PIBSI-TEPA (middle), and *b*-PIBSI-DETA (bottom)

A peak around  $1620\text{ cm}^{-1}$  is clearly observed in the FT-IR spectrum of the *b*-PIBSI dispersant prepared with PEHA. The presence of this peak suggests that instead of succinimide, the dispersants might contain some primary amide (Figure 3.12).<sup>6</sup> If this is the case, less succinimides would be generated and the  $N_{SI}/N_{IB}$  ratio would be larger as experimentally found.

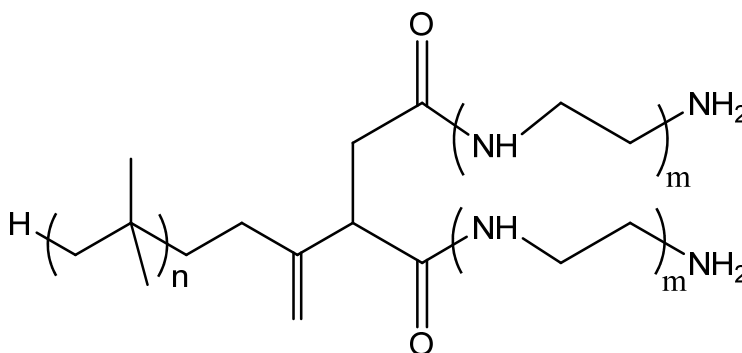


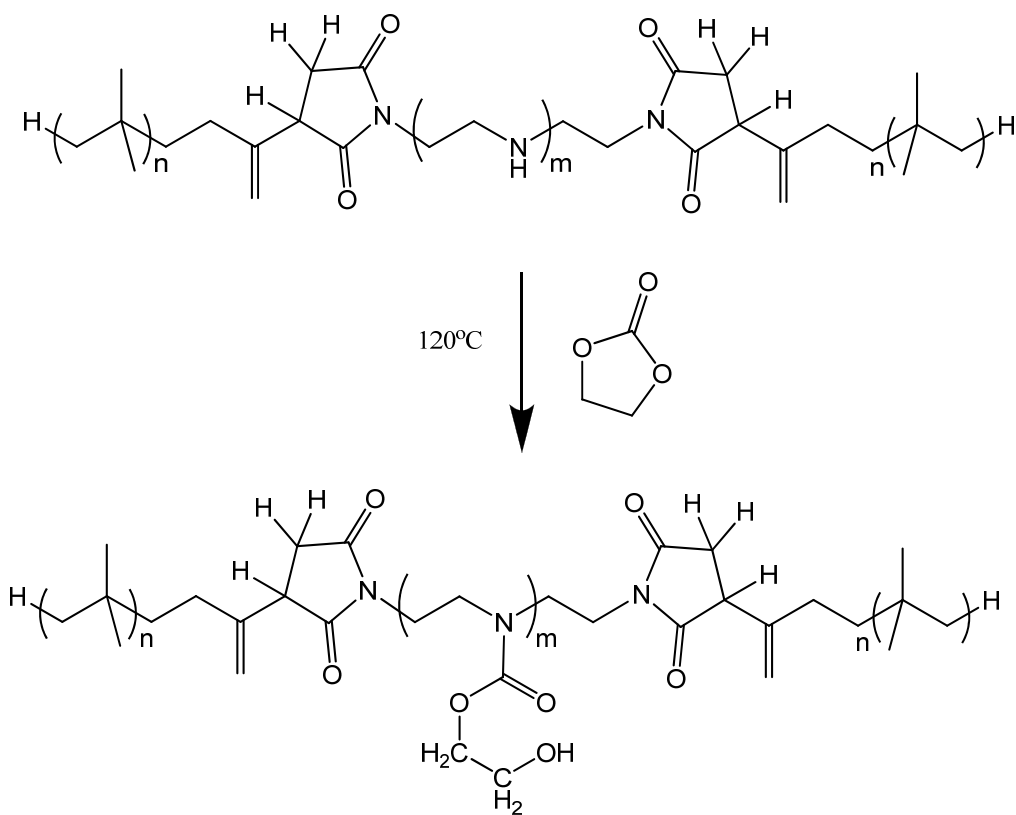
Figure 3.12. Chemical structure of succinamide

The amide peak is not observed in the spectrum of *b*-PIBSI-DETA and it is relatively small in the spectrum of *b*-PIBSI-TEPA. As a result, the modification of these two dispersants with ethylene carbonate is expected to be easier to monitor.

### 3.5. Synthesis and characterization of M-*b*-PIBSI

The synthesis of M-*b*-PIBSI is carried out by reacting a *b*-PIBSI dispersant with ethylene carbonate (EC) (Scheme 3.4). 2-hydroxyethyl *N,N*-dibutyl carbamate (HEDBC) was synthesized in order to enable the characterization of the modified dispersant (Chapter 2). The appearance of the peaks at 3.8 and 4.2 ppm in the  $^1\text{H}$  NMR spectrum

indicates successful modification of the dispersant, and these two peaks can then be used to determine the degree of modification.



Scheme 3.4. Synthesis of M-b-PIBSI

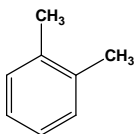
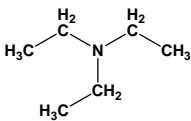
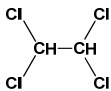
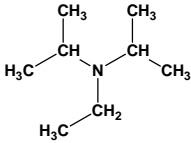
### 3.5.1. Synthesis of M-b-PIBSI-DETA

M-b-PIBSI-DETA was synthesized under various conditions in an attempt to obtain a high degree of modification. Xylenes, tributylamine (TBA), 1,1,2,2-



tetrachloroethane and *N,N*-diisopropylethylamine were used as the solvent for the modification reaction. Unfortunately, low yields were obtained. A high yield of modification was only obtained once with a 2:1 TBA to xylene mixture. Unfortunately, this reaction could not be reproduced. The yields obtained when conducting the modification reaction with different solvents are listed in Table 3.4.

Table 3.4. Yield of M-b-PIBSI-DETA by conducting the modification reaction in different solvents.

Solvent	Boiling Point (°C)	Reaction Yield
Xylenes 	140	Low yield <10%
Triethylamine 	89	Low yield Occasionally high yield
<i>1,1,2,2</i> -tetrachloroethane 	147	React with PIBSIs
<i>N,N</i> -diisopropylethylamine 	127	Low yield <10%

The signature peaks of the modified side chain at 3.8 and 4.2 ppm were observed in the  $^1\text{H}$  NMR spectrum of the M-*b*-PIBSI-DETA samples. However, the signal was usually very weak (Figure 3.13). After numerous attempts, the modification of *b*-PIBSI-DETA was found to be inefficient. This might be due to steric hindrance where the core of *b*-PIBSI-DETA hinders the approach of EC and prevents the reaction.

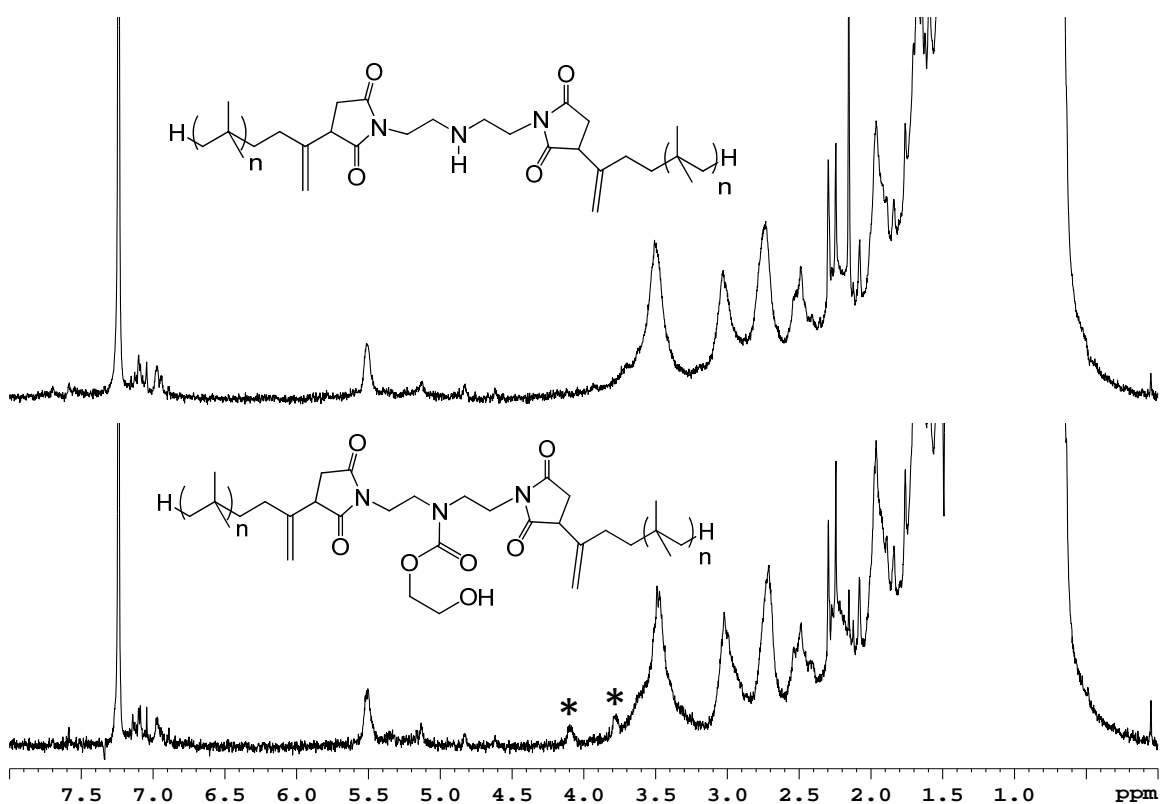


Figure 3.13.  $^1\text{H}$  NMR spectra of *b*-PIBSI-DETA (top) and M-*b*-PIBSI-DETA (bottom); peaks at 3.8 and 4.2 ppm are shown with an asterisk

In order to reduce steric hindrance, *mono*-polyisobutylene succinimide-DETA (*m*-PIBSI-DETA) was used in the modification reaction. The modified *m*-PIBSI-DETA (M-

*m*-PIBSI-DETA) was synthesized as follows. PIBSA (3 g, 1 mmol) was dissolved in 10 mL xylene, and the mixture was heated under nitrogen at 170 °C for 10 hours. DETA (1.55 g, 1.5 mmol) was added into the PIBSA solution, and the mixture was refluxed for 10 hours at 170 °C. After the reaction was completed, 50 mL of xylene was added to the mixture and the solution was washed three times with 0.5 M HCl solution, 0.5 M NaHCO<sub>3</sub> solution, and Milli-Q water. The solvent was removed and the product was further dried in a vacuum oven at 60 °C for 24 hours. The <sup>1</sup>H NMR spectrum of the *m*-PIBSI-DETA dispersant was obtained and it is shown in Figure 3.14.

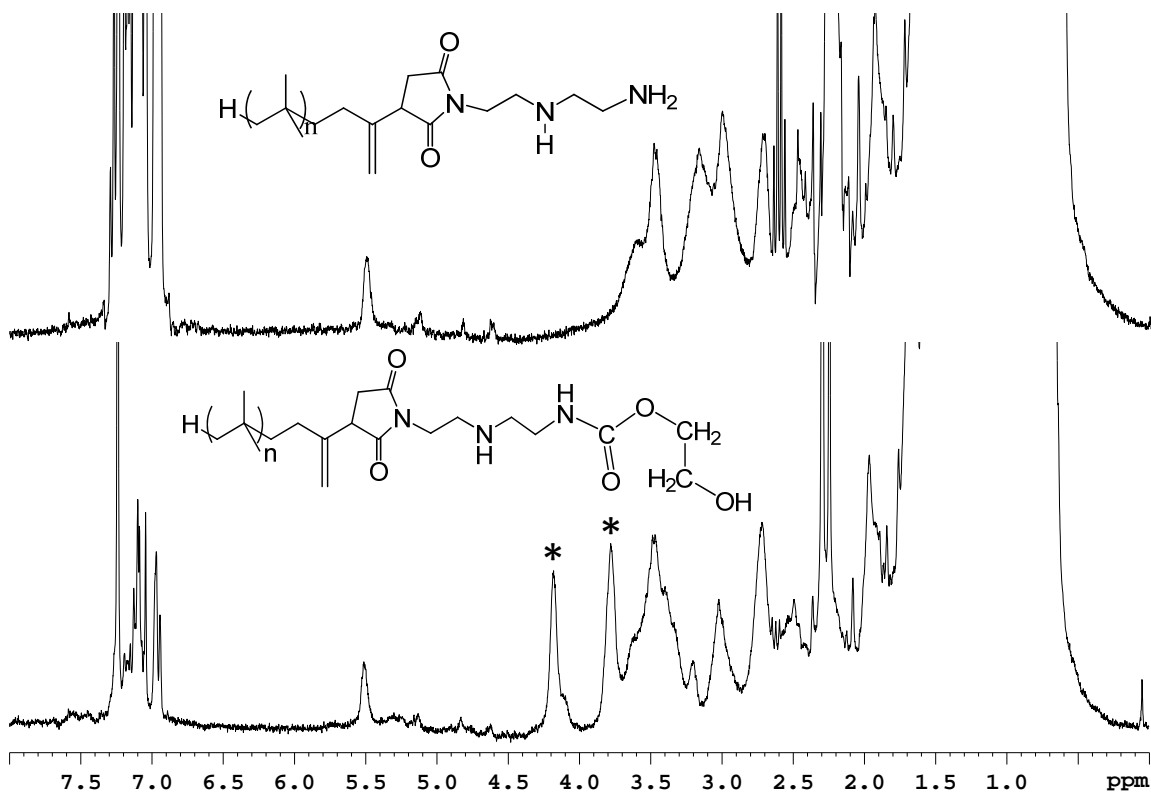


Figure 3.14. <sup>1</sup>H NMR spectra of *m*-PIBSI-DETA (top) and M-*m*-PIBSI-DETA (bottom); Peaks at 3.8 and 4.2 ppm are shown with an asterisk.

Strong peaks at 3.8 and 4.2 ppm are observed. The yield of the modification of *m*-PIBSI-DETA with its more accessible amines is significantly improved as seen from the large intensity of the peaks at 3.8 and 4.2 ppm, suggesting that steric hindrance might indeed be one of the factors hindering the modification of *b*-PIBSI-DETA.

Since the modification yield can be improved by increasing the exposure of the polar core of the dispersant to the solvent, the modification of *b*-PIBSI-TEPA which possesses an 11-atom-linker in its polar core was expected to proceed with a higher yield than the modification of *b*-PIBSI-DETA.

### **3.5.2. Synthesis and characterization of M-*b*-PIBSI-TEPA**

*b*-PIBSI-TEPA is composed of two polyisobutylene tails linked to a TEPA core via two succinimides. Three secondary amines in the polar core are available for reaction with EC. The modification of *b*-PIBSI-TEPA was conducted as follows. *b*-PIBSI-TEPA (1.0 g, 0.24 mmol) was mixed with EC (0.13g, 1.44 mmol). The mixture was dissolved in 2 mL of xylene in a 25 mL round bottom flask which was charged with a water condenser and a nitrogen inlet and outlet. The reaction mixture was heated at 120 °C for 16 hours. The ratio of reactive secondary amines to EC was set to equal 1:2 instead of 1:1 because EC tends to evaporate during the modification reaction. The modification reactions of the dispersants were carried out in a round bottom flask, capped with a water condenser and a nitrogen inlet and outlet. The reaction set up was suggested by Wollenberg.<sup>1</sup> However, with the same settings, the solvent and EC were found to evaporate during the experiments. Since an apolar solvent was used in the reactions, grease could not be used to seal the reaction apparatus. Furthermore, the flow of nitrogen in the reaction system created a positive pressure, which enhanced the evaporation of the

solvent and EC. The extra EC ensured that sufficient amounts of EC would remain in the reaction mixture for the modification.

After the reaction was completed the product mixture was dissolved in 50 mL of xylene and washed with 15 mL of water three times. The organic phase was collected and xylene was removed in a rotary evaporator. The sample was further dried in a vacuum oven at 60 °C for 24 hours. The  $^1\text{H}$  NMR spectrum of the product was obtained (Figure 3.15).

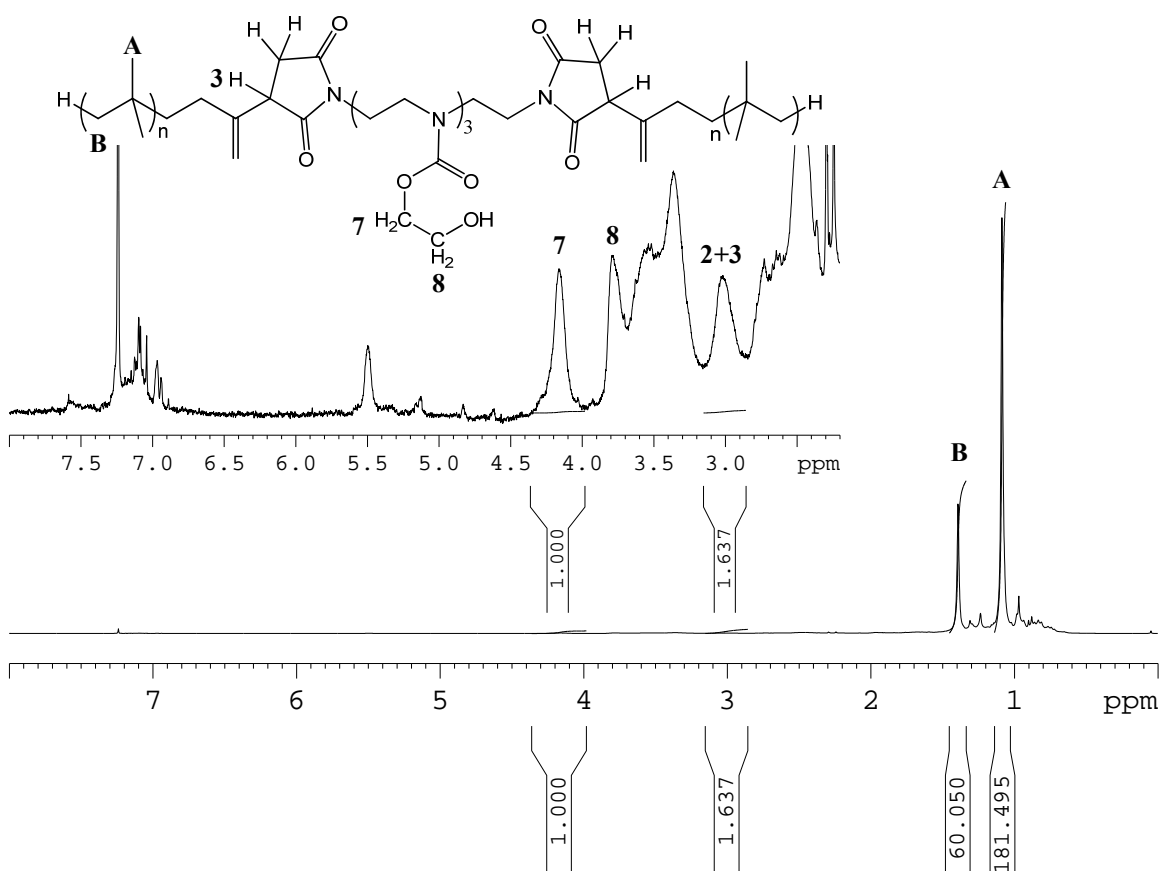


Figure 3.15.  $^1\text{H}$  NMR spectrum of M-b-PIBSI-TEPA

As for *M-m*-PIBSI-DETA, strong peaks at 3.8 and 4.2 ppm were observed. The 4.2 ppm peak is well isolated, and it was used to determine the degree of modification. According to the  $^1\text{H}$  NMR spectrum, the ratio of the peak integral corresponding to proton **7** over that of proton **B** equals 1/60. Since the  $N_{\text{SI}}/N_{\text{IB}}$  ratio of *b*-PIBSI-TEPA equals 1/34 as determined by FT-IR (see Table 3.4), the ratio of the number of secondary amines of the dispersant over that of the IB units equals 3/34. As a result, about 1/6 of the secondary amines are modified by EC, leading to a yield of 17%.

*M-b*-PIBSI-TEPA possesses a  $N_{\text{SI}}/N_{\text{IB}}$  ratio of 1/34, and 17% of the secondary amines in the polar core were modified with a carbamate ethanol side chain.

### 3.6. Conclusions

In this chapter, the synthesis of the *b*-PIBSI and *M-b*-PIBSI dispersants was described, and the chemical composition of the dispersants was investigated. Two molar equivalents of PIBSA were reacted with one molar equivalent of polyamine, DETA, TEPA, or PEHA, to synthesize *b*-PIBSI. *M-b*-PIBSI was obtained by reacting *b*-PIBSI with EC. FT-IR and  $^1\text{H}$  NMR were applied to determine the chemical composition of the dispersants.

The  $N_{\text{SA}}/N_{\text{IB}}$  ratio of PIBSA was determined to equal 1:49 by using the calibration curve established by Walch and Gaymans with FT-IR.<sup>3</sup> The ratio determined by  $^1\text{H}$  NMR was equal to 1:55. The results agree well with each other. Combining both results, the  $N_{\text{SA}}/N_{\text{IB}}$  ratio of PIBSA was found to equal 1:52±3.

Calibration curves were established by FT-IR to relate the  $N_{\text{SI}}/N_{\text{IB}}$  ratio of *b*-PIBSI dispersants to the ratio of the peak height or integral of the absorption bands at

1705  $\text{cm}^{-1}$  and 1390  $\text{cm}^{-1}$  which characterize the SI carbonyl and the IB methyl, respectively. The  $N_{\text{SI}}/N_{\text{IB}}$  ratio was found to be  $1:33 \pm 4$ ,  $1:34 \pm 5$ , and  $1:41 \pm 5$  for *b*-PIBSI-DETA, *b*-PIBSI-TEPA, and *b*-PIBSI-PEHA, respectively.  $^1\text{H}$  NMR was applied to determine the  $N_{\text{SI}}/N_{\text{IB}}$  ratio of *b*-PIBSI-DETA, and it was found to equal  $1:31 \pm 3$ . The ratio obtained with  $^1\text{H}$  NMR and FT-IR were in good agreement, suggesting that both procedures yield reliable results.

The synthesis of M-*b*-PIBSI-DETA was carried out with *b*-PIBSI-DETA whose two SI groups were separated by a 5-atom linker. However, the reaction did not yield efficient modification. A significant improvement of the modification yield was obtained when the modification was carried out using *m*-PIBSI-DETA whose amines are more accessible to EC than that of *b*-PIBSI-DETA. It suggested that the inefficient modification of *b*-PIBSI-DETA might be due to steric hindrance of the amine core of the *b*-PIBSI-DETA dispersant which inhibits the approach of EC.

The modification was carried out with *b*-PIBSI-TEPA whose two SI groups were separated by a 13-atom-linker in the polar core of the dispersant. In the  $^1\text{H}$  NMR spectrum of the modified dispersant, strong peaks at 3.8 and 4.2 ppm which are the characteristics of the modified carbamate ethanol side chain were observed. The yield of the modification was determined to be 17% for the M-*b*-PIBSI-TEPA dispersant.

## **Chapter 4**

# **Preliminary Results for the Determination of the Critical Micelle Concentration of the Dispersants**



## 4.1 Introduction

The concept of an amphiphile was first introduced by Hartley.<sup>1</sup> It refers to a family of compounds which contain moieties with an affinity for water and moieties with an affinity for oil. The dispersants used as oil additives are polymeric amphiphiles. As such, they are composed of one hydrophilic moiety, often referred to as the head group, which is covalently bonded to one or two hydrophobic moieties, generally an alkyl chain also called the tail.<sup>2,3</sup> The dispersant studied in this project is *bis*-polyisobutylene succinimide (*b*-PIBSI) and modified *bis*-polyisobutylene succinimide (*M*-*b*-PIBSI). The structures of these dispersants are shown in Figure 4.1.

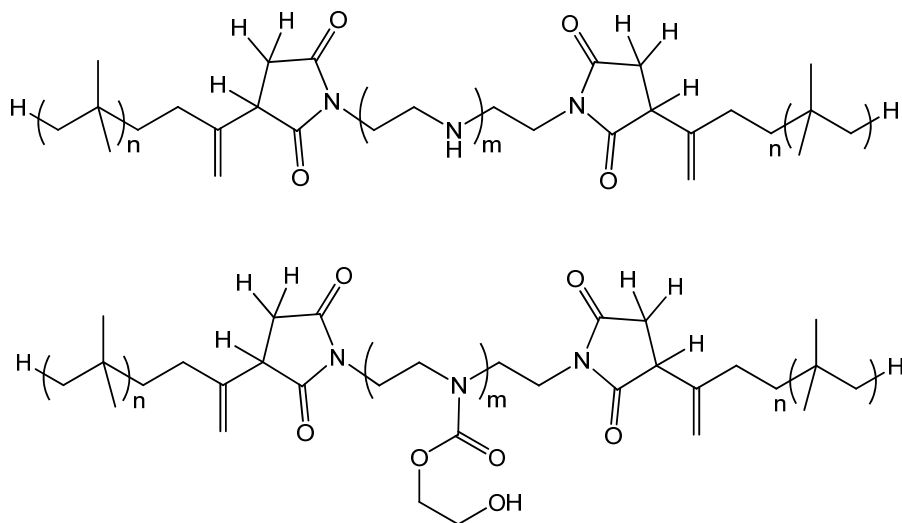


Figure 4.1. Chemical structure of *b*-PIBSI (top) and *M*-*b*-PIBSI (bottom)

*b*-PIBSI is made of two polyisobutylene (PIB) apolar tails linked by a succinimide to a polyamine polar core. The polyamines used in this project are diethylene triamine

(DETA) and tetraethylene pentamine (TEPA) which possess one and three secondary amines, respectively. *M-b*-PIBSI is synthesized by modifying the secondary amine of *b*-PIBSI with ethylene carbonate. *M-b*-PIBSI is the derivative of *b*-PIBSI with an ethanol carbamate replacing the proton of the secondary amines in the polyamine core.

In an apolar solvent such as hexane where the polar moiety of the dispersant is insoluble, the long apolar tails stabilize the polar core of the amphiphilic dispersant, despite the fact that contacts between the polar moiety and the apolar solvent are energetically unfavourable. As the concentration of the dispersant is increased, it reaches a certain concentration where the dispersants start to self-associate into reverse micelles in order to minimize the exposure of the polar moieties to the apolar solvent.<sup>4-6</sup> The concentration at which the dispersants start to form reverse micelles is called the critical micelle concentration (CMC) which is the most important parameter used to describe a dispersant. In reverse micelles, the polar heads are in contact with one another, forming a polar core that is coated by the apolar tails (Figure 4.2). The formation of micelles is a cooperative process that is spontaneous and reversible. Micelles are thermodynamically stable and are in chemical equilibrium with free dispersants (Figure 4.2).<sup>7</sup>

Compounds that are normally insoluble in hexane can be solubilised by the polar core of reverse micelles. As a result, monitoring the solubility of an insoluble additive yields the CMC of a dispersant as it becomes soluble only in the presence of reverse micelles. *bis*-(2,2'-Bipyridine)-ruthenium(II)-5-amino-1,10-phenanthroline hexafluorophosphate ( $[\text{RuNH}_2]2\text{PF}_6$ ) is a chromophore which is barely soluble in hexane. The solubility of  $[\text{RuNH}_2]2\text{PF}_6$  at different dispersant concentrations can be detected by

fluorescence. The concentration at which a significant increase of the  $[\text{RuNH}_2]2\text{PF}_6$  fluorescence is observed represents the CMC of the dispersant.

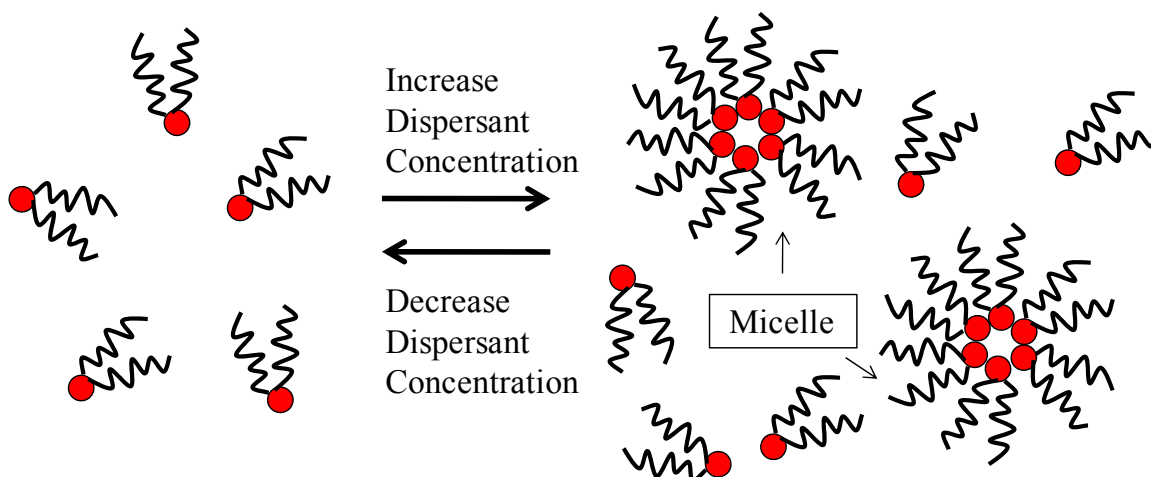


Figure 4.2. Formation of reverse micelles by an amphiphilic polymeric dispersant

## 4.2 Experimental Procedures

### 4.2.1 Chemicals

The solvents were all HPLC grade. Hexane, acetone, toluene, and acetonitrile were purchased from Caledon. Ethanol was obtained from Fisher Scientific. They were used as received. *cis-bis*(2,2'-Bipyridine) dichlororuthenium(II)hydrate ( $\text{Ru}(\text{bpy})_2\text{Cl}_2$ ), ammonium hexafluorophosphate ( $\text{NH}_4\text{PF}_6$ ), and aluminum oxide (neutral, activated) were purchased from Sigma-Aldrich. 5-Amino-1,10-phenanthroline (5-phen) was purchased from Polysciences Inc. (Warrington, PA).

#### 4.2.2 Instrumentation: Steady-state Spectrofluorometer

All the fluorescence spectra were acquired on a Photon Technology International (PTI) fluorometer using the right angle geometry. All the samples were outgassed with a gentle flow of nitrogen for 45 minutes before the measurements. The emission spectra were acquired by exciting the solution at 452 nm and the emission spectra were collected from 470 nm to 800 nm.

#### 4.2.3. Sample Preparation for CMC measurements

The dispersant solutions with concentration ranging from 0.005 g/L to 1 g/L were prepared in hexane.  $[\text{RuNH}_2]_2\text{PF}_6$  was used as the chromophore to probe the formation of the dispersant micelles at the molecular level by fluorescence. A stock solution of  $[\text{RuNH}_2]_2\text{PF}_6$  in acetonitrile with a concentration of 87.6  $\mu\text{M}$  was prepared of which 356 mg was added to a 20 mL vial. Acetonitrile was removed under a gentle flow of nitrogen leaving a thin film of  $[\text{RuNH}_2]_2\text{PF}_6$  at the bottom of the vial. 10 mL of the dispersant solution was added into the vial. The solution was stirred and its fluorescence intensity was monitored over time.

#### 4.3 Chromophore: *bis*-(2,2'-bipyridine)-ruthenium(II)-5-amino-1,10-phenanthroline hexafluorophosphate

The chromophore used to obtain the CMC of the dispersant micelles is *bis*-(2,2'-bipyridine)-ruthenium(II)-5-amino-1,10-phenanthroline hexafluorophosphate ( $[\text{RuNH}_2]_2\text{PF}_6$ ).  $[\text{RuNH}_2]_2\text{PF}_6$  is a chromophore which emits at 600 nm in acetone when excited at 452 nm (Figure 4.3).

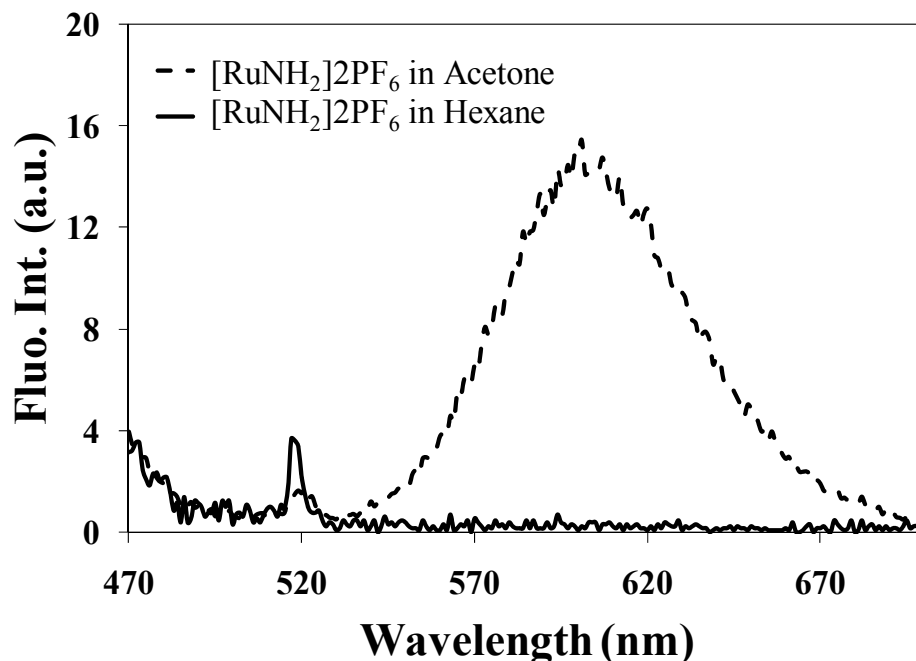
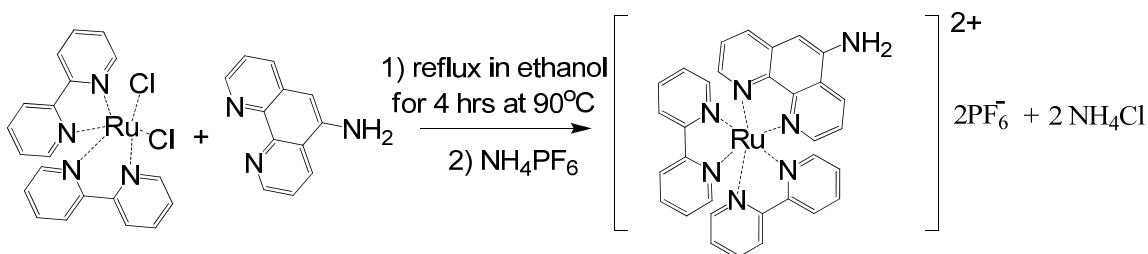


Figure 4.3. Fluorescence spectra of  $[\text{RuNH}_2]_2\text{PF}_6$  in acetone and hexane; the peak at 520 nm for the spectrum in hexane is due to light scattering. ( $\lambda_{\text{ex}}=452$  nm)

#### 4.3.1 Synthesis of $[\text{RuNH}_2]_2\text{PF}_6$

$[\text{RuNH}_2]_2\text{PF}_6$  was synthesized by coupling 5-amino-1,10-phenanthroline with *cis-bis*(bipyridyl) ruthenium (II) dichloride as shown in Scheme 4.1 according to procedures established by Ellis et al.<sup>8</sup> *cis-bis*(2,2'-Bipyridine)dichlororuthenium(II)hydrate ( $\text{Ru}(\text{bpy})_2\text{Cl}_2$ ) (0.34 mmol, 171 mg) was dissolved in 9 mL of hot Milli Q water. 5-Amino-1,10-phenanthroline (5-phen) (0.40 mmol, 84 mg) was dissolved in 17 mL of hot ethanol. The two solutions were combined in a round bottom flask and the mixture was outgassed for 20 minutes. The reaction was complete after refluxing for 4 hours at 100 °C. Ethanol was removed by using a rotary evaporator. The remaining solution was cooled in an ice bath for 20 minutes.

Ammonium hexafluorophosphate ( $\text{NH}_4\text{PF}_6$ ) (1.7 mmol, 270 mg) was added into the ice cooled solution. The product with  $\text{PF}_6^-$  as the counter ion was precipitated out of the water solution. The precipitate was filtered and washed with 1 mL Milli Q water twice. The residue was collected and dried under vacuum for one hour.



Scheme 4.1. Synthesis of  $[\text{RuNH}_2]_2\text{PF}_6$

#### 4.3.2. Purification of $[\text{RuNH}_2]_2\text{PF}_6$

The product is purified by the method established by Ellis et al.<sup>8</sup> and modified by Christina Quinn.<sup>9</sup> A neutral aluminum oxide column was used to remove the impurities present. The dried product was dissolved in a minimal amount of acetone (~1.5 mL) and a solution with a 1:2 ratio of toluene to acetonitrile was used as the eluent. The purified product was collected and dried under vacuum. The product was dissolved in acetone and precipitated from ether. The precipitate was dried under vacuum for one hour. The mass spectrum of the product is shown in Figure 4.4. In the mass spectrum, the group of peaks at 304 m/z represents the mass to charge ratio of the  $[\text{RuNH}_2]^{2+}$  ion. The group of peaks at 754 m/z represents the mass to charge ratio of the  $[\text{RuNH}_2]^{2+}\text{PF}_6^-$  ion. The molecular weight of  $[\text{RuNH}_2]_2\text{PF}_6$  is 898 g/mol.

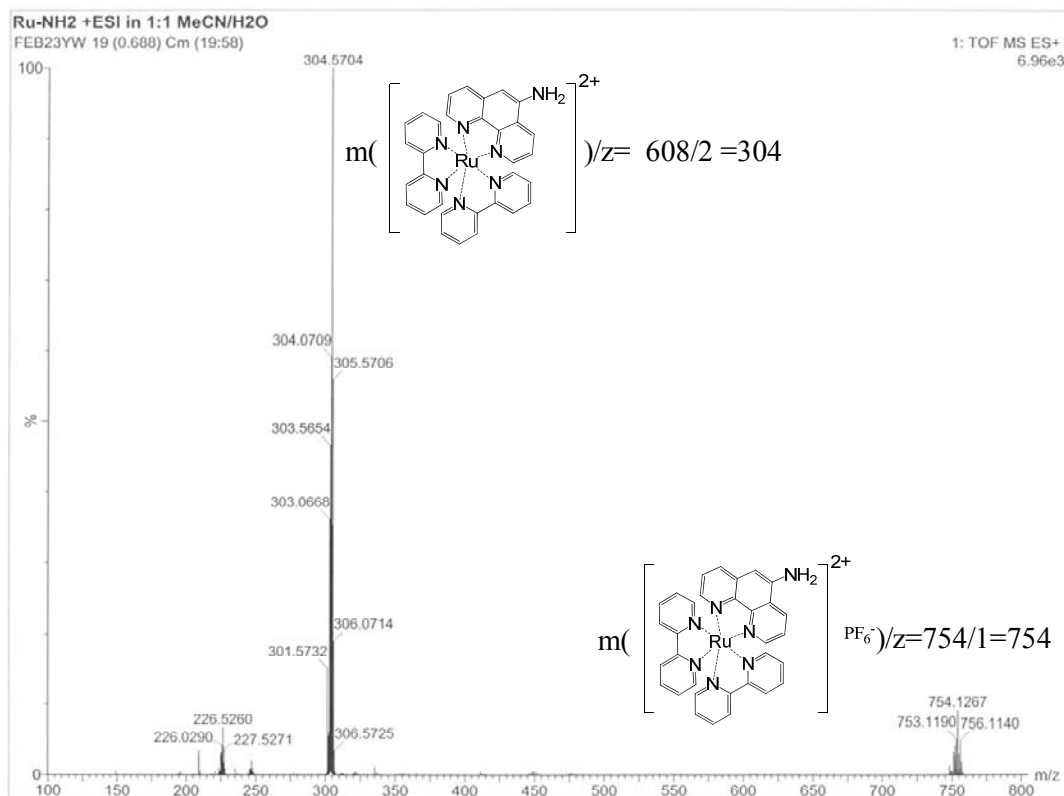


Figure 4.4. Mass spectrometry spectrum of  $[\text{RuNH}_2]_2\text{PF}_6$

#### 4.4. CMC measurements

$[\text{RuNH}_2]_2\text{PF}_6$  was the chromophore used in the CMC characterization. The free amine in the ruthenium complex is expected to enhance its association with the amine-rich core of the reverse micelles.<sup>10</sup>  $[\text{RuNH}_2]_2\text{PF}_6$  is only soluble in polar solvents such as acetone, and it is barely soluble in apolar solvents such as hexane (Figure 4.3). Hexane is a good solvent for the modified and unmodified dispersants. At low dispersant concentration below the dispersant CMC where the dispersants do not form micelles,  $[\text{RuNH}_2]_2\text{PF}_6$  is insoluble and the hexane solution shows weak  $[\text{RuNH}_2]_2\text{PF}_6$  fluorescence intensity. When the dispersant concentration increases to the CMC of the dispersant, the dispersants start to form reverse micelles. The dispersant micelles generate

polar microdomains that solubilise  $[\text{RuNH}_2]_2\text{PF}_6$ . As a result, high fluorescence intensity of  $[\text{RuNH}_2]_2\text{PF}_6$  is observed. Monitoring the fluorescence intensity of  $[\text{RuNH}_2]_2\text{PF}_6$  as a function of dispersant concentration yields the CMC by finding the dispersant concentration where the fluorescence intensity of  $[\text{RuNH}_2]_2\text{PF}_6$  increases significantly.

Figure 4.5 shows the fluorescence spectra of a 0.13 g/L *b*-PIBSI solution with and without  $[\text{RuNH}_2]_2\text{PF}_6$  added. The *b*-PIBSI dispersant solution was excited at 452 nm, and the emission spectra were collected from 470 to 800 nm. The dispersant emits at 490 nm, and  $[\text{RuNH}_2]_2\text{PF}_6$  emits at 590 nm when it is solubilised by the dispersant micelles.

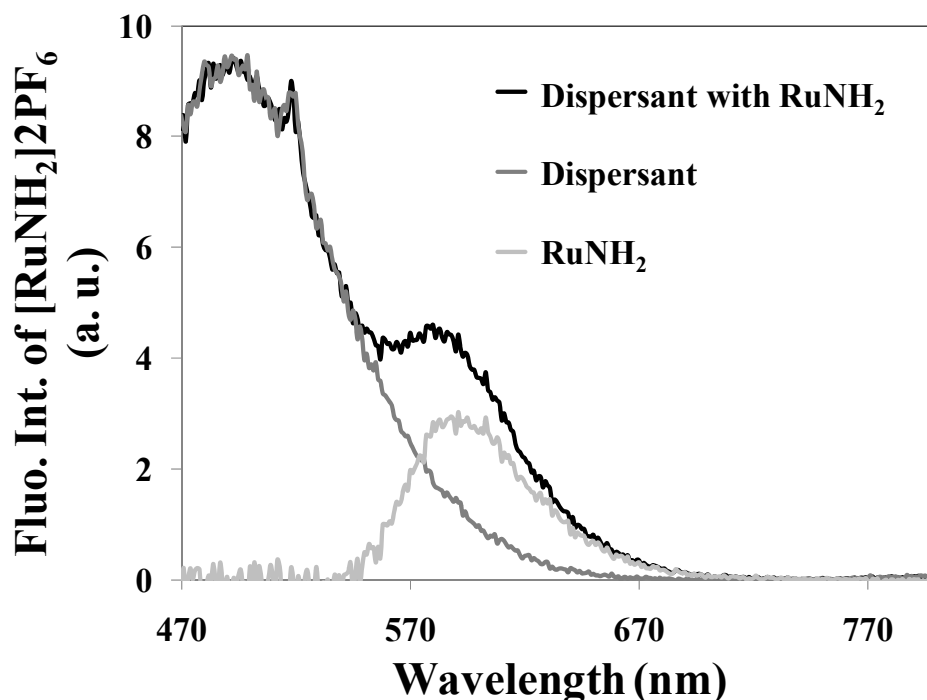


Figure 4.5. Fluorescence spectra of dispersant with  $[\text{RuNH}_2]_2\text{PF}_6$  added, dispersant, and  $[\text{RuNH}_2]_2\text{PF}_6$ ;  $[\text{PIBSI}] = 0.13 \text{ g/L}$ ,  $[[\text{RuNH}_2]_2\text{PF}_6] = 4 \mu\text{M}$



In the fluorescence spectrum of the solution containing both the dispersant and  $[\text{RuNH}_2]2\text{PF}_6$  added, the dispersant emission overlaps that of  $[\text{RuNH}_2]2\text{PF}_6$ . In order to obtain the fluorescence spectrum of  $[\text{RuNH}_2]2\text{PF}_6$  solubilised in the micelles, the spectrum of the dispersant solution was subtracted from that of the solution containing both the dispersant and  $[\text{RuNH}_2]2\text{PF}_6$  to yield the fluorescence spectrum of  $[\text{RuNH}_2]2\text{PF}_6$  only (Figure 4.5).

Preliminary experiments were conducted to determine how long the solubilisation of  $[\text{RuNH}_2]2\text{PF}_6$  in the dispersant solution would take before reaching equilibrium. To this end, the fluorescence of the *b*-PIBSI solution was monitored once a day as the film of  $[\text{RuNH}_2]2\text{PF}_6$  left at the bottom of the vial would slowly dissolve into the polar core of the reverse micelles. The results are shown in Figure 4.6.

In Figure 4.6 A, the fluorescence intensity of  $[\text{RuNH}_2]2\text{PF}_6$  in the *b*-PIBSI-TEPA solution increases continuously with increasing time suggesting that equilibrium was not reached even after waiting for 5 days. A similar trend is observed in Figure 4.6 B, for the *M-b*-PIBSI-TEPA solution although the lower fluorescence intensity obtained on the fifth day could indicate the onset of a plateau and that their equilibrium has been reached. However, more data acquired at longer times are required in order to definitely demonstrate that equilibrium is reached.

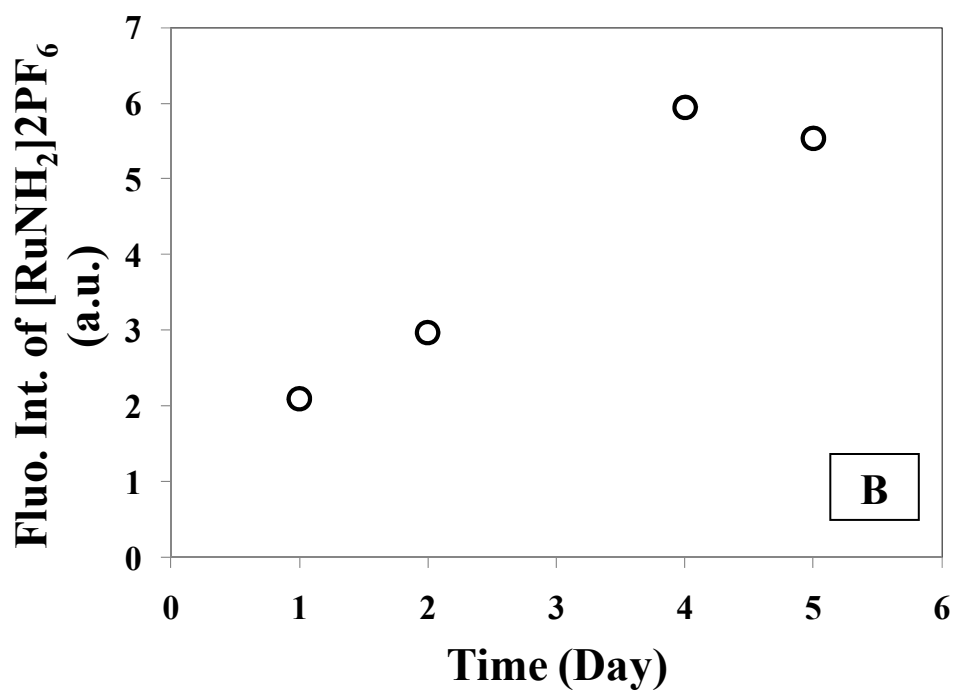
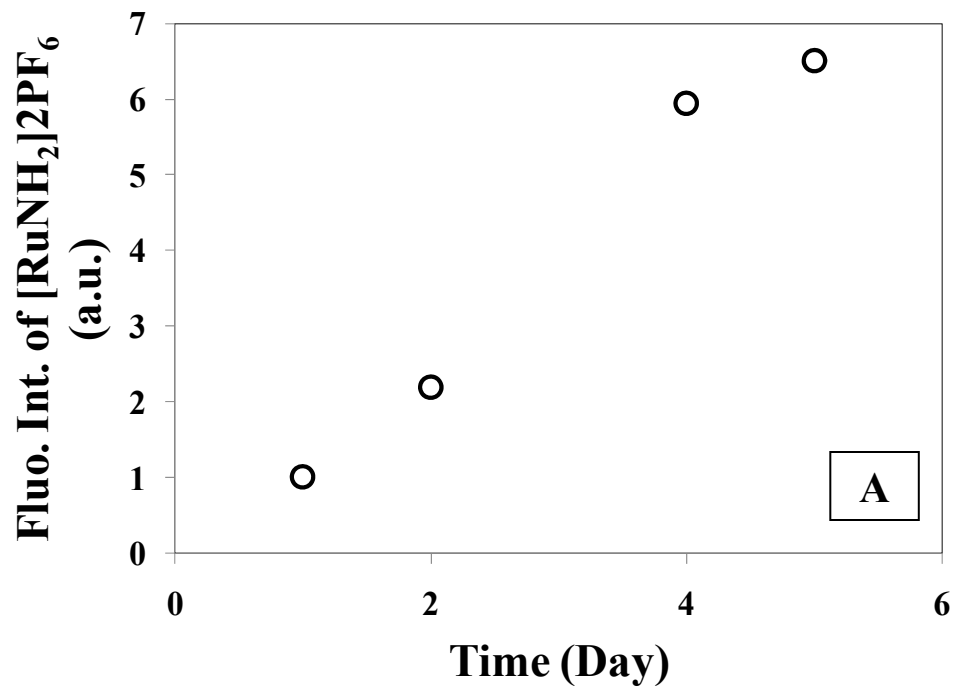


Figure 4.6. Time study of the fluorescence intensity of [RuNH<sub>2</sub>]<sub>2</sub>PF<sub>6</sub> in the dispersant solution; [*b*-PIBSI-TEPA]=1.1 g/L (top), [*M-b*-PIBSI-TEPA]=0.8 g/L (bottom); [[RuNH<sub>2</sub>]<sub>2</sub>PF<sub>6</sub>]=4 μM for both solutions.

Figure 4.7 shows a preliminary trend obtained with the dispersant/[RuNH<sub>2</sub>]<sub>2</sub>PF<sub>6</sub> solutions stirred for 5 days. The fluorescence intensity of [RuNH<sub>2</sub>]<sub>2</sub>PF<sub>6</sub> increases as the dispersant concentration increases indicating that reverse micelles are present at dispersant concentration greater than 0.01 g/L. However, the data were obtained before equilibrium was reached. To obtain a reliable CMC, another set of data will need to be acquired after waiting for longer times to ensure that equilibrium has been reached.

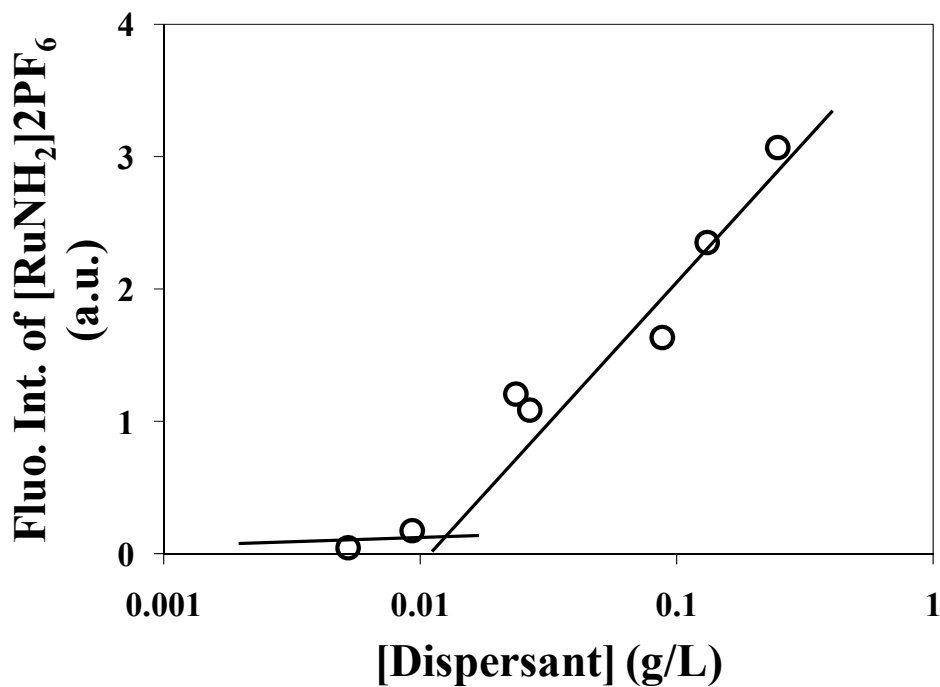


Figure 4.7. CMC measurement of *b*-PIBSI-TEPA after the dispersant/[RuNH<sub>2</sub>]<sub>2</sub>PF<sub>6</sub> solution was stirred for 5 days

## 4.5. Conclusions

The chromophore  $[\text{RuNH}_2]2\text{PF}_6$  was successfully synthesized.  $[\text{RuNH}_2]2\text{PF}_6$  was insoluble in hexane but it could be incorporated in the polar core of *b*-PIBSI micelles. Time-dependent studies indicated that the incorporation of  $[\text{RuNH}_2]2\text{PF}_6$  occurs over a time period longer than 5 days, the largest time period studied so far. To obtain a reliable CMC measurement, the time needed for the solutions to reach equilibrium must be determined so that the fluorescence measurements can be carried out on equilibrated dispersant and  $[\text{RuNH}_2]2\text{PF}_6$  solutions.

## **Chapter 5**

### **Conclusions and Future Work**

## 5.1 Conclusions

This thesis investigated the modification of *bis*-polyisobutylene succinimide (*b*-PIBSI) dispersants with ethylene carbonate (EC) to yield the M-*b*-PIBSI dispersants. Dispersants are usually used in engine oil to reduce sludge formation and ultra fine particle (UFP) emissions.<sup>1-3</sup> The type of dispersant considered in this thesis is composed of two apolar tails and a polar core. UFPs whose surface is covered with polar groups are generated during the normal engine operation. In the apolar engine oil, UFPs aggregate to form large particles in order to minimize contacts between their polar surface and the apolar solvent. Further aggregation induces the large particles to precipitate out of the oil and form sludge which causes various engine problems.<sup>4,5</sup> When dispersants are present in the apolar engine oil, the polar moiety of the dispersant will adsorb onto the surface of the UFPs. The apolar tails of the dispersants extend into the oil, stabilizing the UFPs. As a result, the aggregation of the UFPs is significantly reduced.

As presented in Chapter 3, a series of *b*-PIBSI dispersants were successfully synthesized with the polyamines diethylene triamine (DETA), tetraethylene pentamine (TEPA), and pentaethylene hexamine (PEHA). *b*-PIBSI-TEPA was efficiently modified with EC to form the modified *b*-PIBSI-TEPA dispersant (M-*b*-PIBSI-TEPA) (see Scheme 3.3 and 3.4).<sup>6</sup>

The chemical composition of the *b*-PIBSI dispersants could be estimated by FT-IR.<sup>7</sup> The ratio of the number of succinimide (SI) units ( $N_{SI}$ ) over that of isobutylene (IB) units ( $N_{IB}$ ) was determined by using a calibration curve. The calibration curve related the  $N_{SI}/N_{IB}$  ratio to the IR absorption of the SI carbonyl and the IB methyl in the FT-IR spectra.

The study described in Chapter 3 illustrates how efficiently FT-IR was used to determine the chemical composition of the *b*-PIBSI dispersants. Unfortunately, after the modification of the *b*-PIBSI dispersants, another carbonyl group was formed whose absorption overlapped that of the SI carbonyl in the FT-IR spectra of the *M-b*-PIBSI dispersants. Since it was difficult to separate the overlapping carbonyl absorption peaks in the FT-IR spectra,  $^1\text{H}$  NMR was used instead to determine the degree of modification.

At the early stage of the project, the  $^1\text{H}$  NMR peaks in the NMR spectrum of the modified (*M-b*-PIBSI) and unmodified (*b*-PIBSI) dispersants were difficult to assign. Two strong peaks were observed in the  $^1\text{H}$  NMR spectrum of the dispersants at 1.4 and 1.1 ppm representing the methylene protons and the methyl protons of the PIB backbone, respectively. Since the number of protons of the IB monomers is significantly larger than the number of protons found in the units forming the polar core of the dispersants, the protons in the polar core characteristic of the SI unit could not be easily detected and concentrated (>30 g/L) dispersant sample were used to enhance the  $^1\text{H}$  NMR signal. Several model compounds were prepared to mimic the polar core of the dispersant, and the  $^1\text{H}$  NMR spectra of the model compounds were acquired to be used as reference for the polymer spectra.

Methyl succinic anhydride (MSA) was used as a model compound to mimic the succinic anhydride (SA) of PIBSA. In the  $^1\text{H}$  NMR spectrum of MSA, the peak of proton **1** shown in Figure 5.1 appeared at 2.6 ppm and the peaks of protons **2** and **3** overlapped at 3.2 ppm. In the  $^1\text{H}$  NMR spectrum of PIBSA, the proton **1** peak appeared at 2.6 ppm and the peaks of protons **2** and **3** overlapped at 3.3 ppm. The ratio of the integral of the peak

at 3.3 ppm over the integral of the peak at 1.4 ppm was used to determine the ratio of the number of SA units ( $N_{SA}$ ) over that of the IB units ( $N_{IB}$ ) for PIBSA.

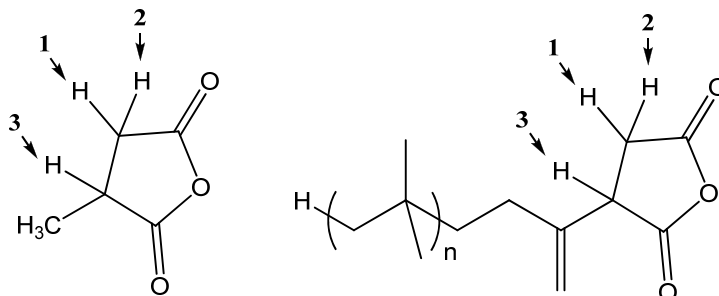


Figure 5.1. Structures of MSA (left) and PIBSA (right)

Another model compound, namely *bis*-methyl succinimide-DETA (*b*-MSI-DETA), was synthesized by reacting two molar equivalents of MSA with one molar equivalent of DETA. *b*-MSI-DETA shown in Figure 5.2 possesses a similar structure as the polar core of *b*-PIBSI-DETA.

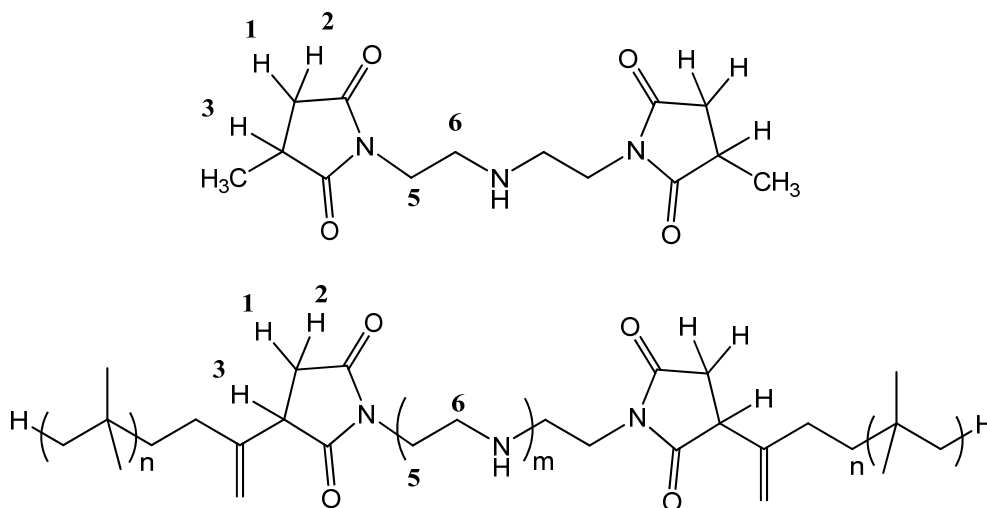


Figure 5.2. Chemical structures of *b*-MSI-DETA (top) and *b*-PIBSI-DETA (bottom)



Using the  $^1\text{H}$  NMR spectrum of *b*-MSI-DETA as reference, the peaks at 2.5 and 3.0 ppm were assigned to the protons on the SI ring, and the peaks at 2.7 and 3.5 ppm to the protons on the ethylene segments in the polar core of *b*-PIBSI-DETA. The ratio of the integral of the peak at 3.5 ppm over the integral of the peak at 1.4 ppm was used to determine the ratio of the number of SI units ( $N_{\text{SI}}$ ) over that of the IB units ( $N_{\text{IB}}$ ).

2-Hydroxyethyl *N,N*-dibutyl carbamate (HEDBC) shown in Figure 5.3 was synthesized by reacting dibutyl amine with EC to mimic the polar core of *M-b*-PIBSI-DETA. HEDBC possesses a similar structure as the polar core of *M-b*-PIBSI-DETA. Using the spectrum of HEDBC as reference, the peaks at 3.8 and 4.2 ppm were assigned to the protons on the ethylene groups of the modified ethanol carbamate side chain of the *M-b*-PIBSI-DETA dispersant. The ratio of the integral of the peak at 4.2 ppm over the integral of the peak at 1.4 ppm was used to determine the degree of modification.

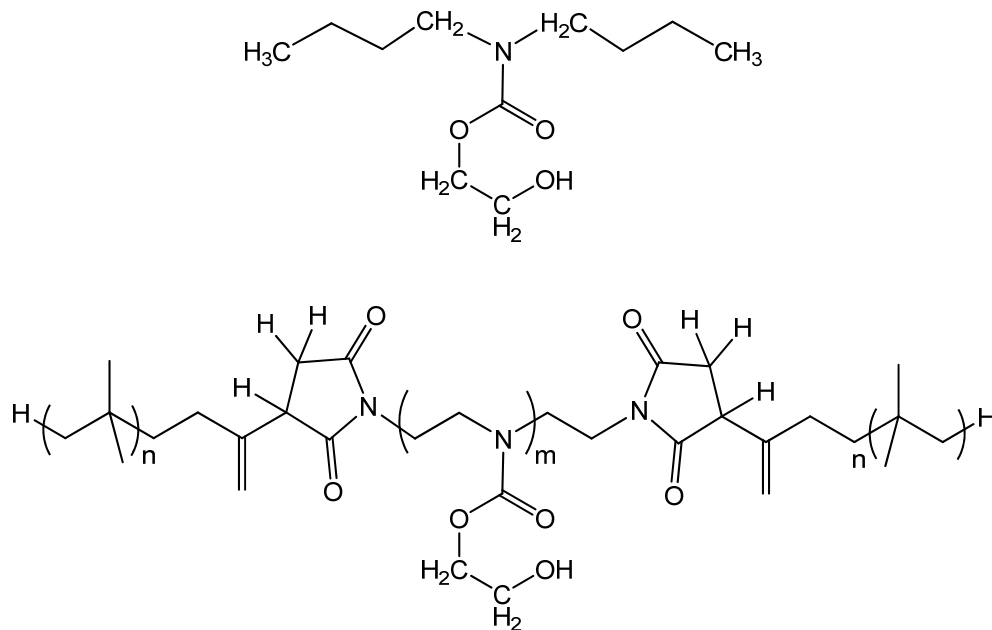


Figure 5.3. Chemical structures of HEDBC (top) and *M-b*-PIBSI-DETA (bottom)

The chemical composition of the *b*-PIBSI dispersants was determined by FT-IR and  $^1\text{H}$  NMR. The results obtained by these two techniques were in relatively good agreement with each other, suggesting that both techniques give reliable results (Table 3.3). Using FT-IR, the  $N_{\text{SI}}/N_{\text{IB}}$  ratios of *b*-PIBSI-DETA, *b*-PIBSI-TEPA, and *b*-PIBSI-PEHA were determined to equal  $1:33\pm 4$ ,  $1:34\pm 5$ , and  $1:41\pm 5$ .

*M-b*-PIBSI-DETA was synthesized under various conditions in order to obtain a high degree of modification. Unfortunately, the yields obtained were very low in all but one example. After numerous fruitless trials, I suspected that EC might be prevented from accessing the secondary amine of the *b*-PIBSI-DETA core due to steric hindrance. In order to confirm whether steric hindrance might be responsible for the poor modification yield, the modification reaction was carried out with *m*-PIBSI-DETA whose amines located at the end of the PIB chain were expected to be more accessible to EC. Strong peaks at 3.8 and 4.2 ppm in the  $^1\text{H}$  NMR spectrum of the *M-m*-PIBSI-DETA dispersant (Figure 3.16) were observed suggesting that steric hindrance might indeed be one of the factors hindering the modification of *b*-PIBSI-DETA.

A higher degree of modification was also obtained with *b*-PIBSI-TEPA where the secondary amines were more accessible than the single one of *b*-PIBSI-DETA. Using a combination of FT-IR and  $^1\text{H}$  NMR techniques, it was estimated that 17% of all amines of *b*-PIBSI-TEPA had been modified.

Preliminary results were also obtained for the determination of the CMC of the dispersants. To this end, *bis*-(2,2'-bipyridine)-ruthenium(II)-5-amino-1,10-phenanthroline hexafluorophosphate ( $[\text{RuNH}_2]2\text{PF}_6$ ) was successfully synthesized by following the

method established by Ellis et al.<sup>8</sup> and modified by Christina Quinn.<sup>9</sup> The fluorescence intensity of [RuNH<sub>2</sub>]<sub>2</sub>PF<sub>6</sub> was monitored over time as it was incorporated into the polar core of the reverse micelles generated by the dispersants. Over a period of five days, the fluorescence signal of [RuNH<sub>2</sub>]<sub>2</sub>PF<sub>6</sub> increased continuously. This study led to the conclusion that a longer time was required to allow [RuNH<sub>2</sub>]<sub>2</sub>PF<sub>6</sub> to equilibrate in the dispersant solutions.

## 5.2 Future Work

### 5.2.1. Why are the N<sub>SA</sub>/N<sub>IB</sub> ratio of PIBSA and the N<sub>SI</sub>/N<sub>IB</sub> ratio of *b*-PIBSI dispersants different?

The N<sub>SA</sub>/N<sub>IB</sub> ratio of PIBSA and the N<sub>SI</sub>/N<sub>IB</sub> ratio of the *b*-PIBSI dispersants were found to equal 1:52±3 and 1:33±4, respectively. Apparently excess SI was generated during the coupling reaction. PIBSA is composed of one PIB tail and a SA polar head, while *b*-PIBSI is composed of two PIB tails linked via two SI moieties. One possible problem might be the proximity of the succinimide moieties in the *b*-PIBSI dispersants which might affect their <sup>1</sup>H NMR and FT-IR response compared to the succinimide model compounds used to build the calibration curves (Figure 3.7 and 3.8). To this end, we are planning to use *bis*-methyl succinimide-DETA (*b*-MSI-DETA) in Figure 5.2 to generate the calibration curve by FT-IR instead of using *N*-methyl succinimide (MSI).

Another experiment to conduct would be to react PIBSA with 1-pyrenemethyl amine (PMA) to generate PIBSI-Py. The molar extinction coefficient of 1-pyrenemethyl succinimide can be used to determine the SI content of PIBSI-Py and compare it with the results obtained by <sup>1</sup>H NMR and FT-IR.

### 5.2.2. Determination of the CMC of *b*-PIBSI and M-*b*-PIBSI dispersants

The dispersant solutions will be allowed to equilibrate with  $[\text{RuNH}_2]_2\text{PF}_6$  for a time period longer than 5 days. After equilibrium has been reached, the fluorescence intensity of  $[\text{RuNH}_2]_2\text{PF}_6$  will be monitored as a function of dispersant concentration. The dispersant concentration above which emission from  $[\text{RuNH}_2]_2\text{PF}_6$  can be detected will be assigned as the CMC of the dispersants.

### 5.2.3. Adsorption of the M-*b*-PIBSI dispersants onto carbon black particles

The other part of this research project is to obtain the adsorption isotherms describing the adsorption of the M-*b*-PIBSI dispersants onto carbon black particles (CBPs), and compare them with that of the unmodified *b*-PIBSI dispersants.

Following a protocol established earlier,<sup>7</sup> a certain amount of dispersant and CBPs will be mixed in a known volume of hexane. The mixture will be stirred for 14 hours. After equilibrium is reached, the solution will be filtered, leaving dispersant in the filtrate that did not adsorb onto the CBPs in the solution. The concentration of the free dispersant in the solution,  $C_{\text{eq}}$ , can be determined by using the change in absorption exhibited by a pH indicator that responds to the number of amines present in the solution.<sup>10,11</sup> The amount of adsorbed dispersant at equilibrium ( $\Gamma$ ) is calculated with Equation 1, where  $C_0$  and  $C_{\text{eq}}$  are the concentrations of dispersant in the solution before and after adsorption, respectively. In Equation 1,  $V$  is the volume of the solution,  $m$  is the mass of the CBPs, and  $A$  is the surface area of the CBPs, which was determined to be  $764 \text{ m}^2/\text{g}$ .<sup>5</sup>

$$\Gamma = \frac{(C_0 - C_{eq}) \times V}{m \times A} \quad (1)$$

The Langmuir model can be used to describe the adsorption of the dispersants onto CBPs. The relation that exists between the amount of dispersant bound to the CBPs ( $\Gamma$ ) and the concentration of unbound dispersant ( $C_{eq}$ ) is given by Equation 2, where  $\Gamma_{max}$  is the maximum amount of dispersant that can be adsorbed onto the CBPs and  $K$  represents the equilibrium constant describing the binding of the dispersant onto the CBPs.

$$\Gamma = \frac{\Gamma_{max} K C_{eq}}{1 + K C_{eq}} \quad (2)$$

Equation 2 can be rearranged into Equation 3 in order to obtain  $\Gamma_{max}$  and  $K$ . By plotting  $1/\Gamma$  versus  $1/C_{eq}$ , a straight line can be obtained, with  $1/(\Gamma_{max} K)$  and  $1/\Gamma_{max}$  being the slope and intercept of the line, respectively.

$$\frac{1}{\Gamma} = \frac{1}{\Gamma_{max} K} \times \frac{1}{C_{eq}} + \frac{1}{\Gamma_{max}} \quad (3)$$

The  $\Gamma_{\max}$  and K values obtained from the analysis of the adsorption isotherm of *M-b*-PIBSI can be compared with that of *b*-PIBSI to determine which dispersant is better suited to stabilize CBPs in solution.

## References

### Chapter 1

1. Wills, J.G., *Lubrication Fundamentals*, Mobil Oil Corporation, New York, 1980.
2. Ranney, M. W., *Lubricant Additives Recent Developments*, Noyes Data Corporation, Park Ridge, 1978.
3. Ritter, S. C & *EN* **2005**, Sept 5, 20-22.
4. Tomlinson, A.; Danks, T. N.; Heyes, D. M. *Langmuir* **1997**, *13*, 5881-5893.
5. Bezot, P.; Hesse-Bezot, C.; Divraison, C. *Carbon* **1997**, *35*, 53-60.
6. Jao, T. C.; Passut, C. A. *Handbook of Detergents, Part D : Formulation*, Showell, M. S. Ed., CRC Press, Taylor and Francis Group, Boca Raton, FL, **2006**, 437-471.
7. Gallopoulos, N. E. *Soc. Autom. Eng.* **1970 SP Paper** No 700506; Edmisten, W. C. Peterson, J. V., Sholts, R. S. *Soc. Autom. Eng.* **1970 SP Paper** No 700509.
8. Anderson, R. G.; Drummond, A. Y.; Stuart, F. A. United State Patent, 1965, 3,202,678.
9. Le Suer, W. M.; Norman, G. R. United States Patent, 1966, 3,272,747.
10. Le Suer, W. M.; Norman, G. R. United States Patent, 1967, 3,172,892, 3,219,666 and 3,341,542.
11. Kertes, A.S.; Kitahara, A.; El Seoud, O.A., *Nonionic Surfactants : Physical Chemistry*, Schick, M., ed., Marcel Dekker, New York, **1987**.
12. Honig, J.G.; Singleterry, C.R., *J. Phys. Chem.* **1956**, *60*,1114.
13. Hinze, W.L., *Organized Assemblies in Chemical Analysis Volume 1 Reverse Micelles*, JAI Press Inc., London, **1994**.
14. Shen, Y.; Duhamel, J., *Langmuir* **2008**, *24*, 10665-10673.

15. Davies, M.; Moreton, D. J., Patent No. WO2009055518.
16. Wollenberg, R. H.; Rafael, S.; Plavac, F. *United States Patent*, **1989**, 4,802,893.

## Chapter 2

1. Shen, Y.; Duhamel, J. *Langmuir* **2008**, *24*, 10665-10673.
2. Housecroft, C. E.; Sharpe, A. G., *Inorganic Chemistry Second Edition*, Pearson, Harlow, **2001**.
3. Wollenberg, R. H.; Rafael, S.; Plavac, F. *United States Patent*, **1989**, 4,802,893.
4. Tessier, M.; Maréchal, E. *Eur. Polym. J.* **1984**, *20*, 281-190.
5. Tessier, M.; Maréchal, E. *Eur. Polym. J.* **1990**, *26*, 499-508.

## Chapter 3

1. Wollenberg, R. H.; Rafael, S.; Plavac, F. *United States Patent* **1989**, 4,802,893.
2. Shen, Y.; Duhamel, J. *Langmuir* **2008**, *24*, 10665-10673.
3. Walch, E.; Gaymans, R. *J. Polymer* **1994**, *35*, 1774-1778.
4. Tessier, M.; Maréchal, E. *Eur. Polym. J.* **1984**, *20*, 281-190.
5. Tessier, M.; Maréchal, E. *Eur. Polym. J.* **1990**, *26*, 499-508.
6. Silverstein, R. M.; Webster, F. X.; Kiemle, D. J. *Spectrometric Identification of Organic Compounds Seventh Edition*, John Wiley & Sons, Hoboken, 2005.

## Chapter 4

1. Hartley, G.S. *Aqueous Solutions of Paraffinic-Chain Salts. A Study of Micelle Formation*, Herman, Paris, 1936.
2. Balzer, D.; Linders, H. *Nonionic Surfactants Alkyl Polyglucosides*, Marcel Dekker, New York, 2000.



3. Kissa, E. *Dispersions Characterization, Testing, and Measurement*, Marcel Dekker, New York, 1999.
4. Hinze, W. L. *Organic Assemblies in Chemical Analysis Volume 1 Reverse Micelles*, JAI PRESS, London, 1994.
5. Pileni, M. P. *Structure and Reactivity in Reverse Micelles*, Elsevier, Paris, 1989.
6. Luisi, P. L.; Straub, B. E. *Reverse Micelles Biological and Technological Relevance of Amphiphilic Structures in Apolar Media*, Plenum Press, New York, 1982.
7. Zana, R. *Dynamics of Surfactant Self-assemblies Micelles, Microemulsions, Vesicles, and Lyotropic Phases*, Taylor& Francis, Boca Raton, 2005.
8. Ellis, C. D.; Margerum, L. D.; Murray, R. W.; Meyer, T. J. *Inorg. Chem.* **1983**, 22, 1283-1291.
9. Quinn, C. Development of a Water-soluble Dye/Quencher System to Study Polymer Chain Folding in Water by Fluorescence, M. Sc. Thesis, University of Waterloo, **2007**.
10. Shen, Y.; Duhamel, J. *Langmuir* **2008**, 24, 10665-10673.

## Chapter 5

1. Tomlinson, A.; Danks, T. N.; Heyes, D. M. *Langmuir* **1997**, 13, 5881-5893.
2. Bezot, P.; Hesse-Bezot, C.; Divraison, C. *Carbon* **1997**, 35, 53-60.
3. Jao, T. C.; Passut, C. A. *Handbook of Detergents, Part D : Formulation*, Showell, M.S. Ed., CRC Press, Taylor and Francis Group, Boca Raton, FL, 2006, pp437-471.
4. Wills, J.G., *Lubrication Fundamentals*, Mobil Oil Corporation, New York, 1980.

5. Ranney, M. W., *Lubricant Additives Recent Developments*, Noyes Data Corporation, Park Ridge, 1978.
6. Wollenberg, R. H.; Rafael, S.; Plavac, F. *U.S. Pat.* **1989**, 4,802,893.
7. Shen, Y.; Duhamel, J. *Langmuir* **2008**, *24*, 10665-10673.
8. Ellis, C. D.; Margerum, L. D.; Murray, R. W.; Meyer, T. *J. Inorg. Chem.* **1983**, *22*, 1283-1291.
9. Quinn, C. Development of a Water-soluble Dye/Quencher System to Study Polymer Chain Folding in Water by Fluorescence, M. Sc. Thesis, University of Waterloo, **2007**
10. Bezot, P.; Hesse-Bezot, C.; Rousset, B.; Diraison, C. *Colloids Surf. A* **1995**, *97*, 53-63.
11. Dubois-Clochard, M. C.; Durand, J. P.; Delfort, B.; Gauteau, P.; Berre, L.; Blanchard, I.; Chevalier, Y.; Gallo, R. *Langmuir* **2001**, *17*, 5901-5910.